The regulatory function of isoprenyl diphosphate synthases in terpene biosynthesis

Dissertation

To Fulfill the

Requirements for the Degree of

„doctor rerum naturalium“ (Dr. rer. nat.)

Submitted to the Council of the Faculty

of Biology and Pharmacy

of the Friedrich Schiller University Jena

by Diplom-Biochemiker Raimund Nagel

born on 27 September 1983 in Halberstadt

1. Gutachter: Prof. Dr. Jonathan Gershenzon (MPI für Chemische Ökologie, Jena)

2. Gutachter: Prof. Dr. Christian Hertweck (Hans-Knöll-Institut, Jena)

3. Gutachter: Prof. Dr. Alain Tissier (Leibniz-Institut für Pflanzenbiochemie, Halle (Saale))

Tag der öffentlichen Disputation: 20.06.2014

Table of Contents

1. Introduction

Terpenes, also called terpenoids, are the most structurally diverse class of metabolites, with currently over 60,000 compounds known (Köksal et al., 2011). Despite this large diversity in structures, terpenes follow the so called 'isoprene rule', which states that they are synthesized from C_5 isopentenoid building blocks (Christianson, 2008). They are ubiquitously present in every living organism and can be classified as part of either primary or secondary metabolism. As primary metabolites terpenes are essential for membrane integrity, e.g. as sterols in eukaryotes, hopanoids in bacteria or prenyllipids in archaea (Kannenberg and Poralla, 1999; Schaller, 2003; Espenshade and Hughes, 2007; Matsumi et al., 2011). The simplest C_{15} and C_{20} terpenes, farnesol and geranylgeraniol, are lipid-anchors for membrane proteins (Yalovsky, 2011; Zverina et al., 2012). Other terpenes are vital hormones, e.g. sterols in mammals, insects and Brassicaceae (Mitchell et al., 1970; Clouse and Sasse, 1998; Kaneko et al., 2011), gibberellins in all plants (Hedden and Thomas, 2012) and juvenile hormones in insects (Belles et al., 2005). Plastoquinone, phylloquinone and ubiquinone are part of electron transport chains and thereby essential for energy production in cellular metabolism (Bueno et al., 2012; Piller et al., 2012). Carotenoids and the phytol side chain of chlorophyll are needed for photosynthesis (Shibata et al., 2004; Cazzonelli and Pogson, 2010). As primary metabolites, terpenes are an integral part of maintaining vital functions of individual cells and the whole organism.

Under situations of abiotic or biotic stress, secondary metabolite terpenes increase the probability of survival for an organism. The simplest terpene with only 5 carbon atoms, isoprene, for example stabilizes the thylakoid membrane of plastids under elevated temperatures (Behnke et al., 2007). Under oxidative stress, tocopherols help organisms to prevent lipid peroxidation (Nowicka et al., 2013). Other terpenes are used to attract pollinators or mating partners, but most are thought to function in defense against herbivores, pathogens and predators (Pichersky and Gershenzon, 2002; Huang et al., 2012; Ponzio et al., 2013)(Figure 1). The defensive role of terpenes is well investigated in plants, whereas for animals, bacteria and fungi it is still a subject of future research. For instance in humans no secondary metabolite terpenes are known to be produced *de novo* and animals produce such terpenes only in a very few cases.

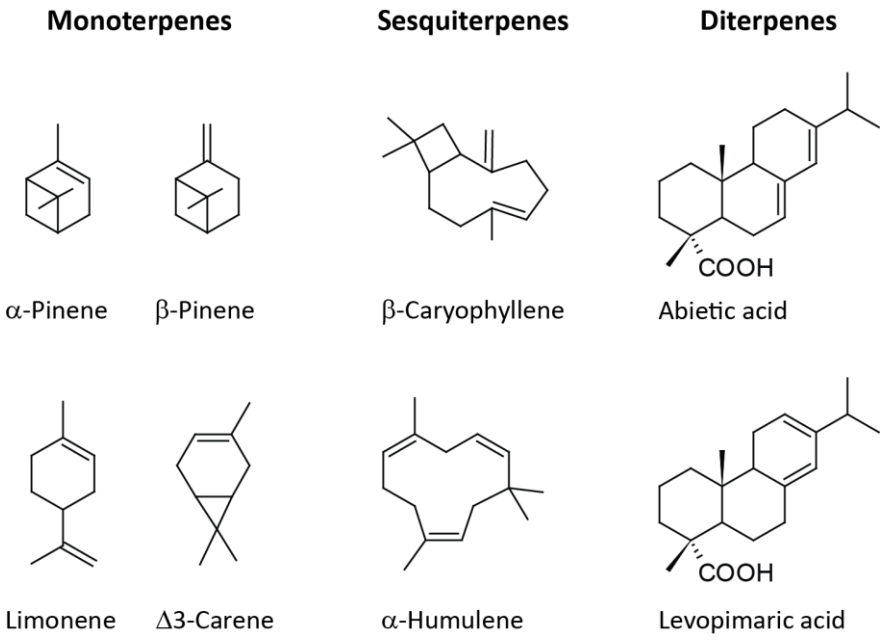

Figure 1: Exemplary defense related terpene structures of *Picea abies*. Major monoterpenes, sequiterpenes and diterpenes of the oleoresin of *Picea abies* are given.

1.1 Terpene biosynthesis

Despite their broad structural and functional diversity, the initial steps of terpene biosynthesis are highly conserved. The basic C_5 building blocks, isopentenyl diphosphate (IDP) and dimethylallyl diphosphate (DMADP), are synthesized by two pathways, the mevalonate (MVA) and the methylerythritol phosphate (MEP) pathways. The MVA pathway uses three units of acetyl-CoA as substrate, whereas the MEP pathway starts from glyceraldehyde 3-phosphate and pyruvate (Arigoni et al., 1997; Rodríguez-Concepción, 2006). In both pathways, specific regulatory enzymes have been identified, for the MVA pathway, 3-hydroxy-3-methyl-glutaryl-CoA reductase (HMGR), and for the MEP pathway, 1-deoxy-D-xylulose 5-phosphate synthase (DXS) and 1-deoxy-D-xylulose 5-phosphate reductoisomerase (DXR) (Hemmerlin et al., 2012). The MVA pathway is common to all eukaryotes and some bacteria, whereas the MEP pathway is present in most bacteria and photosynthetic eukaryotes (Lombard and Moreira, 2011; Hemmerlin et al., 2012). Plants are very distinct since both pathways are present in all species. The MVA pathway is localized in the cytosol and the MEP pathway in the plastids (Hemmerlin et al., 2012). The MVA pathway produces exclusively IDP, later isomerized to DMADP by isopentenyl diphosphate isomerase (IDI). On the other hand, the MEP pathway produces

DMADP and IDP in a fixed ratio of 1:5-6 (Hemmerlin et al., 2012), but IDI adapts the ratio for the requirements of the organism (Berthelot et al., 2012).

After formation of the basic C_5 building blocks, the smallest terpene with only 5 carbon atoms, isoprene, can be produced directly from DMADP (Behnke et al., 2007). However, for the biosynthesis of terpenes larger than C_5, isoprenyl diphosphate synthases (IDS) are needed. IDS catalyze the sequential head-to-tail condensation of IDP with an allylic substrate, usually DMADP, but also GDP, FDP and GGDP (Figure 2). Depending on the stereochemistry of the product formed, IDS can be classified as either *cis*- or *trans*-IDS (Liang et al., 2002). Although carrying out the same reaction, they are evolutionarily and structurally distinct from each other. Still both types need divalent cations as cofactor for catalysis, in most cases Mg^{2+} (Liang et al., 2002; Aaron and Christianson, 2010). Other metal cofactors were tested but most had lower catalytic activities (Tholl et al., 2001; Sen et al., 2007; Sen et al., 2007; Sen et al., 2007; Vandermoten et al., 2009; Barbar et al., 2013). The catalytic activity of *trans*-IDS depends on the first and second aspartate rich motif (FARM/SARM). The FARM has either the sequence DDxxD or DDxxxxD, whereas the SARM is only present as DDxxD. Both motifs bind divalent cations (Mg^{2+}) which themselves bind to the phosphates of IDP and DMADP/GDP/FDP and coordinate both substrates for the formation of the longer products (Aaron and Christianson, 2010). Mutations of the aspartate in either FARM or SARM decrease the catalytic activity (Liang et al., 2002). *Cis*-IDS lack the DDxxD motifs of *trans*-IDS, but instead aspartate and glutamate residues are distributed over the enzyme bind Mg^{2+} and mutations in those residues also decrease the catalytic activity (Liang et al., 2002).

In addition to the classification of *cis*- and *trans*-IDS, IDS can be classified by the length of their products, either short (C_{10}-C_{25}) , medium (C_{30}-C_{45}) or long-chain ($\geq C_{40}$) prenyl diphosphates (Wang and Ohnuma, 2000; Liang et al., 2002). *Trans*-IDS usually are involved in the biosynthesis of short-chain prenyl diphosphates, whereas *cis*-IDS produce longer prenyl diphosphates, with up to 5000 C_5 units in natural rubber (Wang and Ohnuma, 2000; Liang et al., 2002). However, a medium/long-chain *trans*-IDS was recently described from *Arabidopsis thaliana* (Hsieh et al., 2011) as well as a group of short-chain *cis*-IDS in several tomato species (Sallaud et al., 2009; Schilmiller et al., 2009; Akhtar et al., 2013). The product specificity of short-chain *trans*-IDS is to a large extent regulated by the identity of the amino acids on the N-terminal side of the FARM. This is the so called molecular ruler theory because the size of these amino acids limit the size of the active site pocket (Wang and Ohnuma, 2000; Liang et al., 2002). Long-chain *trans*-IDS can be distinguished from short-chain *trans*-IDS by specific amino acid residues, but the length of

the prenyl diphosphate produced cannot be predicted accurately (Wallrapp et al., 2013). Short and long-chain *cis*-IDS also differ in the number of amino acids between conserved regions III and IV of *cis*-IDS (Akhtar et al., 2013). The product length of either C_{10} or C_{15} short-chain *cis*-IDS from tomato depends on individual amino acid changes (Kang et al., 2014).

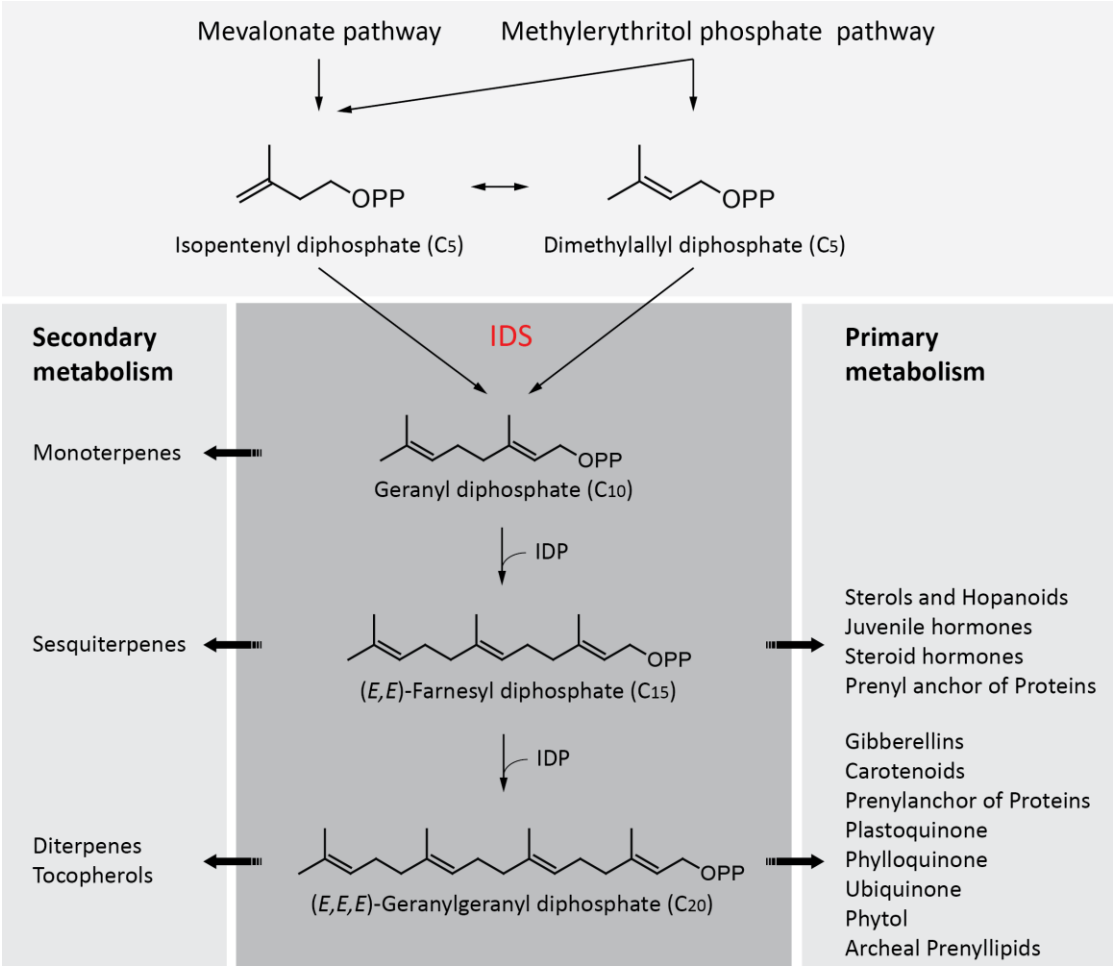

Figure 2: Outline of terpenoid biosynthesis. The schematic diagram depicts the reactions carried out by short-chain isoprenyl diphosphate synthases (IDS). The five carbon building blocks, isopentenyl diphosphate (IDP) and dimethylallyl diphosphate (DMADP), produced either by the cytosolic mevalonate pathway or the plastidial methylerythritol phosphate (MEP) pathway are the substrates for IDS. Sequential condensations of DMADP with 1-3 molecules of IDP mediated by IDS form geranyl- (GDP), farnesyl- (FDP) or geranylgeranyl diphosphate (GGDP). The different prenyl diphosphates are then converted into individual terpenes, which may either be primary or secondary metabolites.

Commonly short-chain *trans*-IDS have been named after their product, e.g. geranyl, farnesyl or geranylgeranyl diphosphate synthases (GDPS, FDPS and GGDPS). This is unfortunate, as one IDS can have more than one product, e.g. IDS1 of *Picea abies* produces GDP and GGDP (Schmidt

et al., 2010). Therefore as an alternative IDS are just named for each species by consecutive numbering in order of discovery. In this dissertation both nomenclatures will be used depending on the original publication.

The prenyl diphosphates produced by IDS are then substrates for terpene synthases and following enzymes give rise to the enormous variety of terpenes produced. Terpenes are classified according to their size as hemiterpenes (C_5), monoterpenes (C_{10}), sesquiterpenes (C_{15}), diterpenes (C_{20}), sesterterpenes (C_{25}), triterpenes (C_{30}), tetraterpenes (C_{40}) and so on (Tholl, 2006; Degenhardt et al., 2009). Therefore by controlling the length of produced terpenes IDS are situated at a central point of terpene biosynthesis.

1.2 Regulation of terpene biosynthesis

Understanding the regulation of terpene biosynthesis holds much interest for human society. For example, terpene regulation has long been known to play a role in diseases linked to elevated cholesterol concentrations (Bhatnagar et al., 2008). More recently the function of FDPS and GGDPS in regulation of protein prenylation in cancer treatment or during pathogen infection has been studied (Dudakovic et al., 2011; Wasko et al., 2011; Dhar et al., 2013). Regulation of terpene biosynthesis is also important in the production of high value terpenes in strains of *Saccharomyces cerevisiae* and *Escherichia coli* engineered to make components of pharmaceutical, fragrance or aroma importance (Martin et al., 2003; Morrone et al., 2010; Fischer et al., 2013; Maury et al., 2013; Paddon et al., 2013). Recently it was proposed to use also engineered plant trichomes of Lamiaceae and Solanaceae for the production of terpenes (Tissier, 2012a, 2012b; Lange and Turner, 2013; Staniek et al., 2013; Tissier et al., 2013). All of these examples deal with a particular form of pathway regulation in diseased cells or engineered organisms and neither is a good representative for regulation of terpene biosynthesis under natural conditions.

1.2.1 Plant terpene biosynthesis

In plants, terpene biosynthesis is highly compartmentalized. The MEP pathway together with IDS producing GDP and GGDP are usually found in the plastids along with the respective terpene synthases while the MVA pathway as well as IDS producing FDP and terpene synthases using it as substrate are usually found in the cytosol (Tholl, 2006; Bohlmann and Keeling, 2008;

Tholl and Lee, 2011). This implies a large need for control to balance terpene biosynthesis not only between primary and secondary metabolism, but also between different subcellular compartments.

For angiosperms *Arabidopsis thaliana* is the most used model in terpene biosynthetic studies because it is easy to grow and the genome was the first to be sequenced. Therefore most genes involved in terpene biosynthesis have been identified. For instance *A. thaliana* has a multitude of IDS genes present: one gene originally identified as a GPPS that was more recently shown to produce medium/long-chain prenyl diphosphates instead; two FPPS in two splicing versions each; and 12 GGPPS of which 10 are described as being functional (Hsieh et al., 2011; Tholl and Lee, 2011; Beck et al., 2013). This large number of IDS enzymes indicates a high degree of redundancy that makes it rather difficult to manipulate individual IDS and decipher if they have regulatory roles. Curiously, although *A. thaliana* has so many IDS present, the actual amounts of terpenes produced or emitted from flowers and leaves is rather low (Chen et al., 2003; Tholl and Lee, 2011; Huang et al., 2012).

Other well studied model plants for terpene biosynthesis include conifers because of their ability to produce large quantities of terpenes. The best investigated plant here is the Eurasian Norway spruce (*Picea abies*), whose genome has become recently available (Nystedt et al., 2013), and its North American relatives Sitka and white spruce (*Picea sitchensis* and *Picea glauca*). The resin of conifer species also called oleoresin is mainly comprised of terpenes. Conifer oleoresin is stored in specialized resin ducts in spruce and pine or in resin blisters in fir (Franceschi et al., 2005). In *P. abies* 6 different IDS and multiple TPS have already been identified to be involved in terpene biosynthesis. Of the 6 IDS, IDS2 produces solely GDP, IDS4 solely FDP, IDS5 and IDS6 produce GGDP, and IDS1 produces GDP and GGDP (Martin et al., 2004; Schmidt and Gershenzon, 2007, 2008; Schmidt et al., 2010; Chen et al., 2011; Schmidt et al., 2011). IDS3 produces short-chain prenyl diphosphates *in vitro*, but has close sequence similarity to the medium/long-chain IDS from *A. thaliana* and therefore might not be involved in resin terpene biosynthesis (Schmidt and Gershenzon, 2008; Hsieh et al., 2011; Schmidt et al., 2011). IDS1 is of particular interest since it produces GDP and GGDP, the precursors for monoterpene and diterpene resin acids, the most abundant terpene classes in oleoresin of needles and bark (Martin et al., 2002; Martin et al., 2003). The oleoresin is employed as a defense against herbivores and pathogens of conifers. In the stem the oleoresin is stored under pressure in resin ducts. If an herbivore attacks the tree and starts to tunnel into the bark, it may rupture a resin duct and the resin flushes the insect out of the entrance hole and seals the

wound or traps the insect in the polymerizing resin (Franceschi et al., 2005). It was also shown that monoterpenes, sesquiterpenes and diterpene resin acids can be toxic or deterrent to insects and their associated pathogens (Gershenzon and Kreis, 1999; Phillips and Croteau, 1999; Keeling and Bohlmann, 2006).

Through its entire life cycle, Norway spruce (*P. abies*) can be attacked by different herbivores and pathogens. Young saplings of 2-5 years as well as young branches of old grown trees are fed on by the large pine weevil (*Hylobius abietis*), which is able to destroy whole plant nurseries and reforested areas. The foliage of older trees is a food source to several sawflies, like *Gilpinia hercyniae*, *Pristiphora abietina* and *Cephalcia abietis*, and moths like *Epinotia tedella, Epinotia pygmaeana* and *Lymantria monacha* (Klimetzek and Vite, 1989). Most of these only have minor growth-reducing effects on Norway spruce with the exception of the nun moth (*Lymantria monacha*), which has devastating consequences during an mass outbreak on entire spruce and pine forests (Wellenstein, 1942; Keena et al., 2010). Although native to Eurasia, the nun moth is also being closely monitored in North America because of its devastating effects on forests and its ability to feed and develop on conifers native to this region (Keena, 2003). Old grown Norway spruce trees can be attacked by several bark beetle species, such as *Ips typographus*, which together with its associated blue stain fungus *Ceratocystis polonica* can be lethal for whole forests (Franceschi et al., 2005)(Figure 3).

In case of herbivore attack, conifers often react by increasing their defenses producing new terpene oleoresin and formation of so called traumatic resin ducts in the cambial layer of the bark (Martin et al., 2002; Franceschi et al., 2005; Abbott et al., 2010; Schmidt et al., 2010; Zulak and Bohlmann, 2010; Schmidt et al., 2011). A higher production rate and larger quantities of oleoresin are associated with a higher resistance against herbivores in spruce trees (Zhao et al., 2011). Especially for IDS1, it was shown that transcript accumulation is an important marker for a higher terpene accumulation (Schmidt et al., 2011). Therefore as a part of this thesis it was investigated, how overexpression of IDS1 influences the amount of terpenes in white spruce and what consequences a changed terpene content has for resistance against needle-feeding herbivores.

Figure 3: Herbivores, pathogens and resulting damage to conifer stands. (A) Large pine weevil (*Hylobius abietis*) feeding on spruce saplings [source: (Lieutier et al., 2004)]; (B) Nun moth (*Lymantria monach*) feeding on spruce needles [source: Petr Kapitola, State Phytosanitary Administration, Czekia, Bugwood.org] ; (C) Bark beetle (*Ips typographus*) tunneling into cambial layer of spruce [source: wikipedia.org]; (D) Blue stain fungus (*Ceratocystis polonica*) stained wood [source: (Lieutier et al., 2004)]; (E) Defoliation of a pine stand after feeding by the nun moth [source: Die Nonne, Waldschutzblatt 52, Landesforstanstalt Eberswalde]; (F) Spruce stand in the Bohemian forest after an bark beetle attack [source: Dr. Axel Schmidt, MPI for Chemical Ecology].

1.2.2 Insect terpene biosynthesis

Terpenes of secondary metabolism in insects are not as well studied as in plants. However, some examples are known from the literature. For example, bark beetles use terpenes as pheromones, either for aggregation (e.g. verbenol) or to warn further bark beetles that a particular tree is already overcrowded (e.g. verbenone) (Gilg et al., 2005; Gilg et al., 2009;

Blomquist et al., 2010; Song et al., 2013). Aphids produce the monoterpenic nepetalactones and nepetalactols to find possible mating partners (Pettersson et al., 2008; Symmes et al., 2012; Fernandez-Grandon et al., 2013), and the sesquiterpene (*E*)-β-farnesene as an alarm pheromone to warn other aphids of an enemy attack (Vandermoten et al., 2012). Other insects are able to sequester toxic terpenes from their food source, among them the monarch butterfly and several leaf beetles (Dobler et al., 2011; Agrawal et al., 2012). Leaf beetles sequester not only terpenes for defense, but depending on the species and their food source also other defensive plant compounds (Blum et al., 1972; Hilker and Schulz, 1994; Schulz et al., 1997; Termonia and Pasteels, 1999; Kuhn et al., 2007). In addition to this exploitation of defensive plant compounds several leaf beetle species have the ability to produce an iridoid-based defense *de novo* (Meinwald et al., 1977; Blum et al., 1978; Pasteels et al., 1982; Soe et al., 2004). The larvae of the horseradish leaf beetle (*Phaedon cochleariae*), for example, have paired exocrine glands on their thoracal and abdominal segments attached to internal reservoirs. In case of an attack the reservoirs release droplets containing the iridoid chrysomelidial (Pasteels et al., 1982; Termonia et al., 2001)(Figure 4).

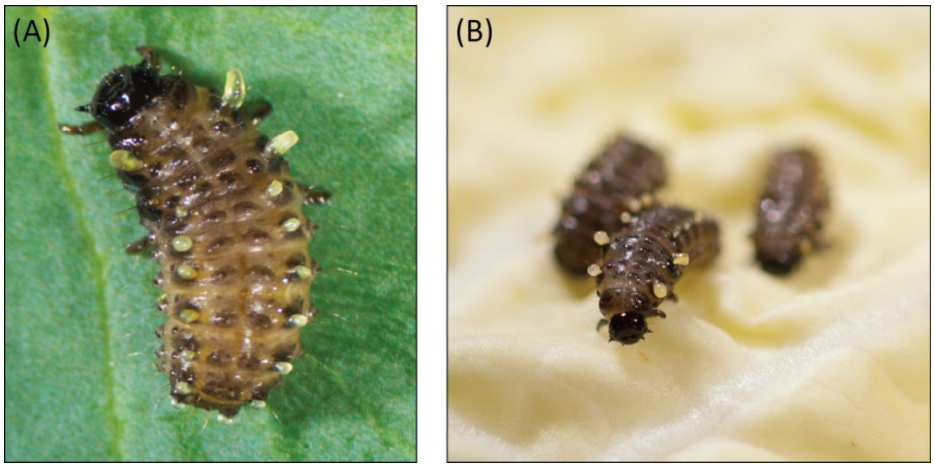

Figure 4: *Phaedon cochleariae* larvae. The larvae show the droplets excreted by the exocrine glands after a simulated attack.

Parts of leaf beetle terpene biosynthesis have already been elucidated. The early biosynthetic steps take place in the larval fat body and use the MVA pathway for DMADP and IDP production (Veith et al., 1994; Burse et al., 2007). The particular IDS producing GDP was identified as part of this thesis. In the following biosynthetic steps, 8-hydroxygeraniol glucoside (8-OH GerGlu) is formed by as yet unidentified enzymes. 8-OH GerGlu is then released into the hemolymph and taken up by glandular cells attached to the reservoirs. After uptake into the

glandular cells, 8-OH GerGlu is converted to chrysomelidial in several enzymatic steps (Pasteels et al., 1982; Pasteels et al., 1990; Lorenz et al., 1993; Soetens et al., 1993; Daloze and Pasteels, 1994; Veith et al., 1994; Veith et al., 1996; Veith et al., 1997; Brückmann et al., 2002; Burse et al., 2007). 3-Hydroxy-3-methyl-glutaryl-CoA reductase (HMGR), an enzyme of the MVA pathway, was already identified to be an important regulatory step for chrysomelidal biosynthesis and is inhibited by the intermediate 8-hydroxygeraniol (Burse et al., 2008)(Figure 5). To look for other modes of regulation, the IDS of *P. cochleariae* was investigated as part of this thesis.

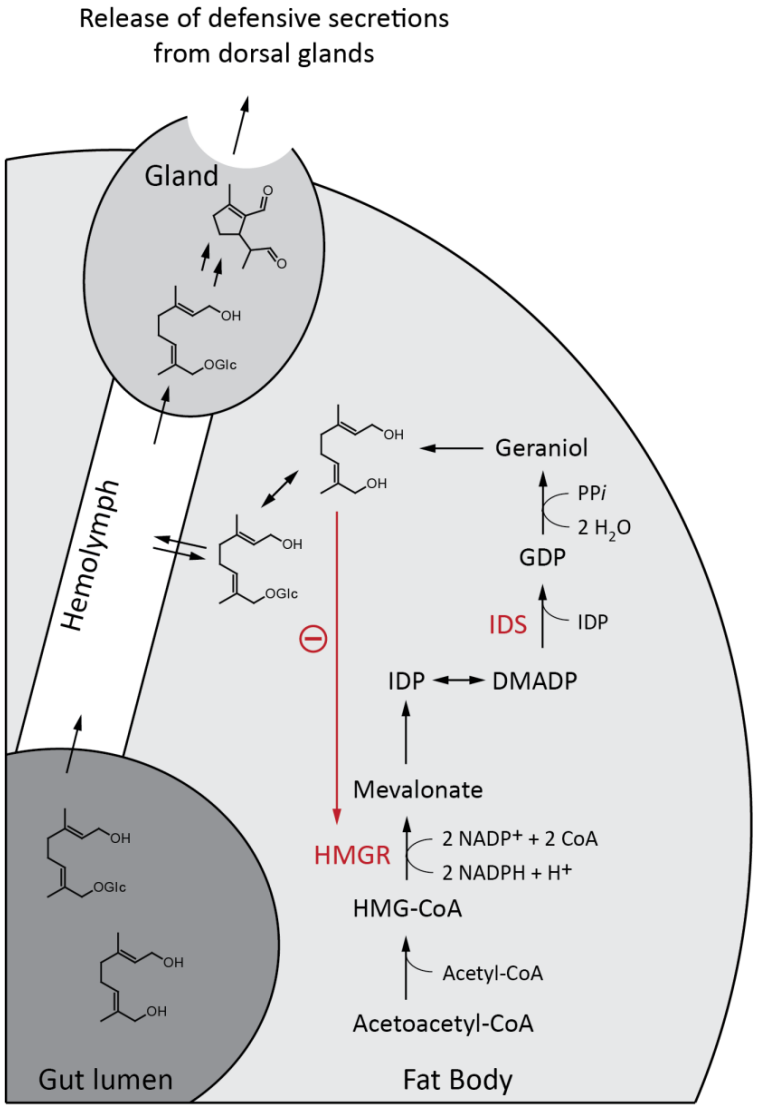

Figure 5: Outline of chrysomelidial biosynthesis in *Phaedon cochleariae* larvae. Early biosynthetic steps take place in the larval fat body. Intermediates are excreted into the hemolymph or sequestered from the food source and subsequentially taken up in to the dorsal glands and converted into chrysomelidial. The regulatory enzymes IDS and HMGR are depicted in red [Adapted from (Burse et al., 2009)].

2. Overview of manuscripts

2.1 Manuscript 1

Raimund Nagel, Jonathan Gershenzon, Axel Schmidt

Nonradioactive assay for detecting isoprenyl diphosphate synthase activity in crude plant extracts using liquid chromatography coupled with tandem mass spectrometry

Analytical Biochemistry **422**; 33–38 (2012)

This publication describes a LC-MS/MS based method to quantify isoprenyl diphosphate synthase enzyme activity, with higher sensitivity than an assay based on radioactivity. The same method also can be used to differentiate between different prenyl diphosphate isomers. As proof of principle, isoprenyl diphosphate synthase enzyme activity was quantified in protein extracts of different plants and their various tissues.

R.N. designed and performed research, analyzed data and wrote the paper
J.G. revised the paper and supervised the work
A.S. designed the research and wrote the paper

2.2 Manuscript 2

Raimund Nagel, Aileen Berasategui, Christian Paetz, Jonathan Gershenzon, Axel Schmidt

Overexpression of an isoprenyl diphosphate synthase in spruce leads to unexpected terpene diversion products that function in plant defense

Plant Physiology **164**; 555-569 (2014)

Overexpression of an IDS in white spruce, increases the total IDS enzyme activity and the *in vivo* prenyl diphosphate concentrations in needles, but not in bark. The major mono-, sesqui- and diterpenes of the resin, as well as primary metabolites, like sterols and carotenoids, were unchanged. Instead in the needles esters of geranylgeraniol with several fatty acids accumulated that can act as a defense against *Lymantria monacha* larvae.

R.N. designed and performed research, analyzed data and wrote the paper

A.B. performed research and analyzed data

C.P. analyzed data

J.G. revised the paper and supervised the work

A.S. designed the research and revised the paper

2.3 Manuscript 3

Sindy Frick, Raimund Nagel, Axel Schmidt, René R. Bodemann, Peter Rahfeld, Gerhard Pauls, Wolfgang Brandt, Jonathan Gershenzon, Wilhelm Boland, and Antje Burse

Metal ions control product specificity of isoprenyl diphosphate synthases in the insect terpenoid pathway

Proceedings of the National Academy of Sciences of the United States of America **110**; 4194-4199. (2013)

An isoprenyl diphosphate synthase (*Pc*IDS1) of *Pheadon cochleariae* was identified and characterized in this publication. Enzyme activity studies revealed a novel mechanism for controlling the product chain length of *Pc*IDS1 depending on the divalent metal co-factor present. RNAi experiments targeting *Pc*IDS1 revealed the involvement of this enzyme in the *de novo* biosynthesis of defensive iridoids.

R.N. performed research and analyzed data
S.F. designed and performed research, analyzed data and wrote the paper
A.B. and A.S. designed research, analyzed data and wrote the paper
R.R.B., P.R. and G.P. performed research and analyzed data
W. Brandt analyzed data
J.G. and W.B. designed research and wrote the paper

3. Manuscripts

3.1 Manuscript 1

Nonradioactive assay for detecting isoprenyl diphosphate synthase activity in crude plant extracts using liquid chromatography coupled with tandem mass spectrometry

Analytical Biochemistry 422 (2012) 33–38

Contents lists available at SciVerse ScienceDirect

Analytical Biochemistry

journal homepage: www.elsevier.com/locate/yabio

Nonradioactive assay for detecting isoprenyl diphosphate synthase activity in crude plant extracts using liquid chromatography coupled with tandem mass spectrometry

Raimund Nagel, Jonathan Gershenzon *, Axel Schmidt

Department of Biochemistry, Max Planck Institute for Chemical Ecology, Beutenberg Campus, D-07745 Jena, Germany

ARTICLE INFO

Article history:
Received 25 October 2011
Received in revised form 22 December 2011
Accepted 23 December 2011
Available online 3 January 2012

Keywords:
Isoprenyl diphosphate synthases
Prenyltransferases
Terpenes
LC–MS/MS
Geranyl diphosphate
Farnesyl diphosphate
Geranylgeranyl diphosphate

ABSTRACT

Terpenoids form the largest class of plant metabolites involved in primary and secondary metabolism. Isoprenyl diphosphate synthases (IDSs) catalyze the condensation of the C_5 terpenoid building blocks, isopentenyl diphosphate and dimethylallyl diphosphate, to form geranyl diphosphate (C_{10}), farnesyl diphosphate (C_{15}), and geranylgeranyl diphosphate (C_{20}). These branch point reactions control the flow of metabolites that act as precursors to each of the major terpene classes—monoterpenes, sequiterpenes, and diterpenes, respectively. Thus accurate and easily performed assays of IDS enzyme activity are critical to increase our knowledge about the regulation of terpene biosynthesis. Here we describe a new and sensitive nonradioactive method for carrying out IDS assays using liquid chromatography coupled with tandem mass spectrometry (LC–MS/MS) to detect the short-chain prenyl diphosphate products directly without dephosphorylation. Furthermore, we were able to separate *cisoid* and *transoid* isomers of both C_{10} enzyme products (geranyl diphosphate and neryl diphosphate) and three C_{15} products [(*E*,*E*)-, (*Z*,*E*)-, and (*Z*,*Z*)-farnesyl diphosphate]. By applying the method to crude protein extracts from various organs of *Arabidopsis thaliana*, *Nicotiana attenuata*, *Populus trichocarpa*, and *Picea abies*, we could determine their IDS activity in a reproducible fashion.

More than 55.000 terpenes or isoprenoids form the largest single class of lower molecular weight plant metabolites and function in many processes in primary and secondary metabolism [1]. The biosynthesis of all terpenoids is initiated by the synthesis of isopentenyl diphosphate (IPP)[1] via the mevalonic acid or the methylerythritol phosphate pathway [2,3]. IPP and its isomer, dimethylallyl diphosphate (DMAPP), are the five-carbon building blocks that undergo sequential condensation reactions to form the prenyl diphosphates, geranyl diphosphate (GPP, C_{10}), farnesyl diphosphate (FPP, C_{15}), and geranylgeranyl diphosphate (GGPP, C_{20}) as precursors for monoterpenes (C_{10}), sesquiterpenes (C_{15}), and diterpenes (C_{20}), respectively, as well as for other compounds such as sterols, carotenoids, and gibberellins. The enzymes catalyzing these sequential condensation reactions are prenyltransferases referred to collectively as isoprenyl diphosphate synthases (IDSs). Each of the short-chain IDS products (GPP, FPP, and GGPP) is formed by a specific enzyme named for its product: GPP synthase (GPPS), FPP synthase (FPPS), and GGPP synthase (GGPPS) (Fig. 1).

Until now, a fast and easy method to determine the products and rate of activity of plant IDSs has not been described. The established assay for measuring IDS enzyme activity *in vitro* in crude extracts of plants or in *Escherichia coli* extracts after heterologous expression of IDSs involves the use of radioactively labeled [^{14}C]IPP as substrate followed by acid or alkaline hydrolysis. The corresponding alcohols are measured by radio-gas chromatography (radio-GC), radio-high-performance liquid chromatography (radio-HPLC), thin layer chromatography (TLC), or liquid scintillation counting (LSC) [4–14]. However, because of the precautions for using radioactive substrates and the complication of hydrolyzing the products, assays are rather laborious, time-consuming, and frequently imprecise. Hydroxylation is carried out either in strongly acidic conditions or by incubation with an alkaline phosphatase. However, both methods have serious disadvantages. Acid hydrolysis may generate multiple products from one prenyl diphosphate such as linalool, α-terpineol, and nerol from neryl diphosphate (NPP, C_{10}) [15]. Thus, it may be difficult to identify

* Corresponding author. Fax: +49 3641 571302.
E-mail address: gershenzon@ice.mpg.de (J. Gershenzon).

[1] *Abbreviations used:* IPP, isopentenyl diphosphate; DMAPP, dimethylallyl diphosphate; GPP, geranyl diphosphate; FPP, farnesyl diphosphate; GGPP, geranylgeranyl diphosphate; IDS, isoprenyl diphosphate synthase; radio-GC, radio-gas chromatography; radio-HPLC, radio-high-performance liquid chromatography; TLC, thin layer chromatography; LSC, liquid scintillation counting; NPP, neryl diphosphate; LC–MS/MS, liquid chromatography coupled with tandem mass spectrometry; PAR: photosynthetically active radiation; Mopso, 3-(*N*-morpholino)-2-hydroxypropanesulfonic acid.

0003-2697/$ - see front matter © 2011 Elsevier Inc. All rights reserved.
doi:10.1016/j.ab.2011.12.037

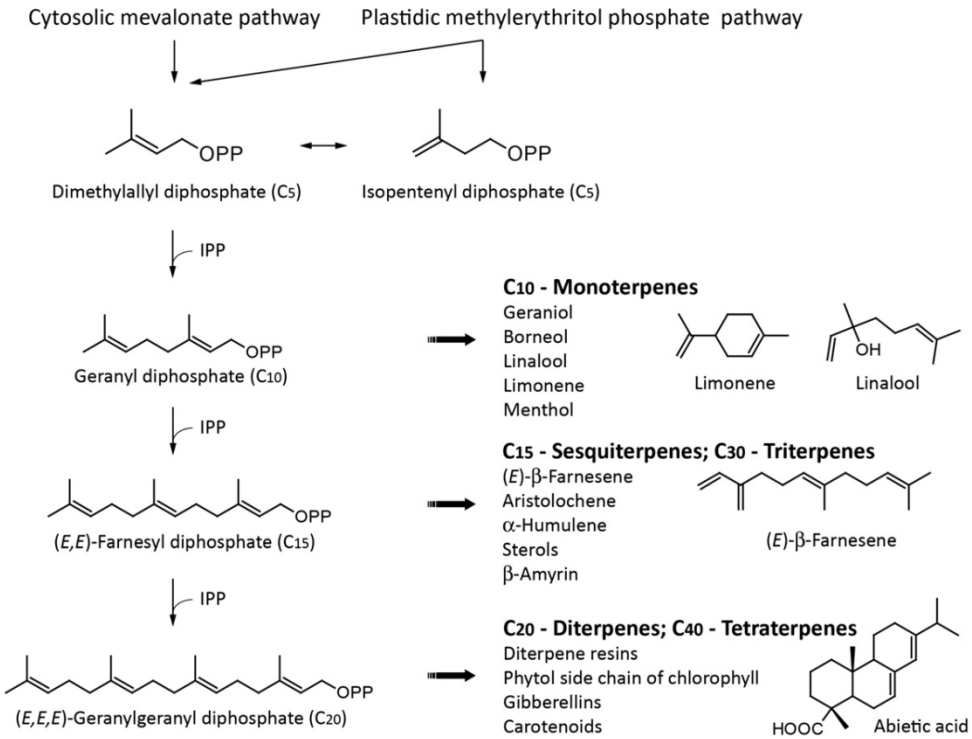

Fig.1. Outline of terpenoid biosynthesis. The schematic diagram depicts the reactions carried out by short-chain isoprenyl diphosphate synthases (IDSs). The five-carbon building blocks isopentenyl diphosphate (IPP) and dimethylallyl diphosphate (DMAPP), produced either by the cytosolic mevalonate pathway or the plastidial methylerythritol phosphate (MEP) pathway, are the substrates for IDSs. Sequential condensations of DMAPP with 1 to 3 molecules of IPP mediated by IDSs form geranyl diphosphate (GPP), farnesyl diphosphate (FPP), or geranylgeranyl diphosphate (GGPP). The catalysts are referred to as GPP synthases, FPP synthases, or GGPP synthases. The different prenyl diphosphates are then converted into representatives of the different terpene classes—GPP to monoterpenes, FPP to sesqui- and triterpenes, and GGPP to di- and tetraterpenes.

the actual enzyme product. Alkaline phosphatases do not usually cause such rearrangements, but a shift of the pH optimum is needed for the reaction to occur and a long incubation time is required for complete cleavage of all prenylated diphosphates. Under these conditions, IDSs can still be active, making this method unsuitable for determining accurate rates of enzyme activity. Moreover, prenyl diphosphates are often poor substrates for commercially available phosphatases [16].

Recently, two unexpected new IDS reaction products were reported with *cisoid* structures instead of *transoid* structures that serve as substrates for new types of terpene synthases, the enzymes converting GPP, FPP, or GGPP to specific terpene skeletons [15,17,18]. The possible involvement of NPP and (*Z,Z*)-FPP, the *cisoid* isomers of GPP and (*E,E*)-FPP, respectively, in other reactions of plant terpenoid biosynthesis now makes it even more crucial to carefully identify IDS products. However, none of the previously described IDS assays is able to differentiate between these *cisoid* and *transoid* isomers without hydrolysis.

Here we describe a new method using liquid chromatography coupled with tandem mass spectrometry (LC–MS/MS) to determine the products and rate of IDS enzyme reaction in crude protein extracts of plants without the need for radioactive substrates or a dephosphorylation step. The protocol can be used to detect IDS enzyme activity in a fast and reliable way in a broad range of plant protein extracts from angiosperms such as *Arabidopsis thaliana*, poplar (*Populus trichocarpa*), and tobacco (*Nicotiana attenuata*) as well as from gymnosperms such as Norway spruce (*Picea abies*). The method can also distinguish between the different *transoid* and *cisoid* isoforms of GPP and FPP as products.

Materials and methods

Chemicals/materials

IPP, DMAPP, GPP, FPP, and GGPP standards, chemical reagents, and LC–MS-grade ammonium bicarbonate were purchased from Sigma–Aldrich (Munich, Germany). GC-grade chloroform was purchased from Roth (Karlsruhe, Germany), and HPLC-grade acetonitrile was purchased from VWR (Darmstadt, Germany). NPP and (*Z,Z*)-FPP were purchased from Echelon Bioscience (Salt Lake City, UT, USA). [1-^{14}C]IPP (50 Ci mol^{-1}) was purchased from Hartmann Analytic (Braunschweig, Germany).

Plant material

A. thaliana (Col-0) was grown from seeds in a climate chamber (22 °C, 55% relative humidity, and 100 μmol m^{-2} s^{-1} photosynthetically active radiation [PAR]) under long-day conditions (16/8-h light/dark) until flowers developed. Flowers and leaves were cut with scissors. *P. abies* tissue was harvested from clone 3369-Schongau (Samenklenge and Pflanzgarten Laufen) planted out originally as 1-year-old seedlings at Jena, Germany, in 2003. Bark and needles from a side branch were harvested in mid-April. *N. attenuata* was

cultivated as described by Baldwin and coworkers [19] and harvested at the rosette stage. *P. trichocarpa* was propagated stem cuttings of clone 606 (NW-FVA, Hann. Münden, Germany) grown in a climate chamber (24 °C, 60% relative humidity, 100 μmol m^{-2} s^{-1} PAR and 16/8-h light/dark). Plants were harvested after reaching 1 m of height. All plant material was immediately frozen in liquid nitrogen after harvest and stored at −80 °C.

Protein extraction

Plant tissues were ground with mortar and pestle under liquid nitrogen by hand to a fine powder. Cooled extraction buffer was added to frozen tissue in a ratio of 1:5 (tissue [g]/buffer [ml]). Extraction buffer was modified after Ref. [5] and contained 250 mM Mopso (pH 6.8), 5 mM ascorbic acid, 5 mM sodium bisulfite, 5 mM dithiothreitol (DTT), 10 mM $MgCl_2$, 1 mM ethylenediaminetetraacetic acid (EDTA), 10% (v/v) glycerol, 1% (w/v) polyvinylpyrrolidone (PVP, M_r = 10,000), 4% (w/v) polyvinylpolypyrrolidone (PVPP), 4% [w/v] Amberlite XAD-4, and 0.1% (v/v) Tween 20. Extraction was carried out in Eppendorf Protein LoBind tubes with an Eppendorf ThermoShaker at 4 °C and 1400 rpm for 30 min. After tubes were centrifuged for 20 min at 4 °C and 20,000*g*, the supernatant was passed through a 2-ml Zeba Spin desalting column with a 7-kDa molecular weight cutoff (MWCO, Thermo Scientific, Rockford, IL, USA) to exchange the buffer to 25 mM Mopso (pH 7.2), 10 mM $MgCl_2$, and 10% (v/v) glycerol according to the manufacturer's protocol. Protein concentration was determined using the Protein Assay Dye (Bradford) Reagent Concentrate (5×) (Bio-Rad, Munich, Germany) and bovine serum albumin as standard (Bio-Rad).

Prenyltransferase assay

Assays were carried out in a total volume of 200 μl with 50 μM IPP and 50 μM DMAPP and a total protein range between 16 and 50 μg per assay. Control assays were done without IPP and DMAPP or were boiled before adding the substrates. Assays were incubated at 30 °C for 2 h, stopped by freezing in liquid nitrogen, and stored for up to 1 week before analysis. Proteins were denatured by adding 500 μl of chloroform and vortexing followed by centrifugation at 3000*g* for 5 min. For LC–MS/MS analysis, the water phase was transferred to a glass vial. Assays for radio-HPLC analysis were performed in the same way except that 50 μM [1-^{14}C]IPP was used as substrate.

LC–MS/MS analysis

Analysis of isoprenoid pyrophosphates was performed after a modified method of Miriyala and coworkers [20] on an Agilent 1200 HPLC system (Agilent Technologies, Boeblingen, Germany) coupled to an API 3200 triple quadrupole mass spectrometer (Applied Biosystems, Darmstadt, Germany). For separation, a ZORBAX Extended C-18 column (1.8 μm, 50 × 4.6 mm, Agilent Technologies, Santa Clara, CA, USA) was used. The mobile phase consisted of 5 mM ammonium bicarbonate in water as solvent A and acetonitrile as solvent B, with the flow rate set at 0.8 ml min^{-1} and the column temperature kept at 20 °C. Separation was achieved by using a gradient starting at 0% B, increasing to 10% B in 2 min, 64% B in 12 min, and 100% B in 2 min (1-min hold), followed by a change to 0% B in 1 min (5-min hold) before the next injection. The injection volume for samples and standards was 20 μl. The mass spectrometer was used in negative electrospray ionization mode. Optimal settings were determined using standards. Ion source gas 1 and gas 2 were set at 60 and 70 psi, respectively, with a temperature of 700 °C. Curtain gas was set at 30 psi, and collision gas was set at 7 psi, with all gases being nitrogen. Ion spray voltage was maintained at −4200 V. Multiple reaction monitoring (MRM) transitions were *m*/*z* 312.9/79 for GPP, *m*/*z* 380.9/79 for (*E*,*E*)-FPP, and *m*/*z* 449/79 for (*E*,*E*,*E*)-GGPP. The same transitions were used for the *cisoid* isomers NPP, (*Z*,*E*)-FPP, and (*Z*,*Z*)-FPP, respectively. For further details of settings see supplementary material (Table S1). Data analysis was performed using Analyst 1.5 build 3385 software (Applied Biosystems).

Radio-HPLC analysis

Analysis was carried on an Agilent 1100 HPLC system (Agilent Technologies, Boeblingen, Germany) coupled to a Radiomatic 500TR series Flow Scintillation Analyzer (Canberra, Rüsselsheim, Germany), having a volume of 0.5 ml for the liquid flow cell. The same separation conditions were used as described under LC–MS/MS analysis. Scintillation fluid (Ultima-Flo AP, PerkinElmer, Rodgau, Germany) was provided in a 4:1 ratio to the column eluent.

Results and discussion

We developed a sensitive, accurate, and reproducible LC–MS/MS method for the detection and quantification of C_{10}, C_{15}, and C_{20} prenyl diphosphates after *in vitro* assays of IDS activity in plant protein extracts. The products were detectable in a linear range from 2 to 270 pmol (GPP), 2 to 230 pmol [(*E*,*E*)-FPP], and 4 to 100 pmol [(*E*,*E*,*E*)-GGPP] per injection (Fig. 2). The limits of detection for GPP, (*E*,*E*)-FPP, and (*E*,*E*,*E*)-GGPP were 0.9, 1.1, and 1.9 pmol, respectively, determined at a signal-to-noise ratio of 1:3. The sensitivity of this nonradioactive method is in the same range as the radio-GC detection used by Martin and coworkers [5] but had a much lower degree of variation. The method is two orders of magnitude more sensitive than analysis by radio-HPLC (see Fig. 1 in supplementary material) and presumably is an even greater improvement over analysis using radio-TLC detection. Technical reproducibility was high, with repeated injections showing ⩽5% variation.

The new IDS assay was first tested on various organs of *A. thaliana* because there is already considerable knowledge on the terpene metabolism of this species. For volatile terpenes, flowers are described to be higher emitters of mono- and sesquiterpenes than leaves [21], suggesting that the levels of endogenous

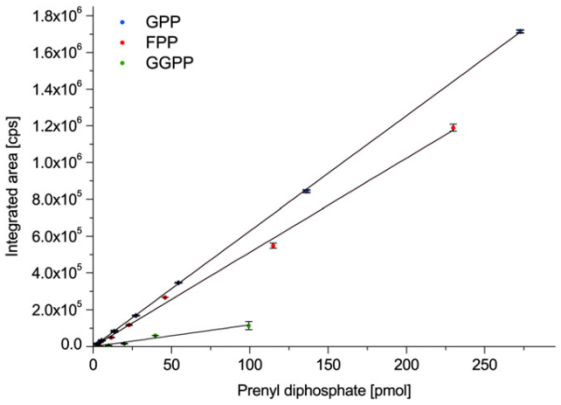

Fig.2. Calibration curves for quantification of GPP, FPP, and GGPP measured by LC–MS/MS under the conditions described. Each point was measured twice. R^2 for linear regression was 0.99 for GPP and FPP and was 0.96 for GGPP. At least three individual dilution series with two injections each were analyzed, and the variation was below 5%. Means ± standard deviations of at least three replicates are depicted.

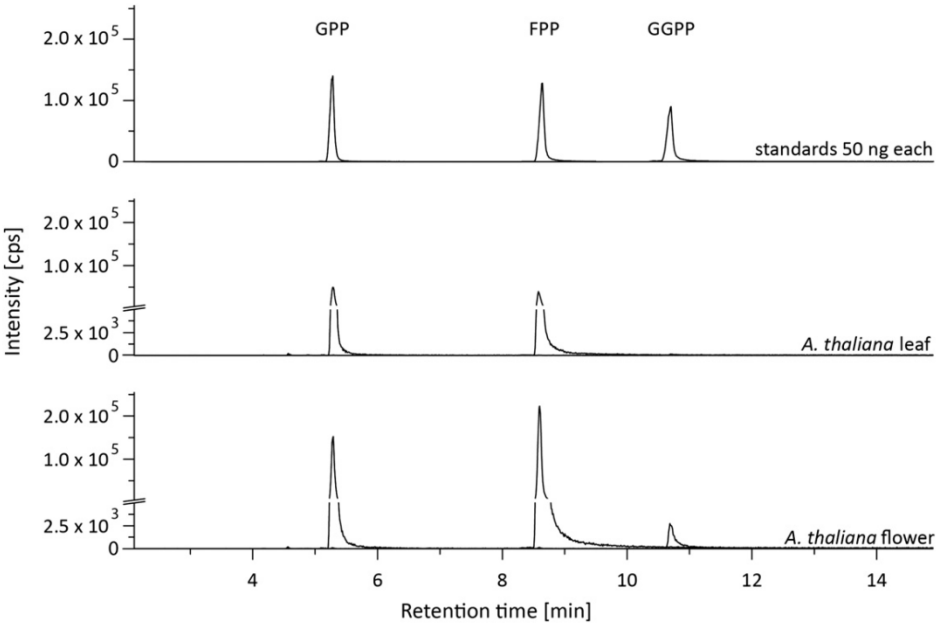

Fig.3. LC–MS/MS analysis of the products of IDS enzyme assays performed with crude protein extracts of *A. thaliana* leaves (middle panel) or flowers (lower panel). Products were identified by comparison with standards of 50 ng each of GPP, (*E,E*)-FPP, and (*E,E,E*)-GGPP (top panel). At least four different biological and two technical replicates of each sample were analyzed, and the standard deviations were below 6% for GPP and FPP and below 10% for GGPP.

Table 1
IDS activity determined in various plant species and organs.

Species	Organ	Activity (pmol h^{-1} µg total $protein^{-1}$)					
		GPP		FPP		GGPP	
		Mean	SD	Mean	SD	Mean	SD
Arabidopsis thaliana	Leaf	3.55	0.07	4.62	0.22	Traces	
Arabidopsis thaliana	Flower	6.00	0.19	19.86	0.82	0.47	0.04
Populus trichocarpa	Leaf	2.75	0.15	9.94	0.58	0.94	0.02
Nicotiana attenuata	Leaf	2.19	0.08	4.05	0.11	Traces	
Picea abies	Needle	5.47	0.14	3.73	0.06	1.50	0.12
Picea abies	Bark	28.93	0.28	26.72	0.31	6.81	0.53

Note. SD, standard deviation.

terpenes and IDS activity might be higher in flowers. Using our methods, IDS activity was detectable for GPP, (*E,E*)-FPP, and (*E,E,E*)-GGPP in both organs. Flower extracts showed 4.3- and 1.6-fold higher levels of (*E,E*)-FPP and GPP formation, respectively, than those found in leaf extracts. (*E,E,E*)-GGPP was also easily detectable in assays of flower extracts, but only traces were found in assays of leaves (Fig. 3 and Table 1). The rate of (*E,E*)-FPP production determined for *A. thaliana* leaf extracts (4.62 pmol h^{-1} µg total $protein^{-1}$) is very similar to the rate of IDS activity previously found for these extracts by Manzano and coworkers (~6 pmol h^{-1} µg total $protein^{-1}$) [4], but these authors measured enzyme activity by scintillation counting and so did not separate and identify the actual assay products. Control assays using boiled protein extracts or without any addition of the substrates showed no detectable products (data not shown).

To demonstrate that the method is not only useful for *A. thaliana*, the same protocol was used to assay IDS activity in extracts of other herbaceous and woody plant species, including both angiosperms and gymnosperms. Tissues investigated were leaves from a wild tobacco species (*N. attenuata*) and the black cottonwood (*P. trichocarpa*) as well as needles and bark of Norway spruce (*P. abies*) (Table 1). IDS activity was found for all samples. The bark of *P. abies* showed the highest activity for formation of GPP and (*E,E*)-FPP (28.9 and 26.7 pmol h^{-1} µg total $protein^{-1}$, respectively), whereas much lower rates were found for (*E,E,E*)-GGPP (6.8 pmol h^{-1} µg total $protein^{-1}$). The measured IDS activities in *P. abies* described by Martin and coworkers [5] were comparable at approximately 15, 10, and 13 pmol h^{-1} µg total $protein^{-1}$ for GPP, (*E,E*)-FPP, and (*E,E,E*)-GGPP, respectively, although these authors used a different plant genotype and radio-GC for product detection. The much higher amounts of IDS activity compared with *A. thaliana* can be attributed to the storage of substantial amounts of monoterpene and diterpene products in the bark of *P. abies* as resin [5,22,23], a phenomenon not found in *A. thaliana*. In *N. attenuata*, the highest IDS activity was measured for GPP and (*E,E*)-FPP formation (2 and 4 pmol h^{-1} µg total $protein^{-1}$, respectively), whereas only traces were detected for (*E,E,E*)-GGPP, confirming the radio-GC-measured pattern found by Jassbi and coworkers that also gave the highest levels for FPP formation [24]. In *P. trichocarpa*, IDS activity levels were 3, 10, and 1 pmol h^{-1} µg total $protein^{-1}$ [for GPP, (*E,E*)-FPP,

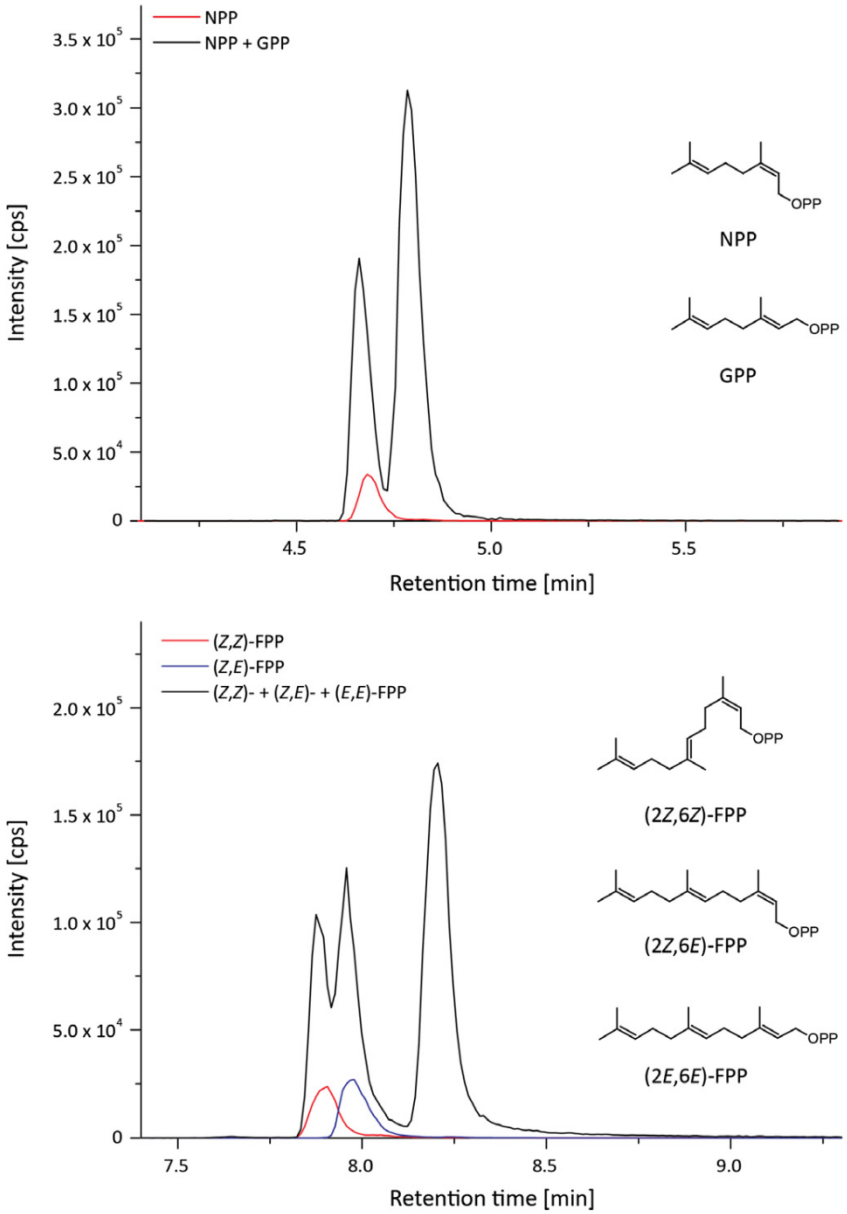

Fig.4. LC–MS/MS separation of short-chain *cisoid* and *transoid* prenyl diphosphate isomers. Separation among the C_{10} compounds, neryl diphosphate and geranyl diphosphate (top panel), and the C_{15} compounds, (*Z*,*Z*)-, (*Z*,*E*)- and (*E*,*E*)-farnesyl diphosphate (lower panel), are depicted. Chromatograms were obtained by coinjection of all isomers together or by individual injection of the *cisoid* isomers.

and (*E*,*E*,*E*)-GGPP, respectively] below the levels found in spruce but above tobacco. To our knowledge, this is the first time IDS has been measured in any poplar species. Although the emission rate of different terpene classes is known for poplar, these data cannot be compared with IDS enzyme activity due to different sampling techniques and variable measurement units [25,26].

The same protocol for measuring IDS activity was also successfully used for functional characterization of putative plant GPP, (*E*,*E*)-FPP, and (*E*,*E*,*E*)-GGPP synthases after heterologous expression in *E. coli* (data not shown). Although the C_{10}, C_{15}, and C_{20} prenyl diphosphate products formed in these assays all were readily quantified, the C_5 substrates, IPP and DMAPP, eluted in a region of the chromatogram where ion suppression by buffer components prevented precise quantification. This limits the method to detection of C_{10}, C_{15}, and C_{20} prenyl diphosphates and excludes the C_5 prenyl diphosphates.

Given the recent discoveries of *cisoid* IDS products in plants, a new IDS assay will not gain wide acceptance unless it is able to distinguish between *cisoid* and *transoid* isomers among the various size classes of prenyl diphosphates. Under the measurement

conditions used, injections of mixtures of NPP and GPP as well as (*Z*,*E*)-, (*Z*,*Z*)-, and (*E*,*E*)-FPP in combination showed a clear, albeit not baseline, separation of these isomers (Fig. 4). Modifications, including smaller injection volumes, altered buffer composition, and a less steep solvent gradient did not improve separation of (*Z*,*Z*)- and (*Z*,*E*)-FPP. Nevertheless, the method can be effectively used to differentiate among the possible C_{10} and C_{15} prenyl diphosphate isomers occurring as IDS products.

Researchers of plant terpenoid metabolism have begun to devote increased attention to IDS enzymes because of their role in directing and modulating flux among the various branches of terpenoid biosynthesis. Our new, nonradioactive, LC–MS-based method of measuring IDS activity obviates the need for dephosphorylation of the assay products prior to analysis and, thus, should increase the speed, precision, and reliability of activity measurements without sacrificing the sensitivity of radio-GC detection. LC–MS detection of prenyl diphosphates could also be valuable in quantifying these biosynthetic intermediates *in vivo* to determine how flux is regulated among the different branches of terpene biosynthesis.

Acknowledgments

We thank Tobias Köllner for (*Z*,*E*)-FPP, Michael Reichelt and Louwrance Wright for useful discussions and advice, Antje Burse and Meredith Schuman for *Populus trichocarpa* and *Nicotiana attenuata* plants, Marion Stäger for technical assistance, and the Max Planck Society for financial support.

Appendix A. Supplementary material

Supplementary data associated with this article can be found, in the online version, at doi:10.1016/j.ab.2011.12.037.

References

[1] J. Bohlmann, C.I. Keeling, Terpenoid biomaterials, Plant J. 54 (2008) 656–669.
[2] D. Arigoni, S. Sagner, C. Latzel, W. Eisenreich, A. Bacher, M.H. Zenk, Terpenoid biosynthesis from 1-deoxy-D-xylulose in higher plants by intramolecular skeletal rearrangement, Proc. Natl. Acad. Sci. USA 94 (1997) 10600–10605.
[3] M. Rodríguez-Concepción, Early steps in isoprenoid biosynthesis: Multilevel regulation of the supply of common precursors in plant cells, Phytochem. Rev. 5 (2006) 1–15.
[4] D. Manzano, A. Busquets, M. Closa, K. Hoyerová, H. Schaller, M. Kamínek, M. Arró, A. Ferrer, Overexpression of farnesyl diphosphate synthase in *Arabidopsis* mitochondria triggers light-dependent lesion formation and alters cytokinin homeostasis, Plant Mol. Biol. 61 (2006) 195–213.
[5] D. Martin, D. Tholl, J. Gershenzon, J. Bohlmann, Methyl jasmonate induces traumatic resin ducts, terpenoid resin biosynthesis, and terpenoid accumulation in developing xylem of Norway spruce stems, Plant Physiol. 129 (2002) 1003–1018.
[6] O. Kim, K. Bang, S. Jung, Y. Kim, D. Hyun, S. Kim, S. Cha, Molecular characterization of ginseng farnesyl diphosphate synthase gene and its up-regulation by methyl jasmonate, Biol. Plant. 54 (2010) 47–53.
[7] A. Masferrer, M. Arró, D. Manzano, H. Schaller, X. Fernández-Busquets, P. Moncaleán, B. Fernández, N. Cunillera, A. Boronat, A. Ferrer, Overexpression of *Arabidopsis thaliana* farnesyl diphosphate synthase (FPS1S) in transgenic *Arabidopsis* induces a cell death/senescence-like response and reduced cytokinin levels, Plant J. 30 (2002) 123–132.
[8] A. Schmidt, J. Gershenzon, Cloning and characterization of isoprenyl diphosphate synthases with farnesyl diphosphate and geranylgeranyl diphosphate synthase activity from Norway spruce (*Picea abies*) and their relation to induced oleoresin formation, Phytochemistry 68 (2007) 2649–2659.
[9] A. Schmidt, B. Wächtler, U. Temp, T. Krekling, A. Seguin, J. Gershenzon, A bifunctional geranyl and geranylgeranyl diphosphate synthase is involved in terpene oleoresin formation in *Picea abies*, Plant Physiol. 152 (2010) 639–655.
[10] T.-H. Chang, F.-L. Hsieh, T.-P. Ko, K.-H. Teng, P.-H. Liang, A.H.-J. Wang, Structure of a heterotetrameric geranyl pyrophosphate synthase from mint (Mentha piperita) reveals intersubunit regulation, Plant Cell 22 (2010) 454–467.
[11] A.B. Gilg, J.C. Bearfield, C. Tittiger, W.H. Welch, G.J. Blomquist, Isolation and functional expression of an animal geranyl diphosphate synthase and its role in bark beetle pheromone biosynthesis, Proc. Natl. Acad. Sci. USA 102 (2005) 9760–9765.
[12] N. Cunillera, M. Arró, D. Delourme, F. Karst, A. Boronat, A. Ferrer, *Arabidopsis thaliana* contains two differentially expressed farnesyl-diphosphate synthase genes, J. Biol. Chem. 271 (1996) 7774–7780.
[13] D.L. Zhang, C.D. Poulter, Analysis and purification of phosphorylated isoprenoids by reversed-phase HPLC, Anal. Biochem. 213 (1993) 356–361.
[14] A. Schmidt, J. Gershenzon, Cloning and characterization of two different types of geranyl diphosphate synthases from Norway spruce (*Picea abies*), Phytochemistry 69 (2008) 49–57.
[15] A.L. Schilmiller, I. Schauvinhold, M. Larson, R. Xu, A.L. Charbonneau, A. Schmidt, C. Wilkerson, R.L. Last, E. Pichersky, Monoterpenes in the glandular trichomes of tomato are synthesized from a neryl diphosphate precursor rather than geranyl diphosphate, Proc. Natl. Acad. Sci. USA 106 (2009) 10865–10870.
[16] T. Kurokawa, K. Ogura, S. Seto, Formation of polyprenyl phosphates by a cell-free enzyme of *Micrococcus lysodeikticus*, Biochem. Biophys. Res. Commun. 45 (1971) 251–257.
[17] C. Sallaud, D. Rontein, S. Onillon, F. Jabès, P. Duffé, C. Giacalone, S. Thoraval, C. Escoffier, G. Herbette, N. Leonhardt, M. Causse, A. Tissier, A novel pathway for sesquiterpene biosynthesis from *Z,Z*-farnesyl pyrophosphate in the wild tomato *Solanum habrochaites*, Plant Cell 21 (2009) 301–317.
[18] J. Bohlmann, J. Gershenzon, Old substrates for new enzymes of terpenoid biosynthesis, Proc. Natl. Acad. Sci. USA 106 (2009) 10402–10403.
[19] I.T. Baldwin, L. Staszak-Kozinski, R. Davidson, Up in smoke: I. Smoke-derived germination cues for postfire annual *Nicotiana attenuata* Torr. Ex. Watson, J. Chem. Ecol. 20 (1994) 2345–2371.
[20] S. Miriyala, T. Subramanian, M. Panchatcharam, H. Ren, M.I. McDermott, M. Sunkara, T. Drennan, S.S. Smyth, H.P. Spielmann, A.J. Morris, Functional characterization of the atypical integral membrane lipid phosphatase PDP1/PPAPDC2 identifies a pathway for interconversion of isoprenols and isoprenoid phosphates in mammalian cells, J. Biol. Chem. 285 (2010) 13918–13929.
[21] J. Rohloff, A.M. Bones, Volatile profiling of *Arabidopsis thaliana:* Putative olfactory compounds in plant communication, Phytochemistry 66 (2005) 1941–1955.
[22] V.R. Franceschi, P. Krokene, E. Christiansen, T. Krekling, Anatomical and chemical defenses of conifer bark against bark beetles and other pests, New Phytologist 167 (2005) 353–376.
[23] A. Schmidt, R. Nagel, T. Krekling, E. Christiansen, J. Gershenzon, P. Krokene, Induction of isoprenyl diphosphate synthases, plant hormones, and defense signalling genes correlates with traumatic resin duct formation in Norway spruce (*Picea abies*), Plant Mol. Biol. 77 (2011) 577–590.
[24] A.R. Jassbi, K. Gase, C. Hettenhausen, A. Schmidt, I.T. Baldwin, Silencing geranylgeranyl diphosphate synthase in *Nicotiana attenuata* dramatically impairs resistance to tobacco hornworm, Plant Physiol. 146 (2008) 974–986.
[25] H. Danner, G.A. Böckler, S. Irmisch, J.S. Yuan, F. Chen, J. Gershenzon, S.B. Unsicker, T.G. Köllner, Four terpene synthases produce major compounds of the gypsy moth feeding-induced volatile blend of *Populus trichocarpa*, Phytochemistry 72 (2011) 897–908.
[26] A. Kessler, I.T. Baldwin, Defensive function of herbivore-induced plant volatile emissions in nature, Science 291 (2001) 2141–2144.

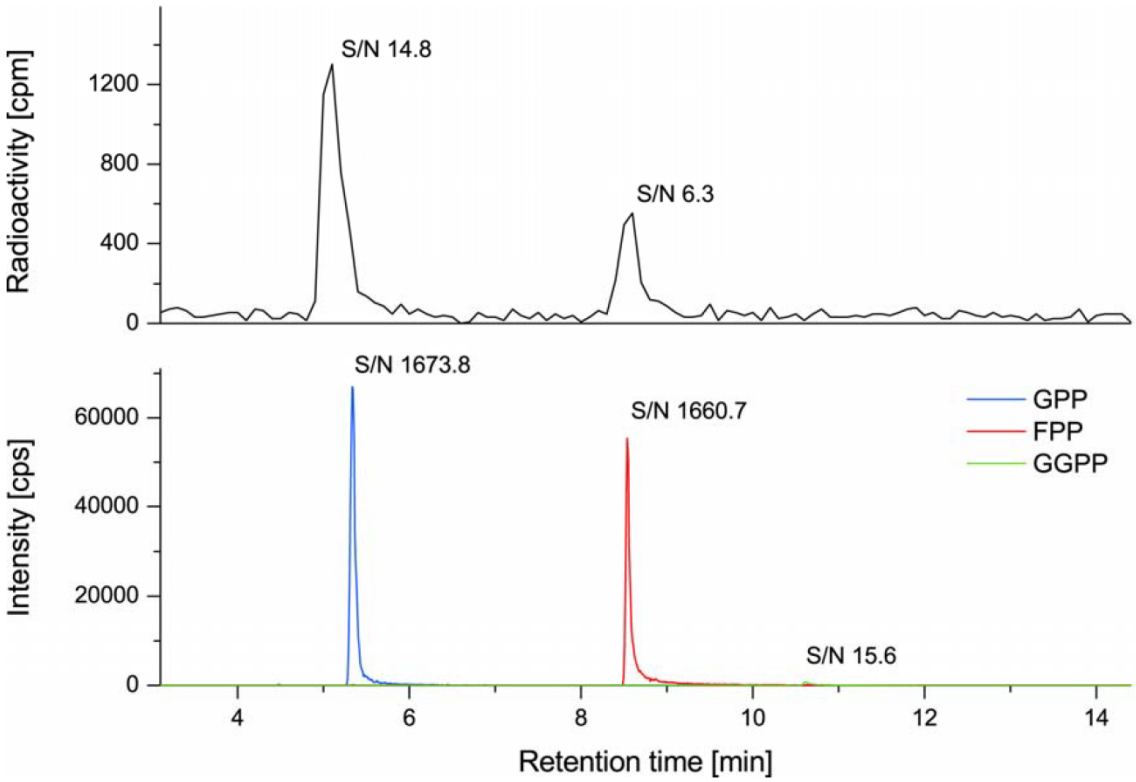

Supplemental Figure 1: Comparison of an IDS assay using the LC-MS/MS detection method described (bottom panel) with the same assay using radio-HPLC for product detection (top panel). Both methods used the same extract, assay conditions and HPLC separation scheme, but the radio-HPLC assay used [1-^{14}C]IPP instead of unlabeled IPP as substrate. To compare sensitivity, the calculated signal to noise ratio (S/N) is given for observed peaks.

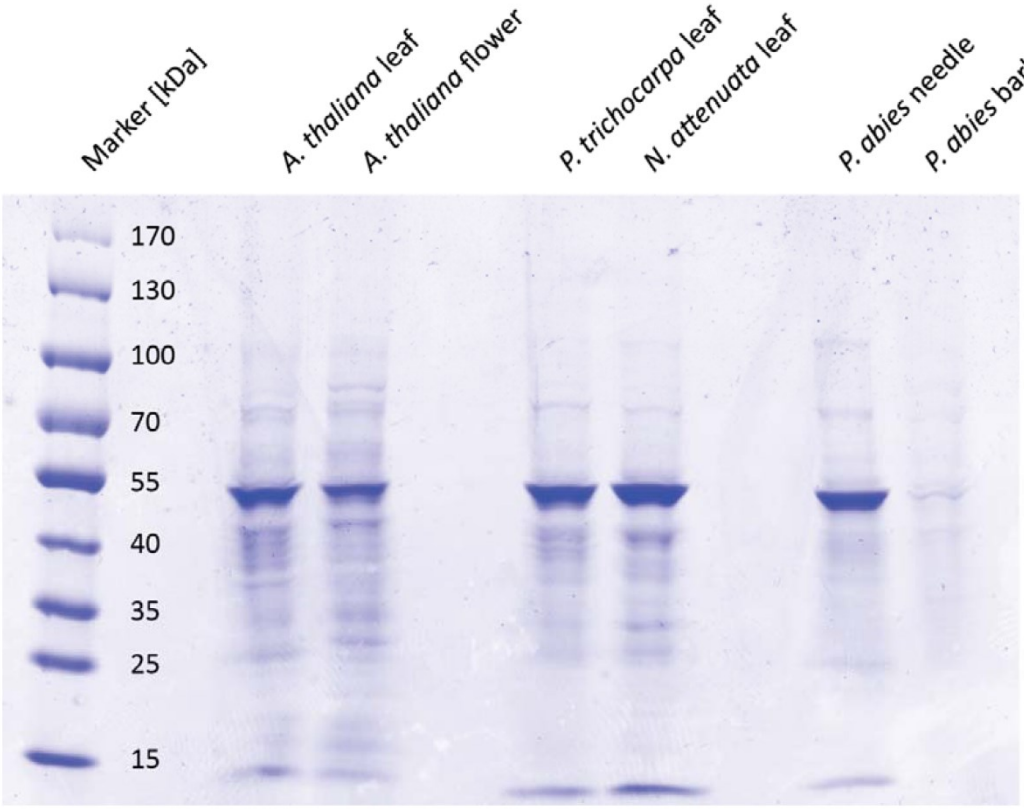

Supplemental Figure 2: Coomassie stained SDS-PAGE showing the crude plant protein extracts used for IDS assays. For leaf and needle extracts, 8 µg of total crude protein were used per assay, while for bark 2.5 µg of crude protein were used.

Supplemental Table 1: Detailed mass spectrometer settings for quantification of principal IDS assay products

compound	parent ion	product ion	DP [V]	EP [V]	CEP [V]	CE [V]	CXP [V]
GPP	312.9	79	-40	-6	-18	-38	0
FPP	380.9	79	-40	-3	-28	-42	0
GGPP	449	79	-45	-10	-22	-50	0

Abbreviations: DP, declustering potential; EP, entrance potential; CEP collision cell entrance potential; CE, collision energy; CXP, collision cell exit potential

3.2 Manuscript 2

Overexpression of an isoprenyl diphosphate synthase in spruce leads to unexpected terpene diversion products that function in plant defense

Overexpression of an Isoprenyl Diphosphate Synthase in Spruce Leads to Unexpected Terpene Diversion Products That Function in Plant Defense[1][W][OPEN]

Raimund Nagel, Aileen Berasategui, Christian Paetz, Jonathan Gershenzon*, and Axel Schmidt

Departments of Biochemistry (R.N., A.B., J.G., A.S.), Insect Symbiosis (A.B.), and Biosynthesis/Nuclear Magnetic Resonance (C.P.), Max Planck Institute for Chemical Ecology, Beutenberg Campus, D–07745 Jena, Germany

Spruce (*Picea* spp.) and other conifers employ terpenoid-based oleoresin as part of their defense against herbivores and pathogens. The short-chain isoprenyl diphosphate synthases (IDS) are situated at critical branch points in terpene biosynthesis, producing the precursors of the different terpenoid classes. To determine the role of IDS and to create altered terpene phenotypes for assessing the defensive role of terpenoids, we overexpressed a bifunctional spruce IDS, a geranyl diphosphate and geranylgeranyl diphosphate synthase in white spruce (*Picea glauca*) saplings. While transcript level (350-fold), enzyme activity level (7-fold), and in planta geranyl diphosphate and geranylgeranyl diphosphate levels (4- to 8-fold) were significantly increased in the needles of transgenic plants, there was no increase in the major monoterpenes and diterpene acids of the resin and no change in primary isoprenoids, such as sterols, chlorophylls, and carotenoids. Instead, large amounts of geranylgeranyl fatty acid esters, known from various gymnosperm and angiosperm plant species, accumulated in needles and were shown to act defensively in reducing the performance of larvae of the nun moth (*Lymantria monacha*), a conifer pest in Eurasia. These results show the impact of overexpression of an IDS and the defensive role of an unexpected accumulation product of terpenoid biosynthesis with the potential for a broader function in plant protection.

Terpenes are a structurally very diverse class of metabolites (Köksal et al., 2011) that have major roles in primary and secondary metabolism (Buchanan et al., 2000; Gershenzon and Dudareva, 2007). The basic pathways of terpene biosynthesis have been well studied. Two separate pathways, the mevalonate (MVA) pathway in the cytosol and peroxisomes and the methylerythritol phosphate (MEP) pathway in plastids, produce the universal C_5 precursors for terpene biosynthesis, dimethylallyl diphosphate (DMADP) and isopentenyl diphosphate (IDP). Next, sequential condensations of DMADP with one to three molecules of IDP yield the elongated C_{10}, C_{15}, and C_{20} intermediates, geranyl diphosphate (GDP), farnesyl diphosphate (FDP), and geranylgeranyl diphosphate (GGDP), respectively (Arigoni et al., 1997; Rodríguez-Concepción, 2006; Hemmerlin et al., 2012).

The enzymes catalyzing these condensation reactions are designated short-chain isoprenyl diphosphate synthases (IDS) and belong to the large family of prenyltransferases (Wang and Ohnuma, 2000; Liang et al., 2002; Fig. 1). The enzymes are named after their main products as GDP synthase, FDP synthase, and GGDP synthase and usually belong to the group of trans-IDS enzymes based on the stereochemistry of the double bond of the reaction product (Kharel and Koyama, 2003; Liang, 2009), although short chain cis-IDS enzymes are known (Sallaud et al., 2009; Schilmiller et al., 2009; Akhtar et al., 2013) The short-chain prenyl diphosphates produced are the substrates for terpene synthases (Chen et al., 2011) that form the huge variety of terpene skeletons, which in turn may be further modified, such as by cytochrome P450 oxidoreductases (Bohlmann and Keeling, 2008) or other oxidative, reductive, and conjugation processes. Thus, the IDS enzymes function at an important branch point in terpene biosynthesis where the pathway splits into routes to the major classes, such as monoterpenes (C_{10}), sesquiterpenes (C_{15}), diterpenes (C_{20}), triterpenes (C_{30}), and tetraterpenes (C_{40}). However, little is known about how IDS control flux into the different branches. A few recent publications have addressed the importance of FDP synthases (Chen et al., 2000; Masferrer et al., 2002; Manzano et al., 2004, 2006; Han et al., 2006; Banyai et al., 2010; Closa et al., 2010; Keim et al., 2012), but only one focuses on a GDP synthase (Lange et al., 2011) and one on a GGDP synthase (Kai et al., 2011).

Among the best known terpenes functioning in antiherbivore defense are the oleoresin components of

[1] This work was supported by the Max Planck Society and the Zwillenberg-Tietz Foundation.

* Address correspondence to gershenzon@ice.mpg.de.

The author responsible for distribution of materials integral to the findings presented in this article in accordance with the policy described in the Instructions for Authors (www.plantphysiol.org) is: Jonathan Gershenzon (gershenzon@ice.mpg.de)

[W] The online version of this article contains Web-only data.

[OPEN] Articles can be viewed online without a subscription.

www.plantphysiol.org/cgi/doi/10.1104/pp.113.228940

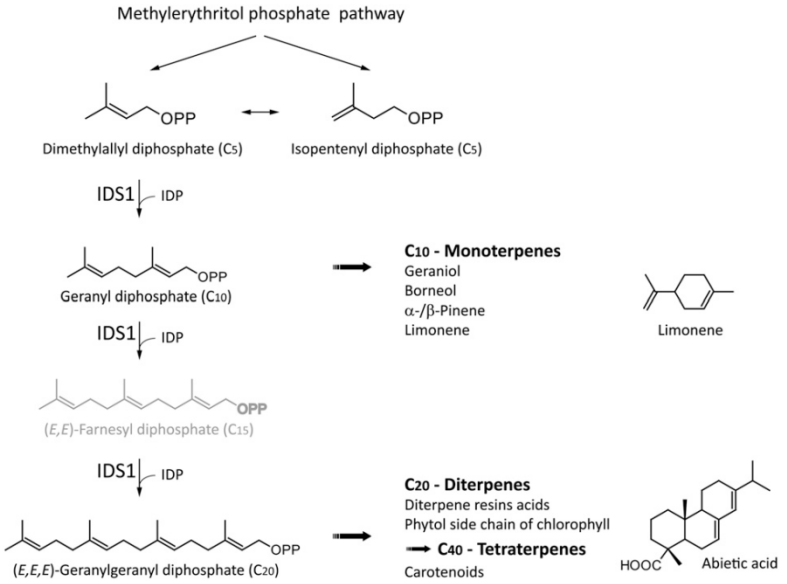

Figure 1. Outline of terpenoid biosynthesis. The schematic diagram depicts the reactions carried out by short-chain IDS1 from *P. abies*. The five-carbon building blocks IDP and DMADP, produced by the plastidial MEP pathway, are the substrates for IDS1. Sequential condensations of DMADP with one to three molecules of IDP mediated by IDS form GDP, FDP, or GGDP. The different prenyl diphosphates are then converted into representatives of the different terpene classes: GDP to monoterpenes and GGDP to diterpenes and tetraterpenes. FDP is produced by IDS1 as an intermediate but is not released. OPP, diphosphate moiety.

conifers such as spruce (*Picea* spp.) that are stored in specialized resin ducts and deter insects such as bark beetles and their associated fungi (Erbilgin et al., 2006; Keeling and Bohlmann, 2006a, 2006b; Zhao et al., 2011; Schiebe et al., 2012). The oleoresin is composed mainly of monoterpenes (C_{10}) and diterpene acids (C_{20}), with very minor amounts of sesquiterpenes (Martin et al., 2002). This composition is congruent with the product profile of an unusual short-chain IDS of *Picea abies* (PaIDS1) that produces both GDP (C_{10}) and GGDP (C_{20}). When bark beetle attack is simulated by methyl jasmonate application to the bark, the expression of the *IDS1* gene is increased and the translated IDS1 protein can be found in cambial cells lining the newly formed traumatic resin ducts that fill them with terpenes (Schmidt et al., 2010, 2011). In contrast to bark, less is known about the regulation of terpenoid biosynthesis and defenses in spruce needles. Treatment with methyl jasmonate increases the amount of stored and emitted needle terpenes (Martin et al., 2003), and feeding of the spruce budworm, *Choristoneura occidentalis*, induced transcript accumulation of an IDS, coding for an enzyme putatively producing GDP or GGDP (Ralph et al., 2006). Similar to the devastating effects of the spruce budworm in North America, the nun moth (*Lymantria monacha*) of Eurasia is also a damaging pest of spruce foliage (Wellenstein, 1942; Klimetzek and Vite, 1989; Keena et al., 2010). The introduction of the nun moth to North America from imported Eurasian timber poses a threat for native North American spruce, since survival and development are possible on species such as *Picea glauca* (Keena, 2003). This suggests that North American spruce should be tested for defenses against the nun moth. Testing herbivores on conifer lines from a common genetic background in which terpene resin formation has been genetically manipulated should be a good approach to investigating the defensive role of these compounds.

In this investigation, we overexpressed *IDS1* in spruce saplings to study its role in terpenoid formation and to generate altered terpene phenotypes.

RESULTS

Characterization of Transgenic *IDS1*-Overexpressing Lines

To learn more about the potential of IDS to regulate the direction and flux through terpene biosynthesis, transgenic *P. glauca* lines were created overexpressing a *P. abies* IDS gene (*PaIDS1*) whose encoded protein produces GDP and GGDP. The protein sequence is more than 99% identical to that of the *P. glauca* IDS1 (PgIDS1; Supplemental Fig. S1) that was deposited in GenBank under accession number KF840686. Transgenic 2-year-old saplings were characterized from three independent *IDS1*-overexpressing lines and three independent lines transformed with an empty vector. *IDS1*-overexpressing saplings had 500-fold higher *IDS1* transcript abundance in needles compared with the empty vector control saplings, but there were no *IDS1* transcript differences in bark. At the metabolite level, no significant differences were observed between *IDS1*-overexpressing lines and controls in monoterpenes, sesquiterpenes, diterpene resin acids, sterols, carotenoids, and chlorophylls (Supplemental Fig. S2).

Overexpression of *IDS1* in Needles Increases *IDS1* Transcript, IDS1 Protein, IDS1 Enzyme Activity, and Isoprenyl Diphosphate Intermediate Levels in Vivo, But There Was No Change in Monoterpene and Diterpene Resin Acid Contents

A single *IDS1*-overexpressing line (line 3) and a single empty vector control line (line 1), both 3 years old, were selected for detailed characterization to compare tissue from different growing seasons as well as different genetic backgrounds. There were no noticeable morphological differences between the two lines. The size, the number of side branches, and the coloration of the needles were all similar (Supplemental Fig. S3). After the spring flush of growth, bark and needles were harvested from both lines and divided by age. Most needles of the first year growth had already abscised. In needles, *IDS1*-overexpressing saplings had 300- to 700-fold higher *IDS1* transcript levels than the vector control saplings, with third year needles of the overexpressing line having a 2.3-fold higher abundance of *IDS1* transcript than the second year needles (Fig. 2B). The IDS1 protein was also much more abundant in needles of the *IDS1*-overxpressing saplings than the controls, as shown by western blots probed with specific antibodies for IDS1 (Fig. 2D). Total IDS enzyme activity as measured by in vitro assay increased substantially for GDP (C_{10}) when comparing the needles of the *IDS1*-overexpressing versus empty vector control lines, about 7-fold (from 8 to 57 pmol h^{-1} μg^{-1} total protein) for second year needles and 17-fold (from 5 to 84 pmol h^{-1} μg^{-1} total protein) for third year needles. However, FDP (C_{15}) production decreased 23-fold in *IDS1*-overexpressing lines (from 7 to 0.3 pmol h^{-1} μg^{-1} total protein) for second year needles and 10-fold (from 3 to 0.3 pmol h^{-1} μg^{-1} total protein) for third year needles compared with controls. On the other hand, GGDP (C_{20}) was only produced

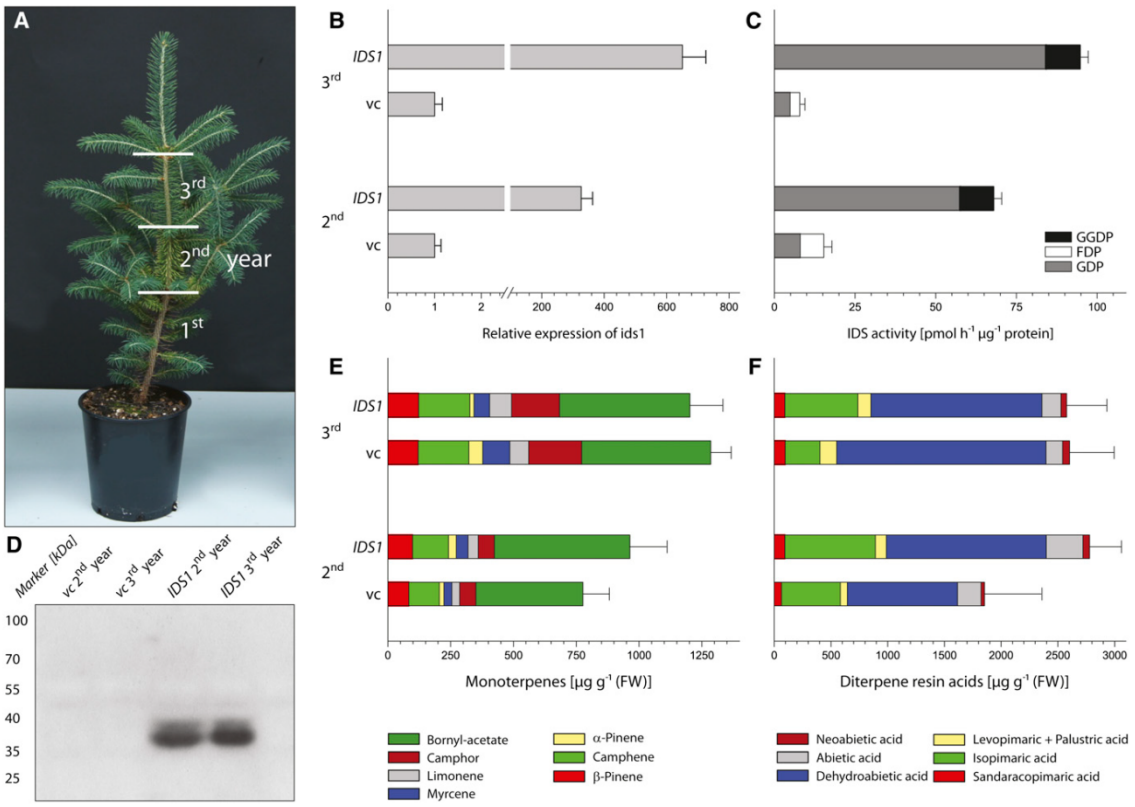

Figure 2. Detailed characterization of needles from 3-year-old *P. glauca IDS1* in comparison with an empty vector control (vc) with respect to second- and third-year growth. A, Photograph of a sapling showing areas of first-, second-, and third-year growth on the main stem. Second- and third-year needles were sampled; first-year needles had abscised. B, Relative expression of *IDS1* as determined by quantitative PCR. C, Total IDS enzyme activity measured in vitro forming GDP (C_{10}), FDP (C_{15}), and GGDP (C_{20}) as determined by LC-MS/MS. D, IDS1 protein abundance measured with a specific antibody by western-blot analysis. E and F, Monoterpene (E) and diterpene resin acid (F) contents as quantified with GC-FID. Data are means ± SD of measurements from five plants of each line. FW, Fresh weight.

in enzyme assays of *IDS1*-overexpressing saplings, with values of 10 pmol h^{-1} μg^{-1} total protein in second and third year needles (Fig. 2C). Despite the increased enzyme activity, individual and total amounts of monoterpenes (0.8–1.3 μg mg^{-1} fresh weight) and diterpene resin acids (1.9–2.7 μg mg^{-1} fresh weight) were not significantly changed in *IDS1*-overexpressing saplings versus empty vector controls; sesquiterpenes were only detected in traces and, therefore, were not quantified (Fig. 2, E and F).

Overexpression of *IDS1* Increases the in Vivo Levels of Prenyl Diphosphate Intermediates

The substantial increases in *IDS1* transcript, IDS1 protein, and in vitro IDS1 enzyme activity upon overexpression in needles were inconsistent with the lack of change in terpene content. To try to reconcile this discrepancy, we also measured the amounts of GDP, FDP, and GGDP as intermediates in planta using a liquid chromatography (LC)-tandem mass spectrometry (MS/MS) method. Since large amounts of plant material were needed for this analysis, we used side branch needles not separated by age instead of stem needles. Needles of side branches have a comparable level of transcript elevation and IDS1 enzyme activity to the stem needles (Supplemental Fig. S4). In needles of *IDS1*-overexpressing saplings, GDP was increased from 0.07 to 0.56 nmol g^{-1} fresh weight (8-fold) compared with vector controls, and GGDP was increased from 1.23 to 5.45 nmol g^{-1} fresh weight (4.5-fold). However, FDP levels (0.07 nmol g^{-1} fresh weight) were not changed (Fig. 3).

Overexpression of *IDS1* Had No Major Effects on Bark Tissue

In bark tissue, *IDS1* transcripts were unchanged or had 2 to 3 times higher levels in *IDS1*-overexpressing saplings than controls for the first, second, and third years of growth (Fig. 4A). These increases were much less than those observed in *IDS1*-overexpressing needles, and there was no significant change in total IDS1 enzyme activity when comparing *IDS1*-overexpressing saplings and vector controls in the bark of different years of growth (GDP as product, 40 pmol h^{-1} μg^{-1} total protein; FDP, 5 pmol h^{-1} μg^{-1} total protein; GGDP, 6 pmol h^{-1} μg^{-1} total protein). Moreover, the levels of most prenyl diphosphates in vivo in bark were not significantly altered by *IDS1* overexpression. The amounts of GDP (0.1 nmol g^{-1} fresh weight) and FDP (0.16 nmol g^{-1} fresh weight) did not differ between *IDS1*-overexpressing saplings and vector controls independent of the age. GGDP levels increased 1.6- and 1.9-fold with *IDS1* overexpression for the first and second year growth, respectively, but these increases were much less than in the needles (Fig. 3). As for the needles, no significant differences in monoterpene (4.5–7.5 mg g^{-1} fresh weight), sesquiterpene (75–185 μg g^{-1} fresh weight), and diterpene resin acid (8.5–12.5 mg g^{-1} fresh weight) amounts were observed between *IDS1* overexpression and control lines (Fig. 4, B–F; Supplemental Fig. S5).

Overexpression of *IDS1* Did Not Affect Terpenoids of Primary Metabolism

The effects of *IDS1* overexpression were also investigated on selected terpenes of primary metabolism, such as sterols, carotenoids, and chlorophylls. For carotenoids and chlorophylls, the first and second years of growth were used, and for sterol analysis, the third year of growth was used. Relative amounts of all three metabolites did not change between vector control and *IDS1*-overexpressing saplings in either the bark or the needles (Fig. 5).

Overexpression of *IDS1* Leads to the Accumulation of Geranylgeranyl Fatty Acid Esters

Instead of increasing the content of monoterpenes and diterpene resin acids, *IDS1* overexpression in *P. glauca* was found to dramatically increase the amounts of esters of geranylgeraniol with fatty acids in comparison with empty vector controls. Palmitic acid (C16:0), anteiso-heptadecanoic acid (14-methylhexadecanoic acid [aiC17:0]), linoleic acid (C18:2), oleic acid (C18:1), and stearic acid (C18:0) were identified as the major components of the acid moieties of the esters (Fig. 6). The occurrence of these esters was initially indicated by the presence of geranylgeraniol in saponified needle extracts of *IDS1*-overexpressing saplings prepared for sterol quantification. This compound was not found in saponified needle extracts of vector control saplings (Supplemental Fig. S6) or after alkaline phosphatase treatment (Supplemental Fig. S7). In addition, high amounts of fatty acids were detected in *IDS1*-overexpressing saplings during a diterpenoid extraction procedure that included methylation with the reagent trimethylsulfonium hydroxide (TMSH), which catalyzes transesterifications (Butte, 1983), but not after treatment with diazomethane, which methylates only free acids (Christie, 2010). Mass spectrometry (MS) and NMR measurements in comparison with those of synthesized standards of geranylgeranyl heptadecanoate and geranylgeranyl octadecanoate confirmed the presence of these and related geranylgeranyl fatty acid esters (Fig. 6B; Supplemental Fig. S8). Final confirmation of the structure of the fatty acid moiety required purification of the geranylgeranyl esters followed by transesterification with TMSH to form fatty acid methyl esters, which were compared with commercially available fatty acid methyl ester standards.

The geranylgeranyl fatty acid esters were major constituents of needles of *IDS1*-overexpressing saplings,

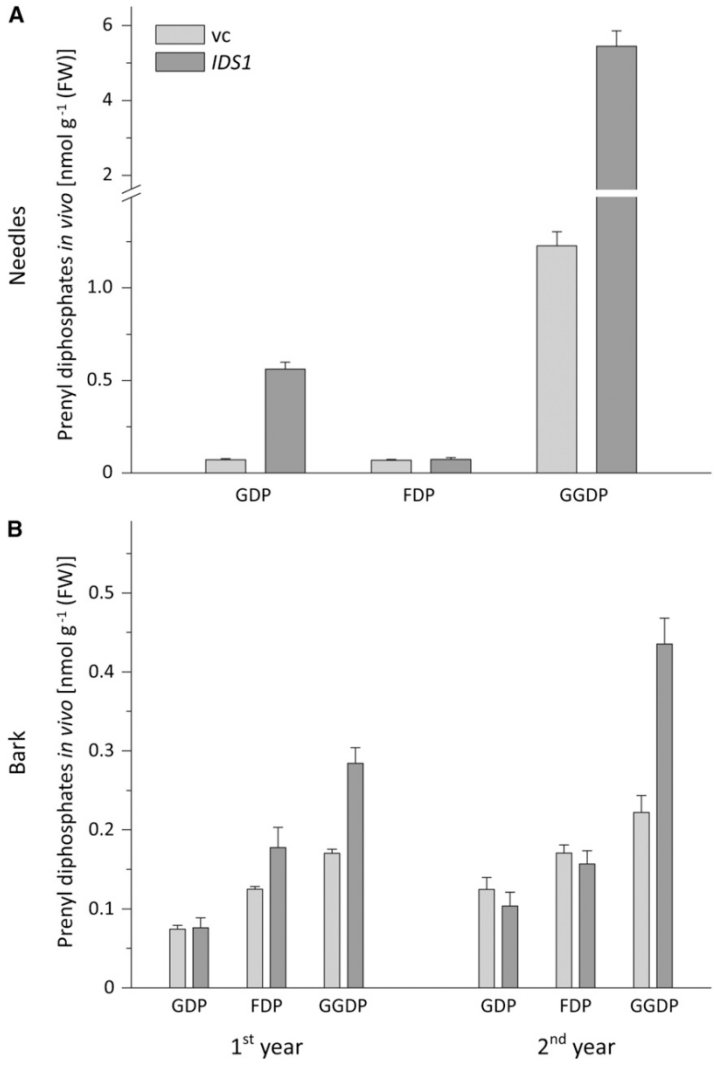

Figure 3. Quantification of in vivo levels of the isoprenoid pathway intermediates GDP, FDP, and GGDP in tissues of *P. glauca IDS1* and an empty vector control line (vc). Measurements were performed on needles (A) and bark (B) by LC-MS/MS. Data are means ± SD of measurements from five plants of each line. FW, Fresh weight.

with 12.2 mg g^{-1} in the second year of growth, 7.76 mg g^{-1} in the third year of growth, and 6.19 mg g^{-1} in needles from side branches not subdivided according to their age. Their composition was dominated by esters with either C18:1 or C18:2 and C16:0 and lesser amounts of esters with aiC17:0 and C18:0 (Table I). In bark of *IDS1*-overexpressing saplings or in bark and needles of empty vector control saplings, these esters were not detectable in amounts greater than 0.5 $\mu g\ g^{-1}$ (Table I; Supplemental Fig. S9). To determine if the accumulation of these prenyl esters is solely a consequence of transformation in the genetic background of *P. glauca*, *IDS1*-overexpressing saplings of *P. abies* were also produced. Needles of 1-year-old *P. abies* saplings had a total amount of geranylgeranyl esters of 8.35 mg g^{-1}, similar to quantities present in transformed *P. glauca*.

Geranylgeranyl Fatty Acid Esters Decrease the Growth and Survival of a Spruce Insect Herbivore

Geranylgeranyl fatty acid esters have previously been reported at low levels in *P. abies* (Ekman, 1980). Their occurrence in large quantities in the needles of our *IDS1*-overexpressing line made it possible to test whether, like many other terpenes, they might have a role in plant defense. For this purpose, larvae of the nun moth, an insect that feeds on the foliage of conifers and other

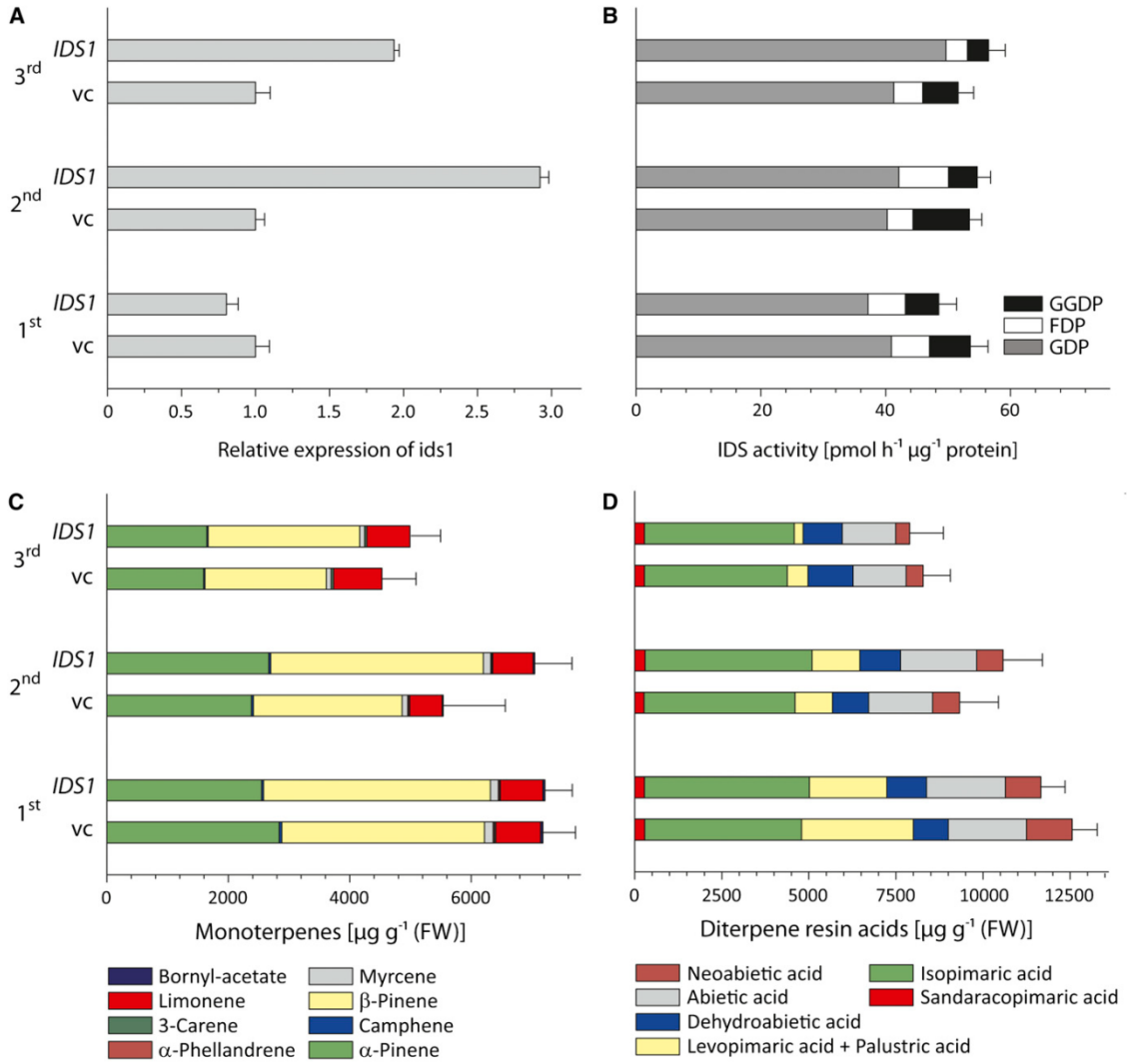

Figure 4. Detailed characterization of bark from 3-year-old *P. glauca IDS1* in comparison with an empty vector control (vc) with respect to bark from first-, second-, and third-year growth transgenic saplings. A, Relative expression of *IDS1* as determined by quantitative PCR. B, Total IDS enzyme activity measured in vitro forming GDP (C_{10}), FDP (C_{15}), and GGDP (C_{20}) as determined by LC-MS/MS. C and D, Monoterpene (C) and diterpene resin acid (D) contents as quantified with GC-FID. The minor monoterpenes are additionally shown separately in Supplemental Figure S5. Data are means ± SD of measurements from five plants of each line. FW, Fresh weight.

trees, were offered foliage from *IDS1*-overexpressing, empty vector control, and wild-type saplings. Larval survival and weight 21 d after hatching were significantly lower on *IDS1*-overexpressing plants than on either the empty vector or wild-type controls ($P < 0.005$, log-rank test; $P < 0.02$, Student's t test; Fig. 7, A and B). Developmental time, time from hatching to pupation, and time from pupation until adulthood did not vary between the treatments (Supplemental Fig. S10). Sex ratios of emerged adults were also the same, with an almost 50:50 ratio for larvae feeding on *IDS1*-overexpressing and control foliage (Supplemental Fig. S11).

To confirm that the higher mortality from feeding on *IDS1*-overexpressing plants is actually caused by the occurrence of geranylgeranyl fatty acid esters, branches from wild-type *P. glauca* saplings were treated with

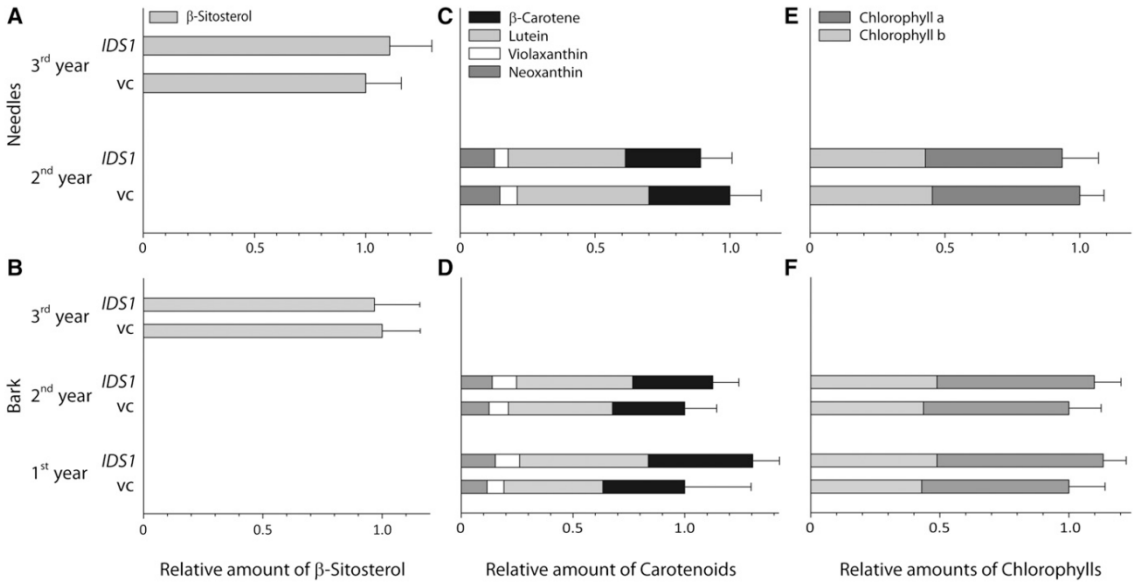

Figure 5. Quantification of other selected isoprenoids in *P. glauca IDS1* compared with an empty vector control line (vc) with respect to first-, second-, and third-year needles and bark. A and B, Relative content of β-sitosterol, a predominant plant sterol, measured by GC-FID. The resulting peak areas, calibrated using the internal standard ergosterol, were expressed relative to the area of the vector control, set to 1. C and D, Relative content of major carotenoids was determined by HPLC with diode-array detector at 455 nm. For each organ and year, the integrated peak areas are expressed relative to that of the vector control, set to 1. E and F, Relative chlorophyll content was determined by HPLC with diode-array detector at 650 nm. For each organ and year, the integrated peak areas are expressed relative to that of the vector control, set to 1. Data are means ± SD of measurements from five plants of each line.

geranylgeranyl stearate dissolved in hexane or hexane as a control. Larvae fed on foliage amended with this purified geranylgeranyl fatty acid ester had a significantly lower survival rate than when fed on controls ($P < 0.001$, log-rank test; Fig. 7C).

DISCUSSION

IDS functions at branch points of terpenoid biosynthesis, catalyzing the formation of intermediates of varying chain length, such as GDP (C_{10}), FDP (C_{15}), and GGDP (C_{20}). However, only scattered information is available about the role of IDS in controlling direction and flux through these pathways. IDS1 isolated from *P. abies* catalyzes the condensation of the C_5 units IDP and DMADP into GDP and GGDP, but not FDP (Schmidt et al., 2010). The C_{10} and C_{20} intermediates, GDP and GGDP, are precursors for the monoterpene hydrocarbons and diterpene resin acids, respectively, the two major classes of terpenes in conifer oleoresin. *P. abies* IDS1 has been suggested to have a major role in conifer oleoresin formation, because of the strong correlations of transcript and protein with the synthesis of resin terpenes in traumatic ducts after methyl jasmonate application (Schmidt et al., 2010, 2011). Here, transgenic spruce lines overexpressing *IDS1* were used to test how increasing enzyme activity would affect terpene amount and composition.

Overexpression of IDS1 Does Not Increase the Content of Typical Resin Monoterpenes and Diterpenes

Overexpression of *IDS1* under the control of the maize (*Zea mays*) ubiquitin promoter led to a massive (up to 700-fold) increase in *IDS1* transcript level in needles but only a 2- to 3-fold increase in bark. Previous measurements on wild-type saplings had shown that *IDS1* transcripts were about 50-fold higher in bark, the site of extensive terpene resin synthesis and storage, than in needles (Schmidt et al., 2010). The strength of the ubiquitin promoter might not be sufficient to increase transcription much further in bark, but in needles, where basal transcription is very low, this promoter could enhance transcription quite significantly. For successful overexpression in bark, another promoter should be chosen, or better, an as-yet-unidentified promoter specific for oleoresin production in ducts.

The elevated transcript levels in needles increased the amount of IDS1 protein, leading to a higher IDS1 enzyme activity and higher in planta levels of the products GDP and GGDP. However, FDP did not

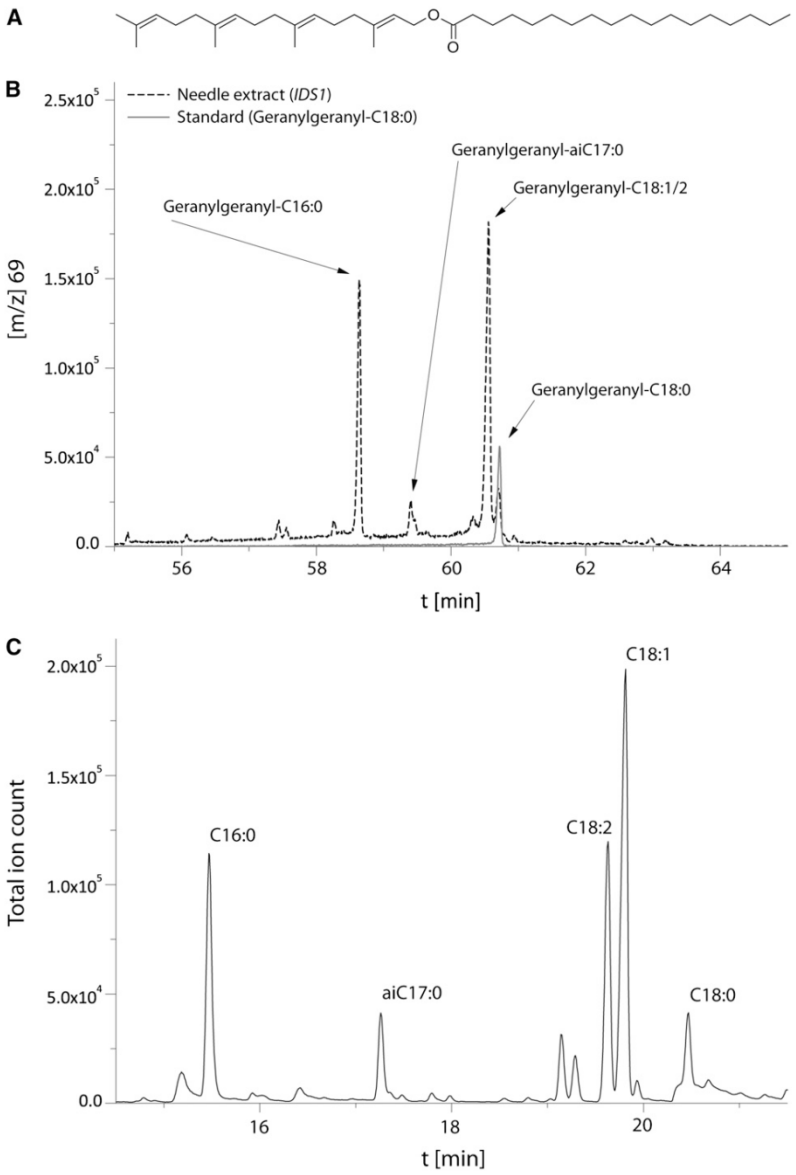

Figure 6. Evidence for the accumulation of geranylgeranyl fatty acid esters in *IDS1*-overexpressing *P. glauca* saplings. A, Structure of geranylgeranyl stearate (geranylgeranyl-C18:0). B, GC-MS chromatogram of a needle extract overlaid with a chromatogram of synthetic geranylgeranyl-C18:0. C, GC-MS chromatogram showing fatty acid methyl esters derived from the hydrolysis of isolated geranylgeranyl fatty acid esters. The peaks just to the left of C18:2 are impurities generated by derivatization with *N*-methyl-*N*-(trimethylsilyl)-trifluoroacetamide and not fatty acid esters. The abbreviation "aiC17:0" stands for 14-methylhexadecanoate, an anteiso fatty acid that is gymnosperm specific.

increase in planta in the needles. The reduction of FDP in the in vitro enzyme assays can be attributed to the ability of IDS1 to use FDP as a substrate for the production of GGDP (Schmidt et al., 2010). Despite the increase in IDS1 protein activity and GDP and GGDP, no significant changes were detected in terpene content, with the exception of a dramatic increase in geranylgeranyl fatty acid esters. The quantities of resin monoterpenes, sesquiterpenes, and diterpene resin acids did not increase in *P. glauca* and are in the same range as already reported for *P. abies* (Martin et al., 2002, 2003). In addition, there were no changes in the levels of the primary isoprenoids measured, including sterols, chlorophylls, and carotenoids. While overexpression of *IDS1* was able to significantly increase the prenyl diphosphate intermediates GDP and GGDP, the lack of increased flux to the resin monoterpenes and diterpenes, respectively, may be due to the low activity of the next step of terpene biosynthesis, catalyzed by terpene synthases.

Table I. *Accumulation of geranylgeranyl (GG) fatty acid esters in transgenic lines of P. glauca and P. abies overexpressing IDS1 or empty vector controls*

Genotype	Tissue	GG-C16:0	GG-aiC17:0	GG-C18:1/C18:2	GG-C18:0	Total
				mg g−1 fresh wt		
P. glauca IDS1	Needles third-year, main stem	5.24 ± 0.14	0.88 ± 0.13	5.03 ± 0.35	1.05 ± 0.17	12.21 ± 0.63
P. glauca IDS1	Needles second-year, main stem	3.05 ± 0.42	0.78 ± 0.06	3.28 ± 0.41	0.65 ± 0.08	7.76 ± 0.89
P. glauca IDS1	Needles, side branch	3.32 ± 0.69	0.80 ± 0.17	3.53 ± 0.73	0.69 ± 0.14	8.35 ± 1.59
P. glauca IDS1	Bark	<0.0002	<0.00002	<0.0002	<0.0001	<0.0005
P. glauca vector control	Needles, side branch	<0.0001	<0.00001	<0.0001	<0.00005	<0.00025
P. glauca vector control	Bark	<0.0002	<0.00002	<0.0002	<0.0001	<0.0005
P. abies IDS1	Needles, main stem	1.76 ± 0.07	0.7 ± 0.01	3.51 ± 0.07	0.23 ± 0.01	6.19 ± 0.14

Another limitation to terpene accumulation in these plant lines may be the broad targeting of *IDS1* overexpression under the control of the maize ubiquitin promoter. In wild-type spruce, this *P. abies* gene and genes encoding later enzymes of terpene resin biosynthesis in spruce are localized in bark cells surrounding resin ducts (Abbott et al., 2010; Schmidt et al., 2010). Here, the resin components are formed and then secreted into the ducts. Resin terpenes in spruce needles are stored in resin ducts (Weng and Jackson, 2000) and thus are likely also produced in the cells immediately surrounding these structures. Therefore, a general overexpression of *IDS1* throughout the needles may not lead to an increase in terpenoids because of the lack of later pathway enzymes in most cells, the absence of a location to store the products, or the missing ability to transport any terpenes produced toward existing storage structures. Instead, the buildup of the intermediate GGDP, but not of GDP, is diverted to the production of geranylgeranyl fatty acid esters.

Transgenic manipulation of IDS expression in other species has had a variety of results. In Arabidopsis (*Arabidopsis thaliana*), knockout of both FDP synthases led to an early developmental arrest of seeds (Closa et al., 2010), while overexpression of Arabidopsis *FDPS1* induced oxidative stress, cell death, and lesions due to altered cytokinin levels (Masferrer et al., 2002; Manzano et al., 2004, 2006). In *Artemisia annua*, FDP synthase overexpression increased the amount of the antimalarial sesquiterpene artemisinin but also had effects on plant morphology (Han et al., 2006; Banyai et al., 2010). In contrast to the cytosol-localized FDP synthases, manipulation of the plastid-localized GDP and GGDP synthases appears to alter terpene levels with fewer other effects on the plant, indicating differences between cytosolic and plastidal regulation of terpene biosynthesis. For example, overexpression of GDP synthase in *Mentha* × *piperita* increased the amount of monoterpenes (Lange et al., 2011), and overexpression of GGDP synthase in *Salvia miltiorrhiza* hairy root cultures increased the amount of the diterpene tanshinone (Kai et al., 2011), while the loss of GGDP synthase activity in *Nicotiana attenuata* decreased the level of defensive diterpene glycosides (Jassbi et al., 2008). In fact, when an FDP synthase, normally found in the cytosol, was expressed in the plastid (together with a terpene synthase), higher terpene amounts were obtained than when the same enzymes were expressed in the cytosol (Wu et al., 2006). Overexpression of a GDP synthase in both compartments had nearly no influence on terpene amount (Wu et al., 2006), because this particular GDP synthase was, in fact, subsequently shown to produce medium/long-chain prenyl diphosphates instead of GDP (Hsieh et al., 2011). In this work, overexpression of the *IDS1* gene, which has a plastid-targeting signal peptide (Schmidt et al., 2010), had no impact on the content of resin monoterpene and diterpenes, but flux was diverted to prenyl esters. Thus, constitutive overexpression of an IDS does not seem to be an appropriate way to increase the amount of resin terpenes. An RNA interference approach is currently under way to further investigate the role of IDS in terpene biosynthesis.

To the best of our knowledge, this work provides the first in planta quantification of GDP, FDP, and GGDP together. GDP has been previously quantified in two publications on spruce and other woody plants, giving concentrations 200-fold higher than what we obtained (Nogués et al., 2006; Ghirardo et al., 2010). These previous values were obtained by acid hydrolysis of the diphosphate moiety to form geraniol, which rearranges to linalool, quantified by proton-transfer reaction MS. The authors themselves (Ghirardo et al., 2010) recognized that their values might be overestimates of in planta GDP levels, since linalool might be formed from other substances under acidic conditions. For GGDP, 10-fold higher amounts in etiolated oat (*Avena sativa*) seedlings were reported (Benz et al., 1983). Large amounts of GGDP might be present in etiolated seedlings to form chlorophyll and initiate photosynthesis rapidly on illumination. The concentration of DMADP reported (Nogués et al., 2006; Ghirardo et al., 2010) is over 100- to 1,000-fold greater than our measurements of GDP, FDP, and GGDP. If this disparity is correct, it indicates a metabolic bottleneck in terpenoid metabolism after the MEP or MVA pathway and prior to the action of IDS enzymes. In some isoprene-emitting woody plant species, including spruce, a large pool of DMADP may be critical in supplying substrate for isoprene biosynthesis (Monson et al., 2013).

To make terpenes larger than C_{10}, more IDP than DMADP is needed, and it is assumed that the ratio between IDP and DMADP is regulated by isopentenyl

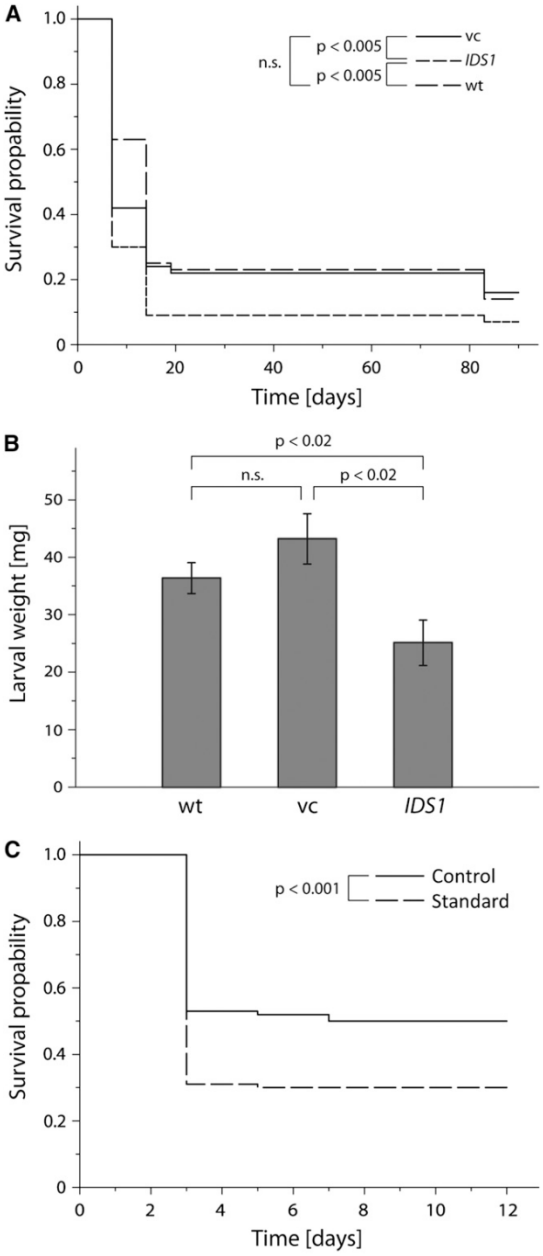

Figure 7. Effect of geranylgeranyl fatty acid esters on the performance of larvae of the nun moth. A, Kaplan-Meier plot of larval survival after feeding on foliage of *IDS1*, empty vector control (vc), or wild-type (wt) saplings. B, Larval mass after 24 d of feeding on the three genotypes. The *IDS1*-overexpressing saplings contain levels of geranylgeranyl fatty acid esters that are over 10^4 times those in either of the control lines. C, Kaplan-Meier plot of larval survival after feeding on foliage dipped in a hexane solution of synthesized geranylgeranyl stearate or dipped in a hexane control. n.s., Not significant.

diphosphate isomerase (Berthelot et al., 2012). In kudzu (*Pueraria lobata*) leaves, which make high levels of isoprene (C_5), this ratio was determined to be about 0.5 (Zhou et al., 2013), but it might be higher in plants that make high levels of terpenes with 10 or more carbon atoms. The greater amount of GGDP in our measurements, especially in needles, in comparison with that of GDP and FDP may be a result of GGDP's role as a precursor for GAs, carotenoids, and the phytol side chain of chlorophyll in photosynthetically active tissue. No detailed data are yet available about the regulatory interactions between the IDS enzymes and isopentenyl diphosphate isomerase and isoprene synthase. However, it was recently demonstrated that IDP and DMADP have inhibitory effects on the initial step of the MEP pathway, 1-deoxy-D-xylulose-5-phosphate synthase (Banerjee et al., 2013). Thus, future efforts should be made to determine whether GDP, FDP, or GGDP are also inhibitory to this enzyme or other MEP or MVA pathway enzymes as well as to determine how metabolic flux is controlled among the IDS-catalyzed steps of terpene biosynthesis.

Elevated Levels of GGDP Are Diverted to Form Geranylgeranyl Fatty Acid Esters

IDS1-overexpressing spruce saplings showed no significant changes in their content of typical *P. glauca* resin monoterpenes and diterpene acids; instead, they exhibited a dramatic increase in a diversion product, esters of geranylgeraniol with various fatty acids. Given a typical concentration of 2.5 to 3.0 mg g^{-1} fresh weight diterpene acids in spruce needles, the amount of GGDP diverted to the esters in *IDS1*-overexpressing plants is about twice the amount of GGDP employed for diterpene acid formation (assuming about half of the mass of geranylgeranyl fatty acid esters, 4–6 mg g^{-1} fresh weight, results from geranylgeraniol). Thus, there has been at least a 3-fold increase in GGDP production in the transgenic plants, which is in broad agreement with the 4.5-fold increase in GGDP measured in vivo.

Despite elevated levels of isoprenoid pathway intermediates, such as GGDP, we did not detect any increase in other primary terpenoids, such as phytol and carotenoids, also formed from GGDP (Fig. 8), indicating that formation of these products is tightly regulated (Cazzonelli and Pogson, 2010). Although we did not measure the levels of the GAs, another group of GGDP metabolites, an increase in these hormones also seems unlikely. First, no obvious morphological differences were found between the transgenic saplings and the controls (Supplemental Fig. S3). Second, GA biosynthesis is known to be regulated mainly by transcriptional changes of transcripts of the early pathway enzymes, *ent*-copalyl diphosphate synthase and *ent*-kaurene synthase, rather than the level of GGDP (Silverstone et al., 1997; Hedden and Thomas, 2012).

The pathway for the formation of geranylgeranyl fatty acid esters likely proceeds from GGDP to geranylgeraniol

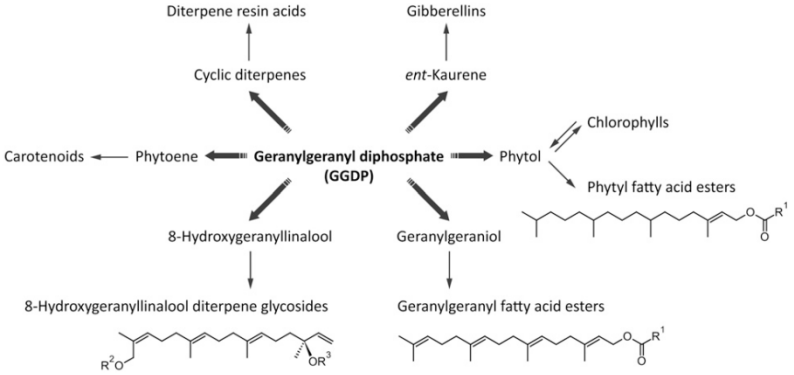

Figure 8. Metabolism of GGDP to primary metabolites, including GAs, chlorophylls, and carotenoids, and to secondary metabolites, including cyclic diterpenes, acyclic fatty acid esters, and acyclic glycosides. For phytyl and geranylgeranyl fatty acid esters, R^1 can be various fatty acids from C_{12} to C_{18} with various degrees of saturation (Ischebeck et al., 2006). For 8-hydroxygeranyllinalool diterpene glycosides, R^2 and R^3 are different monosaccharides or disaccharides with and without malonylation (Heiling et al., 2010).

via phosphatase cleavage (Fig. 8). A prenyl diphosphate phosphatase from *Croton stellatopilosus* was recently identified (but not biochemically characterized) that is part of a family of related phosphatases from eukaryotic as well as prokaryotic sources (Nualkaew et al., 2013). The resulting free geranylgeraniol is then esterified. In Arabidopsis, two enzymes were described as being responsible for the synthesis of esters using the more saturated C_{20} isoprenoid alcohol, phytol, instead of geranylgeraniol (Fig. 8). These are named PHYTYL ESTER SYNTHASE1 and PHYTYL ESTER SYNTHASE2 and are members of the esterase/lipase/thioesterase family of acyltransferases (Lippold et al., 2012). Since both are localized to the plastids, this suggests that the entire sequence for the formation of geranylgeranyl esters via IDS1, phosphatase, and then the ester synthase is localized in plastids. For phytyl fatty acid esters, localization in the plastoglobules was shown (Gaude et al., 2007). An identical localization of geranylgeranyl fatty acid esters can thus be assumed, because of the close structural similarities between these compounds.

Geranylgeranyl Fatty Acid Esters Are Common in Plants and Function in Defense

Esters of geranylgeraniol with fatty acids were already described in *P. abies* wood (Ekman, 1980), in mosses (Liljenberg and Karunen, 1978; Karunen et al., 1980), and in other plants (Lütke-Brinkhaus et al., 1985; McKibben et al., 1985; Jondiko and Pattenden, 1989; Reiter and Lorbeer, 2001; Biedermann et al., 2008). Esters with geraniol instead of geranylgeraniol are also known in rose (*Rosa* spp.) petals (Dunphy, 2006). However, no esters with geraniol were found in our transgenic *P. glauca*, although IDS1 is known to produce GDP and GGDP in vitro (Schmidt et al., 2010) and both intermediates were elevated in planta also, with the GGDP concentration being 12 times higher than that of GDP (Fig. 5A). The occurrence of phytyl esters is also common in plants, as mentioned above (Csupor, 1970; Liljenberg, 1977; Anderson et al., 1984; Pereira et al., 2002; Gaude et al., 2007), indicating that esterification of prenyl alcohols to fatty acid esters is a widespread phenomenon. The unusual anteiso fatty acid found as a component of these esters, anteisoheptadecanoic acid (14-methylhexadecanoic acid), has also already been reported from other conifers of the Pinaceae (Wolff et al., 1997, 2001).

In contrast to phytyl esters, which are known to be involved in chlorophyll *a* and *b* synthesis and in senescence (Ischebeck et al., 2006), the role of geranylgeranyl fatty acid esters had not yet been investigated. Here, we found these compounds to reduce the growth and survival of the conifer needle-feeding larvae of the nun moth, suggesting that they function in plant defense against herbivores (Fig. 7). Their toxicity may be a consequence of hydrolysis in the insect. Gut extracts of the closely related species *Lymantria dispar* possess high esterase activity (Kapin and Ahmad, 1980) that could cause cleavage of the ester bond and the release of geranylgeraniol, which has been described to exert toxic effects on membranes in vitro and against *Staphylococcus aureus* (Funari et al., 2005; Inoue et al., 2005). Interestingly, another group of plant defense compounds, the hydroxygeranyllinalool glycosides found in *N. attenuata* (Jassbi et al., 2008; Heiling et al., 2010; Đinh et al., 2013), share a similar terpene moiety and also can be readily cleaved to release an acyclic diterpene alcohol. The toxicity of geranyllinalool by itself has been reported for ants and termites (Lemaire et al., 1990). In both cases, conjugation of the diterpene moiety with a sugar or fatty acid could function as a strategy for storing these toxins to prevent damage to membranes or other plant components (Fig. 8). In fact, the overaccumulation of geranylgeraniol moieties as fatty acid esters in *IDS1*-overexpressing plants may be essential to avoid autotoxicity. Further experiments are planned to investigate the occurrence of geranylgeranyl fatty acid esters in spruce and their role in defense against other herbivores and pathogens.

MATERIALS AND METHODS

Chemicals

Geranylgeraniol, octadecanoyl chloride, pentadecanoyl chloride, 4-(dimethylamino) pyridine, *para*-cymene, iodine, alkaline bovine phosphatase, Supelco 37 Component FAME Mix, chloroform, dichloromethane, isopentenyl diphosphate, dimethylallyl diphosphate, ammonium bicarbonate, *tert*-butyl methyl ether (TBME), and acetonitrile (LC-MS grade) were purchased from Sigma-Aldrich. *N*-Methyl-*N*-(trimethylsilyl) trifluoroacetamide and TMSH were ordered from Macherey-Nagel. Methyl 14-methylhexadecanoate was purchased from Larodan Fine Chemicals, and tetrahydroabietic acid was from Wako Pure Chemical Industries.

Plant Material

Agrobacterium tumefaciens-mediated transformation of a *Picea glauca* embryogenic cell culture overexpressing *IDS1* from *Picea abies* (Schmidt et al., 2010) was carried out as described previously by Klimaszewska et al. (2001) and Hammerbacher et al. (2011), with the gene under the control of a maize (*Zea mays*) ubiquitin promoter. Somatic embryogenesis and plant regeneration of transgenic saplings were carried out, and plants were transferred to soil. For the analysis of geranylgeranyl fatty acid ester accumulation in *P. abies*, an identical transformation protocol was used. In the case of *P. glauca*, three independent transformed lines plus three empty vector control lines were characterized initially, using four plants per line. For later in-depth characterization, one line each from transformants and controls were chosen using five plants per line.

Monoterpene, Sesquiterpene, and Diterpene Analysis

The protocol was adapted from Lewinsohn et al. (1993). In brief, 100 mg of frozen plant material was ground in 1 mL of TBME with 57 μg mL^{-1} *p*-cymene and 46 μg mL^{-1} tetrahydroabietic acid as internal standards and extracted under continuous shaking for 24 h. The extract was removed, washed with 0.3 mL of 0.1 M $(NH_4)_2CO_3$, pH 8.0, and dried by using a Pasteur pipette filled with 100 mg of Na_2SO_4. The Na_2SO_4 column was further washed with 1 mL of TBME. To 0.4 mL of extract, 50 μL of TMSH was added for methylation of diterpenoid resin acids, which were subsequently analyzed by gas chromatography (GC)-MS and GC-flame ionization detection (FID). The rest was used for monoterpene and sesquiterpene analysis. GC conditions were as described by Schmidt et al. (2011). All terpenes were quantified on a fresh weight basis; the ratio of fresh weight to dry weight is about 3.5 for needles and 4.0 for bark tissues.

Isolation, Purification, and MS Analysis of Geranylgeranyl Fatty Acid Esters

Plant material was extracted with hexane:diethyl ether (9:1, v/v) in a ratio of 100 mg of tissue to 4 mL of solvent for 24 h under continuous shaking. The solvent was evaporated to dryness under a stream of nitrogen. The residual material was taken up in 0.5 mL of hexane:diethyl ether (9:1, v/v), loaded on a 3-mL, 500-mg SPE cartridge (CHROMABOND SiOH; Macherey-Nagel), and equilibrated with 3 mL of hexane:diethyl ether (9:1, v/v). Further elution was done with the same solvent. The first 2 mL was collected, evaporated to dryness, and taken up in 200 μL of chloroform. An Agilent 6890 series GC instrument with an Agilent 5973 mass spectrometer and a Zebron ZB-5HT column (30 m $\times$ 0.25 m $\times$ 0.25 μm; Phenomenex) were used for detection. One microliter of sample was injected in split mode (1:10) with an injector temperature of 310°C and a flow rate of 1 mL min^{-1} helium. Initial oven temperature was 50°C, held for 4 min, then raised by 5°C min^{-1} to 330°C, and held there for 15 min. ChemStation G1701 was used for data analysis. For quantification, geranylgeranyl heptadecanoate was used as an internal standard at a concentration of 25 μg mL^{-1}. Quantification was done using the mass-to-charge ratio (*m/z*) 69 fragment ion and assuming a relative response rate of 1. GC-MS electrospray ionization spectra can be found in Supplemental Figure S12.

NMR Analysis of Geranylgeranyl Fatty Acid Esters

All NMR spectra were measured on a Bruker Avance 500 NMR spectrometer (Bruker Biospin), operating at 500.13 MHz for ^{1}H and 125.75 MHz for ^{13}C. A triple resonance inverse cryoprobe (5 mm) was used to measure spectra at a probe temperature of 300 K. Spectra are referenced to tetramethylsilane at δ 0 ppm. For data processing and spectrometer control, TOPSPIN version 2.1 was used. The all-trans-configuration of the geranylgeranyl moiety could be deduced from chemical shifts in accordance with previously published data and from selective rotating frame nuclear Overhauser effect correlation spectroscopy experiments (Tanaka et al., 1982; Tanaka and Hirasawa, 1989).

Synthesis of Geranylgeranyl Stearate as a Standard in Geranylgeranyl Fatty Acid Ester Analysis

The synthesis was modified after a published method (Vassão et al., 2007). Quantities of 100 mg of geranylgeraniol (purity, 85%) and 30 mg of 4-(dimethylamino)-pyridine were dissolved in 25 mL of dichloromethane on an ice bath, and 100 mg of either octadecanoyl or heptadecanoyl chloride was added. The solution was stirred further for 24 h at room temperature. To stop the reaction, 20 mL of a saturated NaCl solution were added. The organic phase was dried with Na_2SO_4 and concentrated using a rotary evaporator. The reaction products were dissolved in 1 mL of hexane:diethyl ether (9:1, v/v) and purified using a SPE cartridge (CHROMABOND SiOH; Macherey-Nagel) equilibrated and eluted with hexane:diethyl ether (9:1, v/v). The eluate was fractionated and tested for purity by applying 10 μL of each fraction to a silica gel thin-layer chromatography plate, which was developed in hexane:diethyl ether (9:1, v/v) and stained with iodine vapor.

Sterol Analysis

One hundred milligrams of plant material was extracted with 4 mL of dichloromethane:methanol (2:1, v/v), including 60 μg mL^{-1} ergosterol as an internal standard, for 2 h at room temperature under continuous shaking. The solvent was evaporated under a stream of nitrogen, and the sample was dissolved in 2 mL of 2 M KOH in ethanol:water (3:1, v/v) followed by an incubation for 2 h at 60°C. After 2 mL of water was added, extraction was done three times with 2 mL of diethyl ether. The organic phases were combined and evaporated to dryness, and 100 mL of tetrahydrofuran and 100 μL of *N*-methyl-*N*-(trimethylsilyl) trifluoroacetamide were added. An Agilent 6890 series GC device with an Agilent 5973 mass spectrometer and a Zebron ZB-5MSi column (30 m $\times$ 0.25 m $\times$ 0.25 μm; Phenomenex) was used for analysis. One microliter of sample was injected in split mode 1:20 with an injector temperature of 280°C and a flow rate of 1 mL min^{-1} helium. Initial oven temperature was 200°C, held for 2 min, then raised by 15°C min^{-1} to 280°C and by 2°C min^{-1} to 300°C, and held there for 4 min. ChemStation G1701 was used for data analysis and integration of the peak areas.

Carotenoid and Chlorophyll Analysis

Extraction of 100 mg of plant material was carried out with 2 mL of acetone in brown glass vials at 4°C for 24 h under continuous shaking. An 800-μL portion of the extract was diluted with 200 μL of water, and 50 μL was injected on an Agilent 1100 HPLC instrument using a Supelcosil LC-18 column (7.5 cm $\times$ 4.6 mm $\times$ 3 μm; Sigma-Aldrich). Column temperature was kept at 20°C with a flow rate of 1.5 mL min^{-1}. Buffer A was 1 mM $NaHCO_3$ and buffer B was acetone. Starting conditions were 65% B, held for 4 min, followed by an increase to 90% B in 8 min and to 100% B in 8 min, held for 2 min. Carotenoids were detected at 455 nm and chlorophyll at 650 nm. For data analysis and integration of peak areas, ChemStation for LC 3D was used.

SDS-PAGE and Western Blot

Plant material was extracted as described (Nagel et al., 2012), and 34 μg of total protein was separated on a 12% SDS-PAGE gel under reducing conditions and transferred to an Immobilon-P polyvinylidene difluoride membrane (Merck Millipore). The membrane was blocked with 5% skim milk powder in PBS-T (phosphate-buffered saline, 137 mM NaCl, 2.7 mM KCl, 10 mM Na_2HPO_4, 2.0 mM KH_2PO_4, pH 7.4, and 0.05% [v/v] Tween 20). Thereafter, the membrane was incubated with an IDS1 specific polyclonal antibody serum (Schmidt et al., 2010) diluted 1:500 in blocking solution. The secondary antibody was an anti-rabbit horseradish peroxidase (Sigma-Aldrich) diluted 1:5,000 in PBS-T without skim milk powder. Washes between the incubation steps were done with PBS-T. Signal detection was achieved by using West Pico Chemiluminescent Substrate (Thermo Scientific) and Amersham Hyperfilm ECL (GE Healthcare).

Protein Extraction and Quantification of IDS Enzyme Activity

Protein extraction, enzyme assays, and analysis were carried out as described by Nagel et al. (2012). Data analysis was performed using Analyst Software 1.6 Build 3773 (AB Sciex Instruments).

Quantification of Short-Chain Prenyl Diphosphates in Planta

A 0.75-g portion of plant material was extracted three times with 5 mL of methanol:water (7:3, v/v), including a total of 0.3 μg of geranyl *S*-thiolodiphosphate and farnesyl *S*-thiolodiphosphate each (Echelon Biosciences). Extracts were combined, and 5 mL of water was added. Extracts were purified using 150 mg (6 mL) of CHROMABOND HR-XA columns (Macherey-Nagel), conditioned with 5 mL of methanol and 5 mL of water. After application of extract, the column was washed with 4 mL of water followed by 5 mL of methanol. Prenyl diphosphates were eluted with 3 mL of 1 M ammonium formate in methanol, evaporated under a stream of nitrogen to dryness, and dissolved in 250 μL of water:methanol (1:1). Quantification was done using an Agilent 1260 HPLC system (Agilent Technologies) coupled to an API 5000 triple-quadrupole mass spectrometer (AB Sciex Instruments). For separation, a ZORBAX Extended C-18 column (1.8 μm, 50 mm × 4.6 mm; Agilent Technologies) was used. The mobile phase consisted of 5 mM ammonium bicarbonate in water as solvent A and acetonitrile as solvent B, with the flow rate set at 1.2 mL min^{-1}, and the column temperature was kept at 20°C. Separation was achieved by using a gradient starting at 5% B, increasing to 7% B in 5 min and 100% B in 1 min (0.5-min hold), followed by a change to 0% B in 1.5 min (1-min hold) before the next injection. The injection volume for samples and standards was 2 μL; autosampler temperature was 4°C. The mass spectrometer was used in the negative electrospray ionization mode. Optimal settings were determined using standards. Levels of ion source gases 1 and 2 were set at 60 and 70 pounds per square inch (p.s.i.), respectively, with a temperature of 700°C. Curtain gas was set at 30 p.s.i., and collision gas was set at 7 p.s.i., with all gases being nitrogen. Ion spray voltage was maintained at −4,200 V. Multiple reaction monitoring was used to monitor analyte parent ion-to-product ion formation: *m/z* 312.9/79 for GDP, *m/z* 380.9/79 for FDP, *m/z* 449/79 for GGDP, *m/z* 329/79 and 329/159 for geranyl *S*-thiolodiphosphate, and *m/z* 379/79 and 379/159 for farnesyl *S*-thiolodiphosphate. Data analysis was performed using Analyst Software 1.6 Build 3773 (AB Sciex Instruments).

Quantitative Real-Time PCR and Quantitative Genomic PCR

RNA isolation, complementary DNA synthesis, and quantitative PCR from needle tissue were done as described by Schmidt et al. (2011). Quantitative genomic PCR was done from needle tissue as described by Schmidt et al. (2010).

Cloning of PgIDS1 and Alignment with PaIDS1

RNA was isolated from bark tissue of *P. glauca*, and the *PgIDS1* sequence was amplified with the primers and conditions described by Schmidt et al. (2010). The resulting fragment was cloned into pCR 4-TOPO (Invitrogen) and transformed into *Escherichia coli* strain TOP10F (Invitrogen) according to the manufacturer's instructions. Positive clones were selected, and sequence analysis was carried out using an ABI 3100 automatic sequencer (Applied Biosystems). The DNAStar Lasergene program version 9.0 (MegAlign) was used to align *PgIDS1* (GenBank accession no. KF840686) with *PaIDS1* (GenBank accession no. GQ369788).

Insect Assays

Eggs of nun moth (*Lymantria monacha*) were collected in fall 2011 near Herzberg/Elster, Germany, and kept at −8°C for 2 months plus 2 weeks at +4°C and then at room temperature until hatching. Hatched larvae were selected randomly for the different treatments and placed in groups of 50 larvae in Steri Vent Containers (Duchefa). Cut branches of wild-type, vector control *IDS1*-overexpressing spruce saplings were inserted in a water-filled 2-mL tube through a hole in the lid of each container and changed every third day. Larvae were counted once per week, and numbers were equalized every second week in each treatment group. Larval weight was determined separately for each individual after 21 d. To determine the time needed for pupation and the sex of the emerging adult, containers were checked for pupae every day after the first pupation event occurred, and pupae were placed in separate containers. In total, 300 larvae were fed on vector control and *IDS1*-overexpressing saplings, and 150 larvae were fed on wild-type plants.

For the feeding assay with geranylgeranyl stearate standard applied to branches from wild-type spruce saplings, ends of cut branches were placed in water-filled 2-mL tubes through a hole in the lid and swirled in hexane including 2 mg mL^{-1} geranylgeranyl stearate or pure hexane for 10 s. Newly treated branches were placed in a container with nun moths every day, and larvae were counted on days 3, 5, 7, 9, and 12. One hundred larvae were used for each treatment.

Statistical Analysis

The statistical significance of nun moth weight gain was tested by pairwise comparison using Student's *t* test. Survival curves were compared using a log-rank test.

Sequence data from this article can be found in the GenBank/EMBL data libraries under accession number KF840686 (*PgIDS1*).

Supplemental Data

The following materials are available in the online version of this article.

Supplemental Figure S1. Amino acid alignment of PgIDS1 and PaIDS1.

Supplemental Figure S2. Initial characterization of three independent IDS1 transgenic lines.

Supplemental Figure S3. General morphology of vector control and *IDS1*-overexpressing *Picea glauca* saplings.

Supplemental Figure S4. *IDS1* expression and total IDS enzyme activity of side branch needles.

Supplemental Figure S5. Content of sesquiterpenes and minor monoterpenes in bark.

Supplemental Figure S6. Identification of geranylgeraniol in saponified plant material.

Supplemental Figure S7. Determination of the origin of geranylgeraniol in needles of *IDS1*-overexpressing saplings.

Supplemental Figure S8. NMR analysis of geranylgeranyl fatty acid esters in needles.

Supplemental Figure S9. Abundance of geranylgeranyl fatty acid esters in bark and needles of IDS1-overexpressing saplings.

Supplemental Figure S10. Developmental times of *Lymantria monacha* fed on IDS1-overexpressing foliage versus controls.

Supplemental Figure S11. Sex ratio of *Lymantria monacha* fed on *IDS1*-overexpressing foliage versus controls.

Supplemental Figure S12. GC-MS spectra of geranylgeranyl fatty acid esters.

ACKNOWLEDGMENTS

We thank Dr. Paulina Dabrowska (Max Planck Institute of Chemical Ecology) for the synthesis of diazomethane, Annett Engelmann and Dr. Katrin Möller (Landeskompetenzzentrum Forst Eberswalde) for collecting and providing nun moth eggs, and Ines Lassowskat (Institute of Plant Biochemistry) and Dr. Michael Reichelt (Max Planck Institute for Chemical Ecology) for useful discussions regarding prenyl diphosphate purification.

Received September 19, 2013; accepted December 16, 2013; published December 17, 2013.

LITERATURE CITED

Abbott E, Hall D, Hamberger B, Bohlmann J (2010) Laser microdissection of conifer stem tissues: isolation and analysis of high quality RNA, terpene synthase enzyme activity and terpenoid metabolites from resin

ducts and cambial zone tissue of white spruce (*Picea glauca*). BMC Plant Biol **10:** 106–121

Akhtar TA, Matsuba Y, Schauvinhold I, Yu G, Lees HA, Klein SE, Pichersky E (2013) The tomato *cis*-prenyltransferase gene family. Plant J **73:** 640–652

Anderson WH, Gellerman JL, Schlenk H (1984) Effect of drought on phytyl wax esters in *Phaseolus* leaves. Phytochemistry **23:** 2695–2696

Arigoni D, Sagner S, Latzel C, Eisenreich W, Bacher A, Zenk MH (1997) Terpenoid biosynthesis from 1-deoxy-D-xylulose in higher plants by intramolecular skeletal rearrangement. Proc Natl Acad Sci USA **94:** 10600–10605

Banerjee A, Wu Y, Banerjee R, Li Y, Yan H, Sharkey TD (2013) Feedback inhibition of deoxy-D-xylulose-5-phosphate synthase regulates the methylerythritol 4-phosphate pathway. J Biol Chem **288:** 16926–16936

Banyai W, Kirdmanee C, Mii M, Supaibulwatana K (2010) Overexpression of farnesyl pyrophosphate synthase (FPS) gene affected artemisinin content and growth of *Artemisia annua* L. Plant Cell Tissue Organ Cult **103:** 255–265

Benz J, Fischer I, Rüdiger W (1983) Determination of phytyl diphosphate and geranylgeranyl diphosphate in etiolated oat seedlings. Phytochemistry **22:** 2801–2804

Berthelot K, Estevez Y, Deffieux A, Peruch F (2012) Isopentenyl diphosphate isomerase: a checkpoint to isoprenoid biosynthesis. Biochimie **94:** 1621–1634

Biedermann M, Haase-Aschoff P, Grob K (2008) Wax ester fraction of edible oils: analysis by on-line LC-GC-MS and GC x GC-FID. Eur J Lipid Sci Technol **110:** 1084–1094

Bohlmann J, Keeling CI (2008) Terpenoid biomaterials. Plant J **54:** 656–669

Buchanan BB, Gruissem W, Jones RL (2000) Biochemistry and Molecular Biology of Plants. John Wiley & Sons, New York

Butte W (1983) Rapid method for the determination of fatty acid profiles from fats and oils using trimethylsulphonium hydroxide for transesterification. J Chromatogr A **261:** 142–145

Cazzonelli CI, Pogson BJ (2010) Source to sink: regulation of carotenoid biosynthesis in plants. Trends Plant Sci **15:** 266–274

Chen DH, Ye HC, Li GF (2000) Expression of a chimeric farnesyl diphosphate synthase gene in *Artemisia annua* L. transgenic plants via *Agrobacterium tumefaciens*-mediated transformation. Plant Sci **155:** 179–185

Chen F, Tholl D, Bohlmann J, Pichersky E (2011) The family of terpene synthases in plants: a mid-size family of genes for specialized metabolism that is highly diversified throughout the kingdom. Plant J **66:** 212–229

Christie WW (2010) Lipid Analysis: Isolation, Separation, Identification and Structural Analysis of Lipids, Ed 4. Oily Press, Bridgwater, UK

Closa M, Vranová E, Bortolotti C, Bigler L, Arró M, Ferrer A, Gruissem W (2010) The *Arabidopsis thaliana* FPP synthase isozymes have overlapping and specific functions in isoprenoid biosynthesis, and complete loss of FPP synthase activity causes early developmental arrest. Plant J **63:** 512–525

Csupor L (1970) [Phytol in yellowed leaves]. Planta Med **19:** 37–41

Đinh ST, Gális I, Baldwin IT (2013) UVB radiation and 17-hydroxygeranyllinalool diterpene glycosides provide durable resistance against mirid (*Tupiocoris notatus*) attack in field-grown *Nicotiana attenuata* plants. Plant Cell Environ **36:** 590–606

Dunphy PJ (2006) Location and biosynthesis of monoterpenyl fatty acyl esters in rose petals. Phytochemistry **67:** 1110–1119

Ekman R (1980) Geranylgeranyl esters in Norway spruce wood. Phytochemistry **19:** 321–322

Erbilgin N, Krokene P, Christiansen E, Zeneli G, Gershenzon J (2006) Exogenous application of methyl jasmonate elicits defenses in Norway spruce (*Picea abies*) and reduces host colonization by the bark beetle *Ips typographus*. Oecologia **148:** 426–436

Funari SS, Prades J, Escribá PV, Barceló F (2005) Farnesol and geranylgeraniol modulate the structural properties of phosphatidylethanolamine model membranes. Mol Membr Biol **22:** 303–311

Gaude N, Bréhélin C, Tischendorf G, Kessler F, Dörmann P (2007) Nitrogen deficiency in *Arabidopsis* affects galactolipid composition and gene expression and results in accumulation of fatty acid phytyl esters. Plant J **49:** 729–739

Gershenzon J, Dudareva N (2007) The function of terpene natural products in the natural world. Nat Chem Biol **3:** 408–414

Ghirardo A, Koch K, Taipale R, Zimmer INA, Schnitzler JP, Rinne J (2010) Determination of de novo and pool emissions of terpenes from four common boreal/alpine trees by $^{13}CO_2$ labelling and PTR-MS analysis. Plant Cell Environ **33:** 781–792

Hammerbacher A, Ralph SG, Bohlmann J, Fenning TM, Gershenzon J, Schmidt A (2011) Biosynthesis of the major tetrahydroxystilbenes in spruce, astringin and isorhapontin, proceeds via resveratrol and is enhanced by fungal infection. Plant Physiol **157:** 876–890

Han JL, Liu BY, Ye HC, Wang H, Li ZQ, Li GF (2006) Effects of overexpression of the endogenous farnesyl diphosphate synthase on the artemisinin content in *Artemisia annua* L. J Integr Plant Biol **48:** 482–487

Hedden P, Thomas SG (2012) Gibberellin biosynthesis and its regulation. Biochem J **444:** 11–25

Heiling S, Schuman MC, Schoettner M, Mukerjee P, Berger B, Schneider B, Jassbi AR, Baldwin IT (2010) Jasmonate and ppHsystemin regulate key malonylation steps in the biosynthesis of 17-hydroxygeranyllinalool diterpene glycosides, an abundant and effective direct defense against herbivores in *Nicotiana attenuata*. Plant Cell **22:** 273–292

Hemmerlin A, Harwood JL, Bach TJ (2012) A raison d'être for two distinct pathways in the early steps of plant isoprenoid biosynthesis? Prog Lipid Res **51:** 95–148

Hsieh FL, Chang TH, Ko TP, Wang AHJ (2011) Structure and mechanism of an *Arabidopsis* medium/long-chain-length prenyl pyrophosphate synthase. Plant Physiol **155:** 1079–1090

Inoue Y, Hada T, Shiraishi A, Hirose K, Hamashima H, Kobayashi S (2005) Biphasic effects of geranylgeraniol, teprenone, and phytol on the growth of *Staphylococcus aureus*. Antimicrob Agents Chemother **49:** 1770–1774

Ischebeck T, Zbierzak AM, Kanwischer M, Dörmann P (2006) A salvage pathway for phytol metabolism in *Arabidopsis*. J Biol Chem **281:** 2470–2477

Jassbi AR, Gase K, Hettenhausen C, Schmidt A, Baldwin IT (2008) Silencing geranylgeranyl diphosphate synthase in *Nicotiana attenuata* dramatically impairs resistance to tobacco hornworm. Plant Physiol **146:** 974–986

Jondiko IJO, Pattenden G (1989) Terpenoids and an apocarotenoid from seeds of *Bixa orellana*. Phytochemistry **28:** 3159–3162

Kai GY, Xu H, Zhou CC, Liao P, Xiao JB, Luo XQ, You LJ, Zhang L (2011) Metabolic engineering tanshinone biosynthetic pathway in *Salvia miltiorrhiza* hairy root cultures. Metab Eng **13:** 319–327

Kapin MA, Ahmad S (1980) Esterases in larval tissues of gypsy moth, *Lymantria dispar* (L.): optimum assay conditions, quantification and characterization. Insect Biochem **10:** 331–337

Karunen P, Mikola H, Ekman R (1980) Occurrence of steryl and wax esters in *Dicranum elongatum*. Physiol Plant **48:** 554–559

Keeling CI, Bohlmann J (2006a) Diterpene resin acids in conifers. Phytochemistry **67:** 2415–2423

Keeling CI, Bohlmann J (2006b) Genes, enzymes and chemicals of terpenoid diversity in the constitutive and induced defence of conifers against insects and pathogens. New Phytol **170:** 657–675

Keena MA (2003) Survival and development of *Lymantria monacha* (Lepidoptera: Lymantriidae) on North American and introduced Eurasian tree species. J Econ Entomol **96:** 43–52

Keena MA, Vandel A, Pultar O (2010) Phenology of *Lymantria monacha* (Lepidoptera: Lymantriidae) laboratory reared on spruce foliage or a newly developed artificial diet. Ann Entomol Soc Am **103:** 949–955

Keim V, Manzano D, Fernández FJ, Closa M, Andrade P, Caudepón D, Bortolotti C, Vega MC, Arró M, Ferrer A (2012) Characterization of *Arabidopsis* FPS isozymes and FPS gene expression analysis provide insight into the biosynthesis of isoprenoid precursors in seeds. PLoS ONE **7:** e49109

Kharel Y, Koyama T (2003) Molecular analysis of *cis*-prenyl chain elongating enzymes. Nat Prod Rep **20:** 111–118

Klimaszewska K, Lachance D, Pelletier G, Lelu MA, Seguin A (2001) Regeneration of transgenic *Picea glauca*, *P. mariana*, and *P. abies* after cocultivation of embryogenic tissue with *Agrobacterium tumefaciens*. In Vitro Cell Dev Biol Plant **37:** 748–755

Klimetzek D, Vite JP (1989) Tierische Schädlinge. *In* H Schmidt-Vogt, ed, Die Fichte, Vol 2. Verlag Paul Parey, Hamburg, Germany, pp 40–131

Köksal M, Hu H, Coates RM, Peters RJ, Christianson DW (2011) Structure and mechanism of the diterpene cyclase *ent*-copalyl diphosphate synthase. Nat Chem Biol **7:** 431–433

Lange BM, Mahmoud SS, Wildung MR, Turner GW, Davis EM, Lange I, Baker RC, Boydston RA, Croteau RB (2011) Improving peppermint

essential oil yield and composition by metabolic engineering. Proc Natl Acad Sci USA **108:** 16944–16949

Lemaire M, Nagnan P, Clement JL, Lange C, Peru L, Basselier JJ (1990) Geranyllinalool (diterpene alcohol): an insecticidal component of pine wood and termites (Isoptera: Rhinotermitidae) in four European ecosystems. J Chem Ecol **16:** 2067–2079

Lewinsohn E, Savage TJ, Gijzen M, Croteau R (1993) Simultaneous analysis of monoterpenes and diterpenoids of conifer oleoresin. Phytochem Anal **4:** 220–225

Liang PH (2009) Reaction kinetics, catalytic mechanisms, conformational changes, and inhibitor design for prenyltransferases. Biochemistry **48:** 6562–6570

Liang PH, Ko TP, Wang AHJ (2002) Structure, mechanism and function of prenyltransferases. Eur J Biochem **269:** 3339–3354

Liljenberg C (1977) Occurrence of phytolpyrophosphate and acyl esters of phytol in irradiated dark-grown barley seedlings and their possible role in biosynthesis of chlorophyll. Physiol Plant **39:** 101–105

Liljenberg C, Karunen P (1978) Changes in content of phytyl and geranylgeranyl esters of germinating *Polytrichum commune* spores. Physiol Plant **44:** 369–372

Lippold F, vom Dorp K, Abraham M, Hölzl G, Wewer V, Yilmaz JL, Lager I, Montandon C, Besagni C, Kessler F, et al (2012) Fatty acid phytyl ester synthesis in chloroplasts of *Arabidopsis*. Plant Cell **24:** 2001–2014

Lütke-Brinkhaus F, Weiss G, Kleinig H (1985) Prenyl lipid formation in spinach chloroplasts and in a cell-free system of *Synechococcus* (cyanobacteria): polyprenols, chlorophylls, and fatty acid prenyl esters. Planta **163:** 68–74

Manzano D, Busquets A, Closa M, Hoyerová K, Schaller H, Kamínek M, Arró M, Ferrer A (2006) Overexpression of farnesyl diphosphate synthase in *Arabidopsis* mitochondria triggers light-dependent lesion formation and alters cytokinin homeostasis. Plant Mol Biol **61:** 195–213

Manzano D, Fernández-Busquets X, Schaller H, González V, Boronat A, Arró M, Ferrer A (2004) The metabolic imbalance underlying lesion formation in *Arabidopsis thaliana* overexpressing farnesyl diphosphate synthase (isoform 1S) leads to oxidative stress and is triggered by the developmental decline of endogenous HMGR activity. Planta **219:** 982–992

Martin D, Tholl D, Gershenzon J, Bohlmann J (2002) Methyl jasmonate induces traumatic resin ducts, terpenoid resin biosynthesis, and terpenoid accumulation in developing xylem of Norway spruce stems. Plant Physiol **129:** 1003–1018

Martin DM, Gershenzon J, Bohlmann J (2003) Induction of volatile terpene biosynthesis and diurnal emission by methyl jasmonate in foliage of Norway spruce. Plant Physiol **132:** 1586–1599

Masferrer A, Arró M, Manzano D, Schaller H, Fernández-Busquets X, Moncaleán P, Fernández B, Cunillera N, Boronat A, Ferrer A (2002) Overexpression of *Arabidopsis thaliana* farnesyl diphosphate synthase (FPS1S) in transgenic *Arabidopsis* induces a cell death/senescence-like response and reduced cytokinin levels. Plant J **30:** 123–132

McKibben GH, Thompson MJ, Parrott WL, Thompson AC, Lusby WR (1985) Identification of feeding stimulants for boll weevils from cotton buds and anthers. J Chem Ecol **11:** 1229–1238

Monson RK, Jones RT, Rosenstiel TN, Schnitzler JP (2013) Why only some plants emit isoprene. Plant Cell Environ **36:** 503–516

Nagel R, Gershenzon J, Schmidt A (2012) Nonradioactive assay for detecting isoprenyl diphosphate synthase activity in crude plant extracts using liquid chromatography coupled with tandem mass spectrometry. Anal Biochem **422:** 33–38

Nogués I, Brilli F, Loreto F (2006) Dimethylallyl diphosphate and geranyl diphosphate pools of plant species characterized by different isoprenoid emissions. Plant Physiol **141:** 721–730

Nualkaew N, Guennewich N, Springob K, Klamrak A, De-Eknamkul W, Kutchan TM (2013) Molecular cloning and catalytic activity of a membrane-bound prenyl diphosphate phosphatase from *Croton stellatopilosus* Ohba. Phytochemistry **91:** 140–147

Pereira AS, Siqueira DS, Elias VO, Simoneit BRT, Cabral JA, Aquino Neto FR (2002) Three series of high molecular weight alkanoates found in Amazonian plants. Phytochemistry **61:** 711–719

Ralph SG, Yueh H, Friedmann M, Aeschliman D, Zeznik JA, Nelson CC, Butterfield YSN, Kirkpatrick R, Liu J, Jones SJM, et al (2006) Conifer defence against insects: microarray gene expression profiling of Sitka spruce (*Picea sitchensis*) induced by mechanical wounding or feeding by spruce budworms (*Choristoneura occidentalis*) or white pine weevils (*Pissodes strobi*) reveals large-scale changes of the host transcriptome. Plant Cell Environ **29:** 1545–1570

Reiter B, Lorbeer E (2001) Analysis of the wax ester fraction of olive oil and sunflower oil by gas chromatography and gas chromatography-mass spectrometry. J Am Oil Chem Soc **78:** 881–888

Rodríguez-Concepción M (2006) Early steps in isoprenoid biosynthesis: multilevel regulation of the supply of common precursors in plant cells. Phytochem Rev **5:** 1–15

Sallaud C, Rontein D, Onillon S, Jabès F, Duffé P, Giacalone C, Thoraval S, Escoffier C, Herbette G, Leonhardt N, et al (2009) A novel pathway for sesquiterpene biosynthesis from *Z,Z*-farnesyl pyrophosphate in the wild tomato *Solanum habrochaites*. Plant Cell **21:** 301–317

Schiebe C, Hammerbacher A, Birgersson G, Witzell J, Brodelius PE, Gershenzon J, Hansson BS, Krokene P, Schlyter F (2012) Inducibility of chemical defenses in Norway spruce bark is correlated with unsuccessful mass attacks by the spruce bark beetle. Oecologia **170:** 183–198

Schilmiller AL, Schauvinhold I, Larson M, Xu R, Charbonneau AL, Schmidt A, Wilkerson C, Last RL, Pichersky E (2009) Monoterpenes in the glandular trichomes of tomato are synthesized from a neryl diphosphate precursor rather than geranyl diphosphate. Proc Natl Acad Sci USA **106:** 10865–10870

Schmidt A, Nagel R, Krekling T, Christiansen E, Gershenzon J, Krokene P (2011) Induction of isoprenyl diphosphate synthases, plant hormones and defense signalling genes correlates with traumatic resin duct formation in Norway spruce (*Picea abies*). Plant Mol Biol **77:** 577–590

Schmidt A, Wächtler B, Temp U, Krekling T, Séguin A, Gershenzon J (2010) A bifunctional geranyl and geranylgeranyl diphosphate synthase is involved in terpene oleoresin formation in *Picea abies*. Plant Physiol **152:** 639–655

Silverstone AL, Chang C, Krol E, Sun TP (1997) Developmental regulation of the gibberellin biosynthetic gene GA1 in *Arabidopsis thaliana*. Plant J **12:** 9–19

Tanaka Y, Hirasawa H (1989) Sequence analysis of polyprenols by 500 MHz ^{1}H-NMR spectroscopy. Chem Phys Lipids **51:** 183–189

Tanaka Y, Sato H, Kageyu A (1982) Structural characterization of polyprenols by ^{13}C-n.m.r. spectroscopy: signal assignments of polyprenol homologues. Polymer (Guildf) **23:** 1087–1090

Vassão DG, Kim SJ, Milhollan JK, Eichinger D, Davin LB, Lewis NG (2007) A pinoresinol-lariciresinol reductase homologue from the creosote bush (*Larrea tridentata*) catalyzes the efficient in vitro conversion of p-coumaryl/coniferyl alcohol esters into the allylphenols chavicol/eugenol, but not the propenylphenols p-anol/isoeugenol. Arch Biochem Biophys **465:** 209–218

Wang KC, Ohnuma S (2000) Isoprenyl diphosphate synthases. Biochim Biophys Acta **1529:** 33–48

Wellenstein G, editor (1942) Die Nonne in Ostpreußen (1933–1937): Freilandstudien der Waldstation für Schädlingsbekämpfung in Jagdhaus Rominten. Monographien zur Angewandten Entomologie, No. 15. Parey, Berlin

Weng C, Jackson ST (2000) Species differentiation of North American spruce (*Picea*) based on morphological and anatomical characteristics of needles. Can J Bot **78:** 1367–1383

Wolff RL, Christie WW, Coakley D (1997) The unusual occurrence of 14-methylhexadecanoic acid in Pinaceae seed oils among plants. Lipids **32:** 971–973

Wolff RL, Lavialle O, Pédrono F, Pasquier E, Deluc LG, Marpeau AM, Aitzetmüller K (2001) Fatty acid composition of Pinaceae as taxonomic markers. Lipids **36:** 439–451

Wu SQ, Schalk M, Clark A, Miles RB, Coates R, Chappell J (2006) Redirection of cytosolic or plastidic isoprenoid precursors elevates terpene production in plants. Nat Biotechnol **24:** 1441–1447

Zhao T, Krokene P, Hu J, Christiansen E, Björklund N, Långström B, Solheim H, Borg-Karlson AK (2011) Induced terpene accumulation in Norway spruce inhibits bark beetle colonization in a dose-dependent manner. PLoS ONE **6:** e26649

Zhou C, Li Z, Wiberley-Bradford AE, Weise SE, Sharkey TD (2013) Isopentenyl diphosphate and dimethylallyl diphosphate/isopentenyl diphosphate ratio measured with recombinant isopentenyl diphosphate isomerase and isoprene synthase. Anal Biochem **440:** 130–136

Supplemental Figure 1

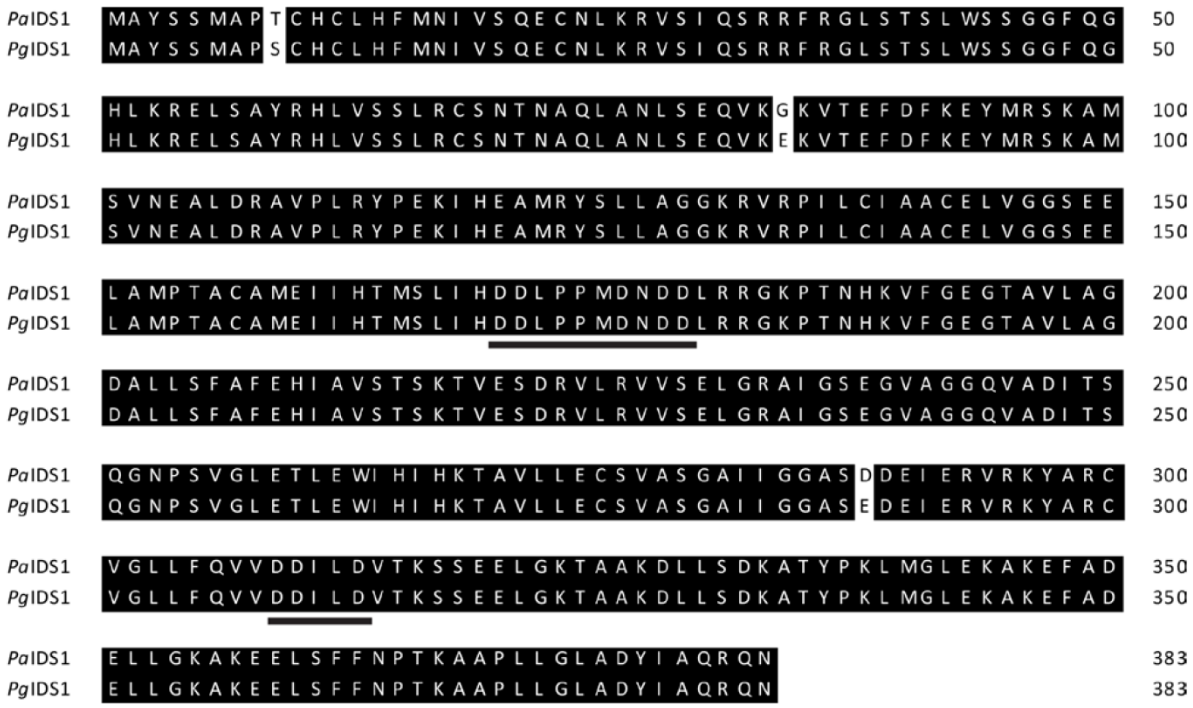

Supplemental Figure 1: Alignment of deduced amino acid sequences of *Pa*IDS1 (accession no. GQ369788) and *Pg*IDS1 (accession no. KF840686). Identical amino acids are boxed in black. The Asp-rich motifs conserved among IDSs are indicated by the black lines.

Supplemental Figure 2

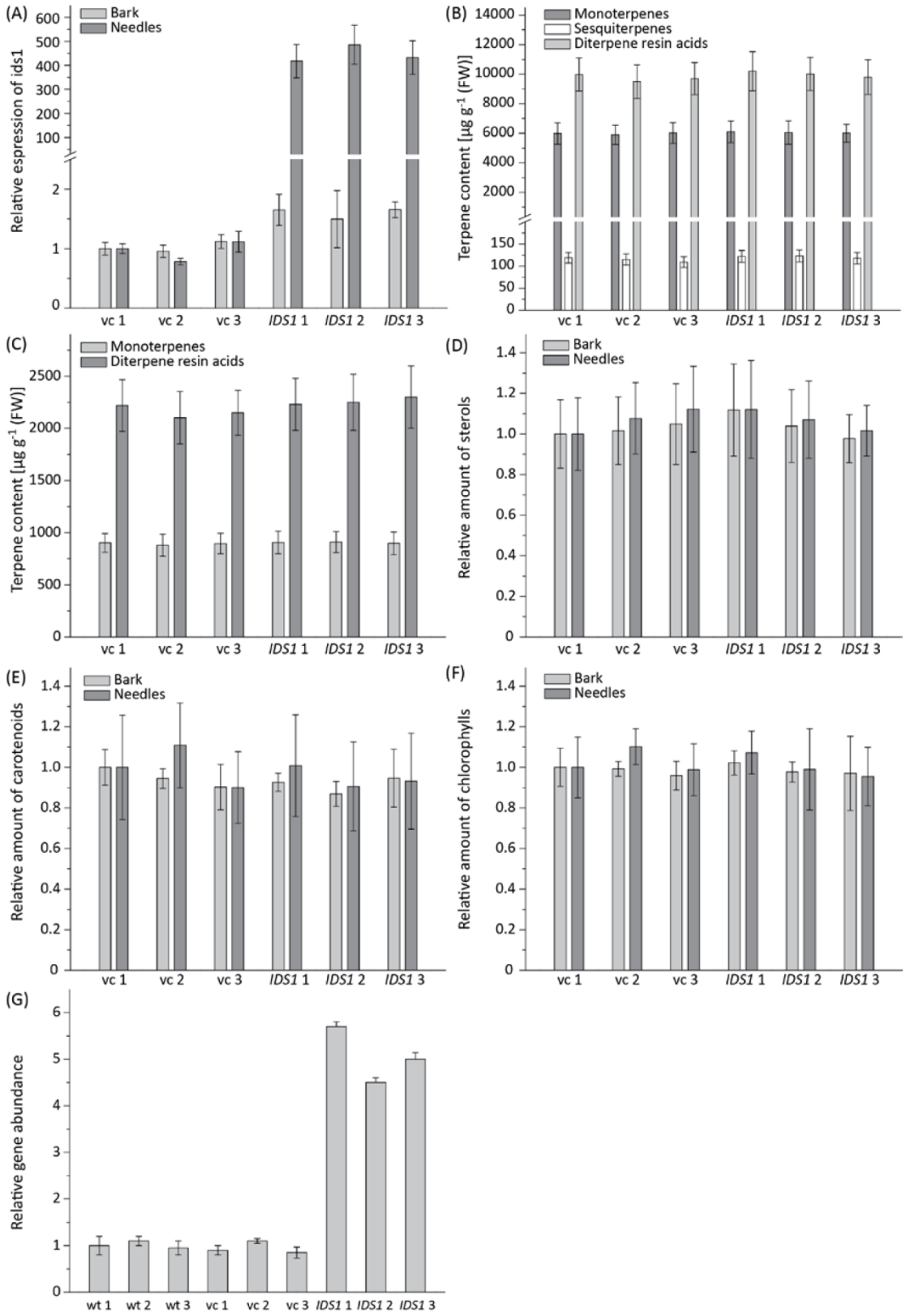

Supplemental Figure 2: Initial characterization of transgenic *P. glauca* saplings overexpressing *IDS1* (*IDS1*) compared with those transformed with an empty vector as a control (vc). Data for three independently-transformed lines of each type are shown. (A) Relative expression of *IDS1* in bark and needles as determined by qPCR. (B) Terpene content of bark (C) Terpene content of needles (D) Sterol content of bark and needles as measured by GC-FID. (E) Carotenoid and (F) chlorophyll content of bark and needles as measured by HPLC-UV/DAD. (G) Relative gene abundance as determined by genomic-qPCR. Data are means ± SD of four plants of each line.

Supplemental Figure 3

Supplemental Figure 3: Morphology of three-year-old *P. glauca* saplings transformed with (A) empty vector as control or (B) an *IDS1*-overexpressing construct.

Supplemental Figure 4

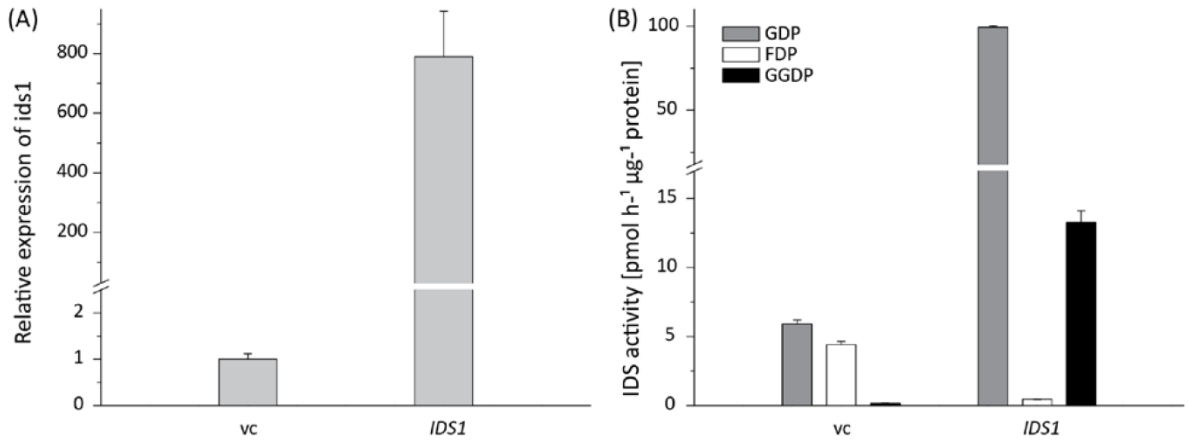

Supplemental Figure 4: Comparison of side branch needles of a *P. glauca IDS1*-overexpressing line (*IDS1*) and an empty vector control line (vc) for (A) relative expression of *IDS1* as determined by qPCR and (B) total IDS enzyme activity as measured in vitro by LC-MS/MS. Data are means ± SD of measurements from five plants of each line.

Supplemental Figure 5

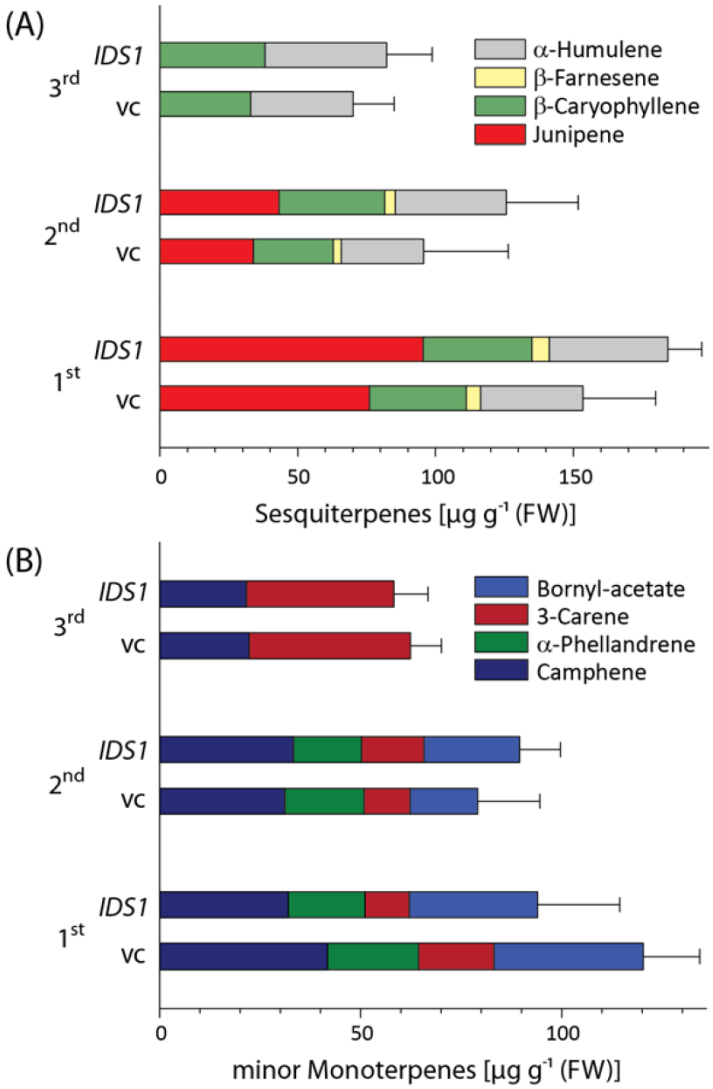

Supplemental Figure 5: Comparison of bark (A) sesquiterpene and (B) minor monoterpene content as measured by GC-FID between three-year-old *P. glauca IDS1*-overexpressing saplings (*IDS1*) and vector control (vc) saplings in 1st, 2nd and 3rd year growth. Data are means ± SD of measurements from five plants of each line.

Supplemental Figure 6

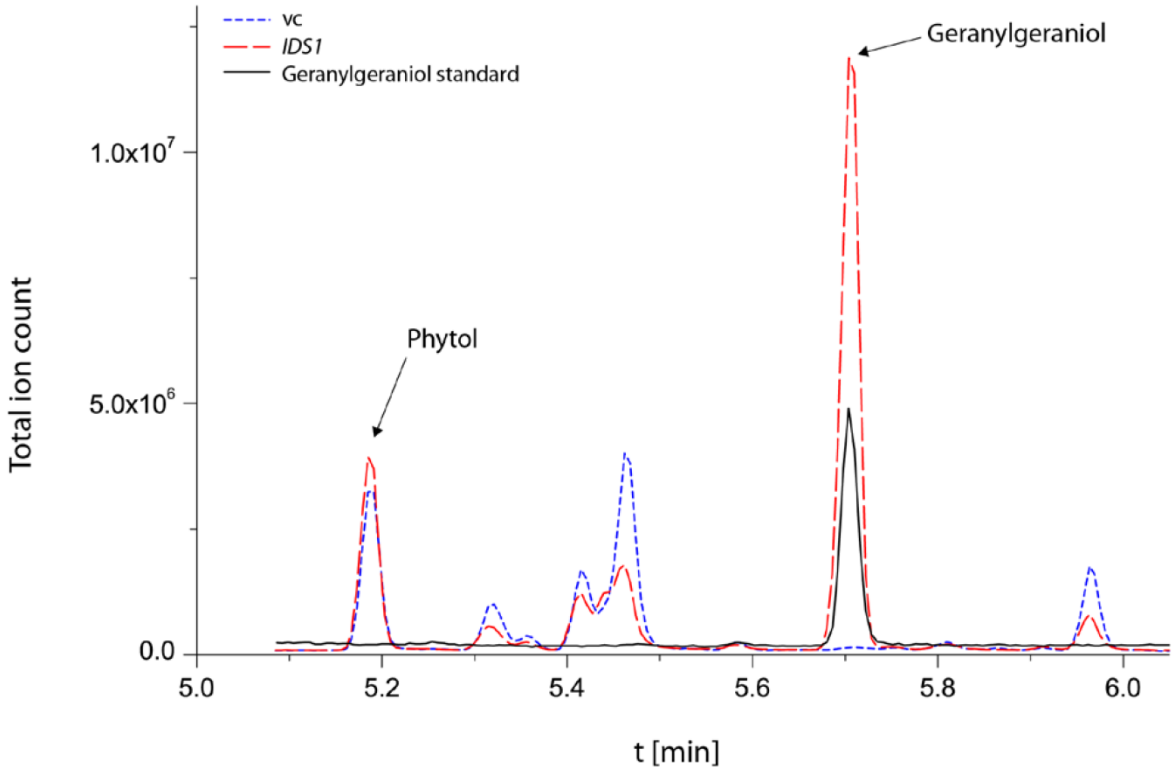

Supplemental Figure 6: GC-MS chromatogram of saponified and silylated lipid extract of either vector control or *IDS1*-overexpressing plants, as well as a silylated authentic geranylgeraniol standard.

Supplemental Figure 7

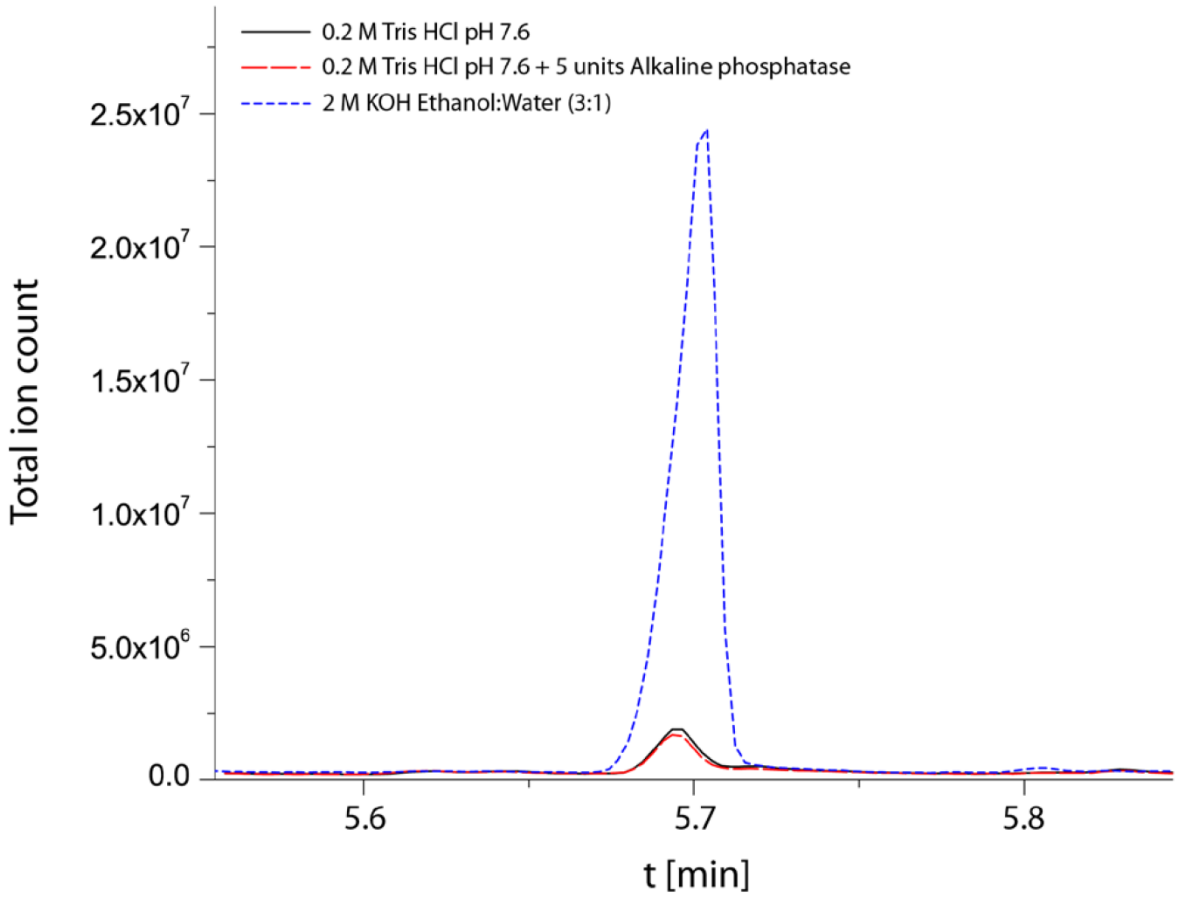

Supplemental Figure 7: Characterization of geranylgeranyl fatty acid esters from *IDS1*-overexpressing *P. glauca* lines. Hydrolysis was attempted in strong base and with alkaline phosphatase, but was only successful in the former case, suggesting compounds were carboxylate esters and not phosphate esters. Peak at 5.7 min is that of geranylgeraniol.

Supplemental Figure 8

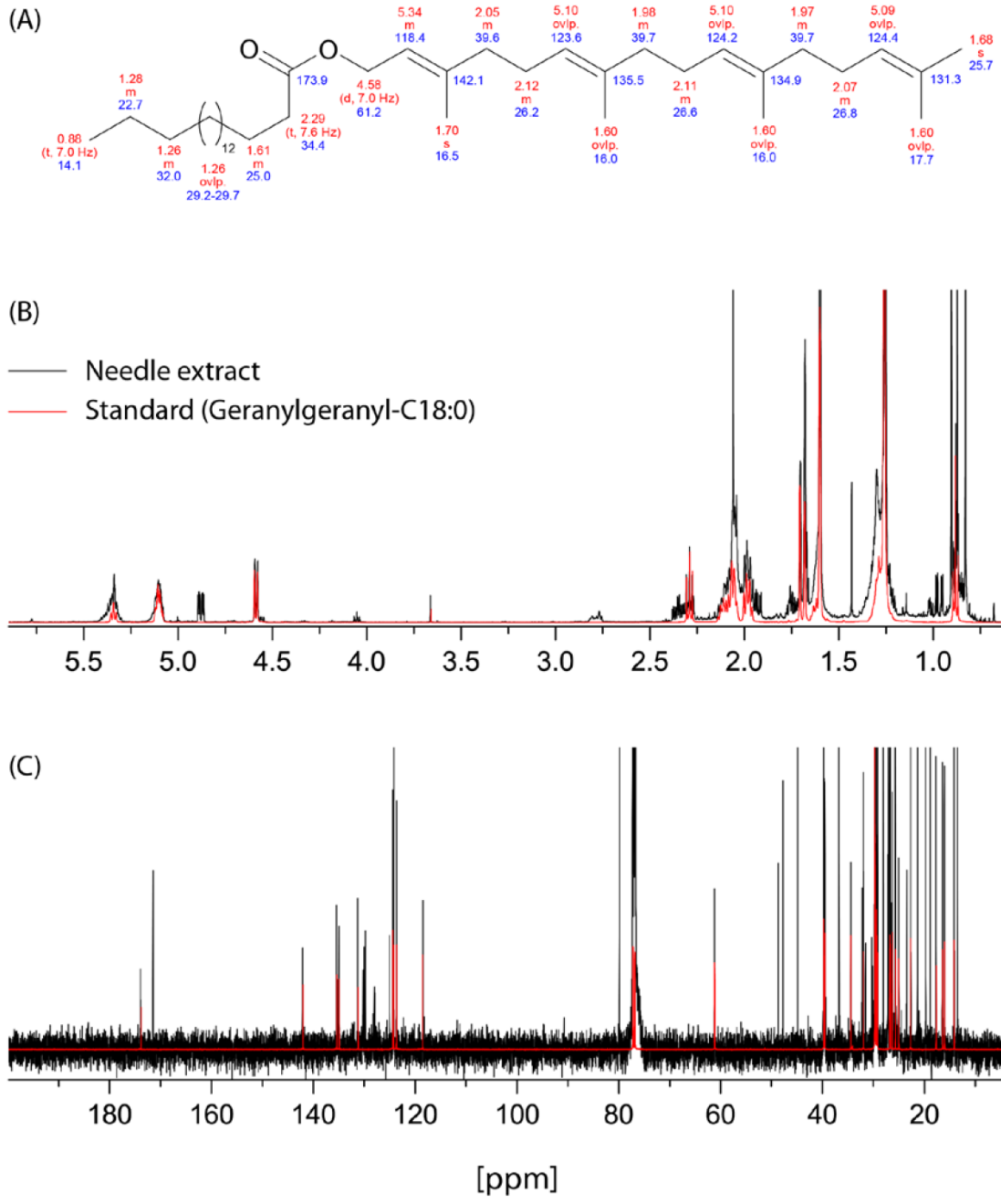

Supplemental Figure 8: NMR analysis of geranylgeranyl fatty acid esters in needle extracts of *IDS1*-overexpressing *P. glauca* plants. (A) Chemical shifts of synthesized geranylgeranyl-C18:0, ^{13}C in blue and ^{1}H in red. (B) ^{1}H-NMR and (C) ^{13}C-NMR spectra of needle extract from *IDS1*-overexpressing saplings overlaid on spectrum of geranylgeranyl-C18:0 standard.

Supplemental Figure 9

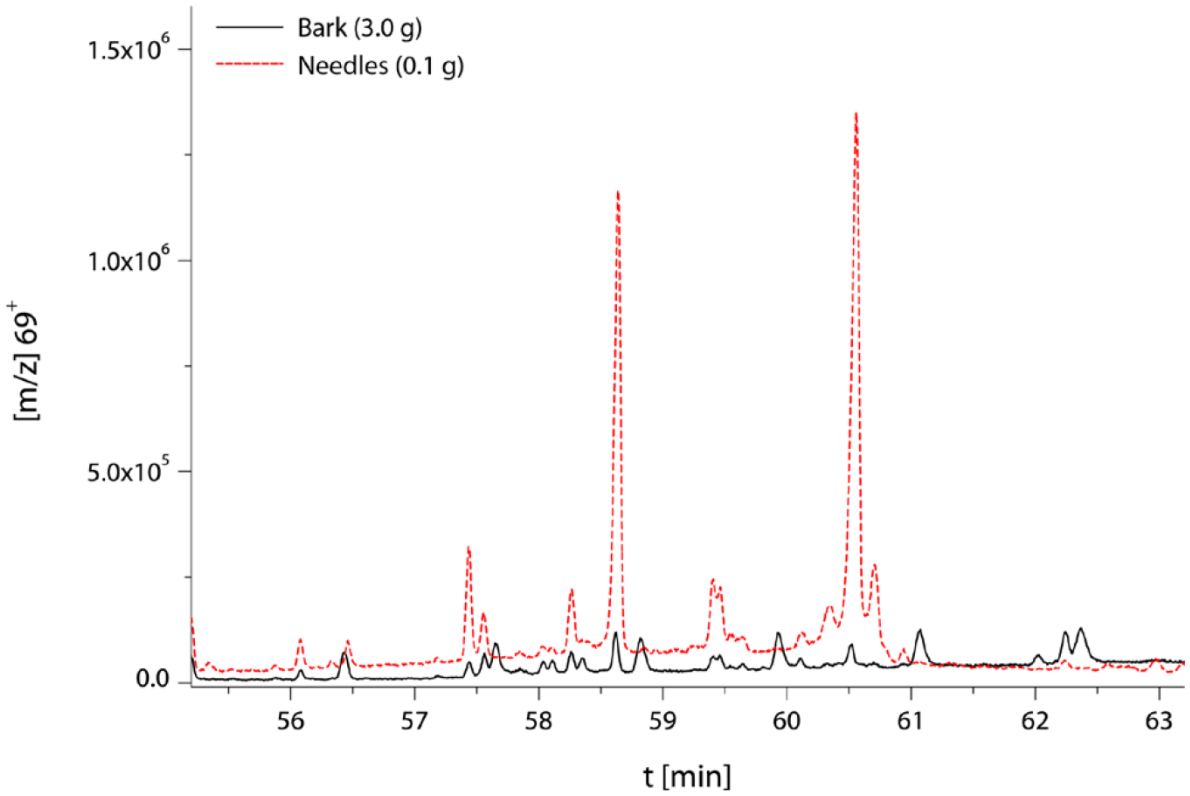

Supplemental Figure 9: Low abundance of geranylgeranyl fatty acid esters in bark vs. needles of *IDS1*-overexpressing *P. glauca* saplings is shown by GC-MS comparison of extracts. Bark extract is 30-fold more concentrated than needle extract, but gives only small peaks. Major peak at ~58.6 min is that of geranylgeranyl–C16:0 and peak at ~60.6 min is that of geranylgeranyl-C18:1 and C18:2.

Supplemental Figure 10

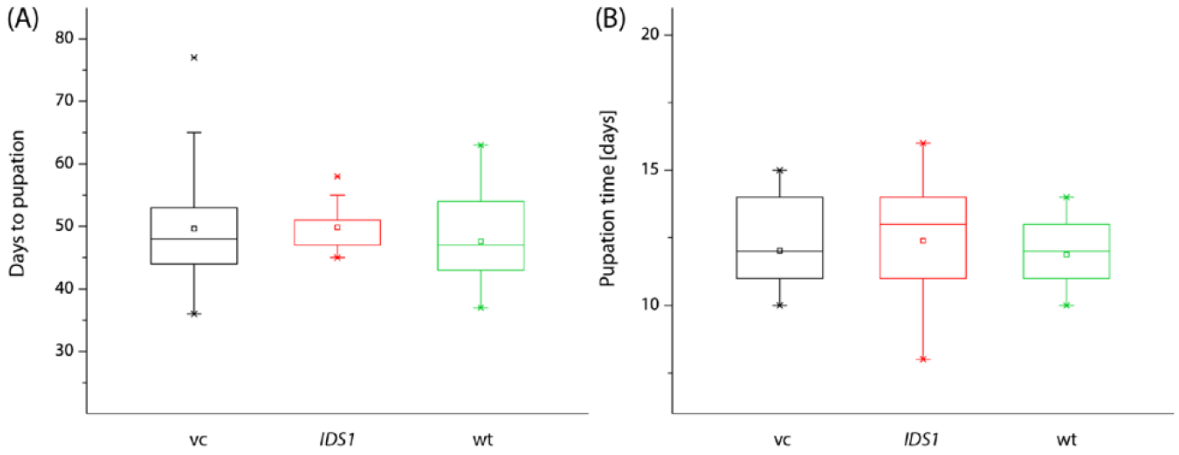

Supplemental Figure 10: Effect of geranylgeranyl fatty acid esters on development of *Lymantria monacha* larvae feeding on *IDS1*-overexpressing (*IDS1*), empty vector control (vc) and wild-type control (wt) saplings. (A) Time from hatching to pupation and (B) time from pupation to emergence of adult moths.

Supplemental Figure 11

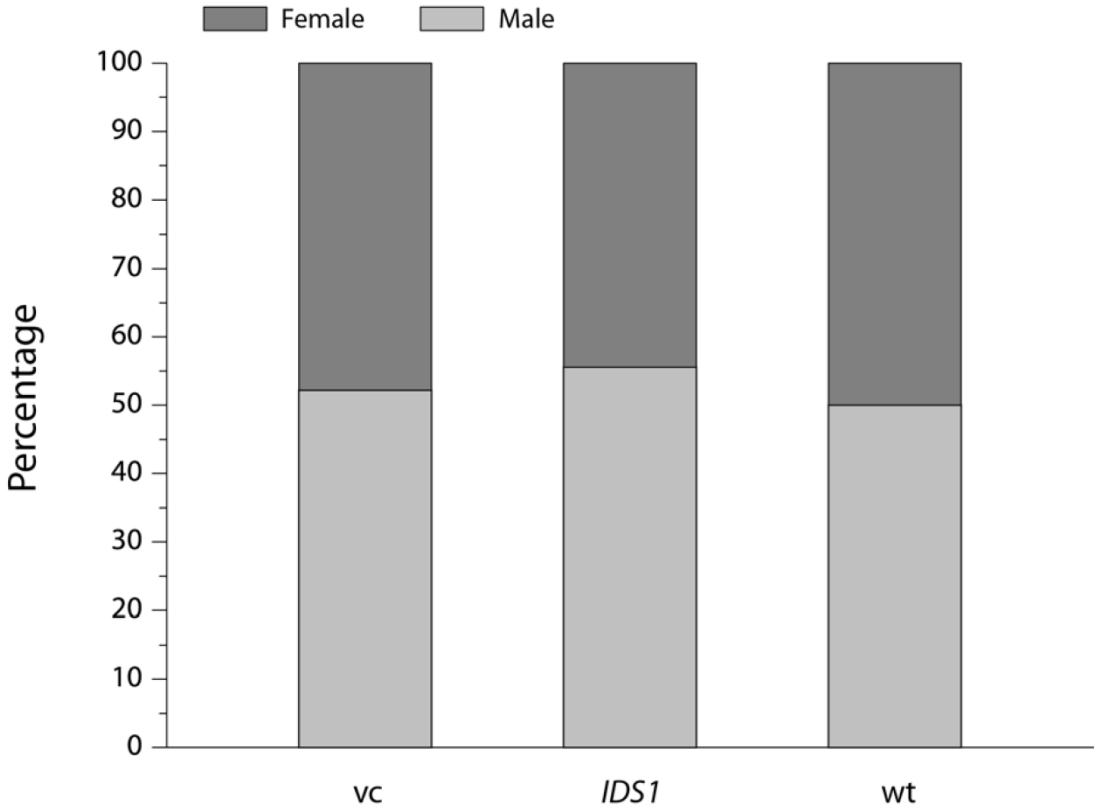

Supplemental Figure 11: Effect of geranylgeranyl fatty acid esters on sex ratio of emerging *Lymantria monacha* adults after larval feeding on *IDS1*-overexpressing (*IDS1*), empty vector control (vc) and wild-type control (wt) saplings.

Supplemental Figure 12

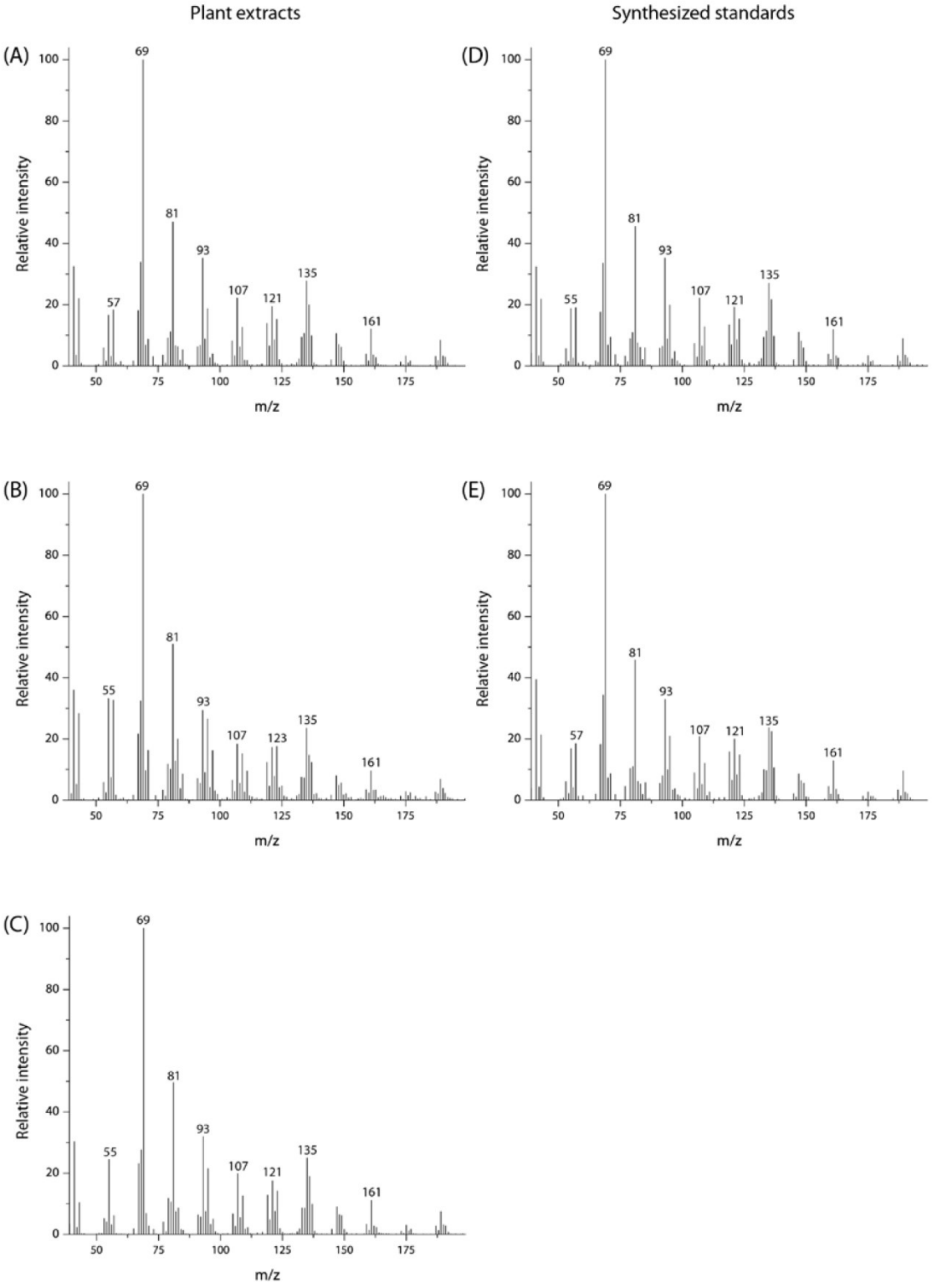

Supplemental Figure 12: EI-MS spectra of geranylgeranyl fatty acid esters. (A) geranylgeranyl-C16:0; (B) geranylgeranyl-aiC17:0; (C) mixture of geranylgeranyl-C18:1 and geranylgeranyl-C18:2; (D) geranylgeranyl-C17:0; (E) geranylgeranyl-C18:0. A-C were isolated from plant extracts and D and E were synthesized as standards.

3.3 Manuscript 3

Metal ions control product specificity of isoprenyl diphosphate synthases in the insect terpenoid pathway

Metal ions control product specificity of isoprenyl diphosphate synthases in the insect terpenoid pathway

Sindy Frick[a], Raimund Nagel[b], Axel Schmidt[b], René R. Bodemann[a], Peter Rahfeld[a], Gerhard Pauls[a], Wolfgang Brandt[c], Jonathan Gershenzon[b], Wilhelm Boland[a], and Antje Burse[a,1]

Departments of [a]Bioorganic Chemistry and [b]Biochemistry, Max Planck Institute for Chemical Ecology, Beutenberg Campus, D-07745 Jena, Germany; and [c]Department of Bioorganic Chemistry, Leibniz Institute of Plant Biochemistry, D-06120 Halle/Saale, Germany

Edited by Jerrold Meinwald, Cornell University, Ithaca, NY, and approved January 29, 2013 (received for review December 12, 2012)

Isoprenyl diphosphate synthases (IDSs) produce the ubiquitous branched-chain diphosphates of different lengths that are precursors of all major classes of terpenes. Typically, individual short-chain IDSs (scIDSs) make the C_{10}, C_{15}, and C_{20} isoprenyl diphosphates separately. Here, we report that the product length synthesized by a single scIDS shifts depending on the divalent metal cofactor present. This previously undescribed mechanism of carbon chain-length determination was discovered for a scIDS from juvenile horseradish leaf beetles, *Phaedon cochleariae*. The recombinant enzyme *P. cochleariae* isoprenyl diphosphate synthase 1 (*Pc*IDS1) yields 96% C_{10}-geranyl diphosphate (GDP) and only 4% C_{15}-farnesyl diphosphate (FDP) in the presence of Co^{2+} or Mn^{2+} as a cofactor, whereas it yields only 18% C_{10} GDP but 82% C_{15} FDP in the presence of Mg^{2+}. In reaction with Co^{2+}, *Pc*IDS1 has a K_m of 11.6 μM for dimethylallyl diphosphate as a cosubstrate and 24.3 μM for GDP. However, with Mg^{2+}, *Pc*IDS1 has a K_m of 1.18 μM for GDP, suggesting that this substrate is favored by the enzyme under such conditions. RNAi targeting *Pc*IDS1 revealed the participation of this enzyme in the de novo synthesis of defensive monoterpenoids in the beetle larvae. As an FDP synthase, *Pc*IDS1 could be associated with the formation of sesquiterpenes, such as juvenile hormones. Detection of Co^{2+}, Mn^{2+}, or Mg^{2+} in the beetle larvae suggests flux control into C_{10} vs. C_{15} isoprenoids could be accomplished by these ions in vivo. The dependence of product chain length of scIDSs on metal cofactor identity introduces an additional regulation for these branch point enzymes of terpene metabolism.

cobalt | kinetic | prenyltransferase | secretions | silencing

Terpenes are an extensive group of natural products serving essential biological functions in Eukaryota, Bacteria, and Archaea. The more than 55,000 terpenes identified thus far are crucial components of intracellular signal-transduction pathways, electron transport chains, and membranes, or they can function as hormones, photosynthetic pigments, and semiochemicals (1, 2). Despite their structural diversity, terpenes are derived from the universal linear C_{10}, C_{15}, C_{20}, and larger diphosphate intermediates whose synthesis is catalyzed by isoprenyl diphosphate synthases (IDSs), also known as prenyltransferases (3). Depending on the stereochemistry of the double bond of the reaction product, these enzymes are classified as either *trans*-IDSs or *cis*-IDSs (4, 5).

Here, we focus on *trans*-IDSs, which can be further divided into enzymes producing short-chain (C_{10}–C_{20}), medium-chain (C_{25}–C_{35}), and long-chain (C_{40}–C_{50}) IDS products (6). Short-chain IDSs (scIDSs) are named for their main end products. Geranyl diphosphate synthases (GDPSs; EC 2.5.1.1) catalyze the alkylation of the homoallylic isopentenyl diphosphate (C_5-IDP) by the allylic dimethylallyl diphosphate (C_5-DMADP) resulting in geranyl diphosphate (GDP), the ubiquitous C_{10}-building block of many monoterpenes. Farnesyl diphosphate synthases (FDPSs; EC 2.5.1.10) form farnesyl diphosphate (FDP), the C_{15} precursor of sesquiterpenes, and geranylgeranyl diphosphate synthases (GGDPSs; EC 2.5.1.29) produce geranylgeranyl diphosphate (GGDP), the C_{20} backbone of diterpenes.

Whereas FDPSs and GGDPSs occur nearly ubiquitously in plants, animals, fungi, and bacteria, GDPSs have mainly been described in plants and insects to date (7). In plants, they participate in the biosynthesis of defenses against herbivores and pathogens, as well as in the formation of attractants for pollinators and seed-dispersing animals (1). Most plant GDPSs make GDP as a single product (8). However, occasionally, the enzymes are bifunctional and also produce FDP [*Pb*GDPS from the orchid *Phalaenopsis bellina* (9)] or GGDP [*Pa*IDS1 from the spruce *Picea abies* (10)] in addition to GDP. So far, only a few GDPSs have been characterized in insects (7). Strikingly, most of them have the ability to form multiple products.

The GDPSs cloned from the bark beetle *Ips pini*, for example, displayed prenyltransferase and terpene synthase activity in succession (11), resulting in the formation of precursors for the de novo synthesis of monoterpenoid aggregation pheromones such as ipsdienol, which coordinates the colonization of coniferous trees (12). Bifunctionality was also observed from the scIDSs characterized from different aphid species (13–17). Here, the recombinant proteins generated both GDP and FDP in parallel, and hence may be involved in the biosynthesis of either aphid sex pheromones or the sesquiterpene (*E*)-β-farnesene, the most common component of alarm pheromones. How nature accomplishes mixed-product formation by scIDSs in insects as well as in plants is still poorly understood.

Generally, catalysis by scIDSs follows a sequential mechanism called "head-to-tail alkylation." During chain elongation, the allylic cosubstrate (DMADP or GDP) undergoes coupling with IDP through electrophilic alkylation at its carbon-carbon double bond (18, 19). The reaction depends for activation on a trinuclear metal cluster, usually containing Mg^{2+} or Mn^{2+} (20). Based on earlier studies describing the role of metal cofactors for scIDS catalysis, we tested the product composition of a unique scIDS discovered from juvenile horseradish leaf beetles, *Phaedon cochleariae*, in the presence of different metal ions. To our surprise, we found that the enzyme *P. cochleariae* isoprenyl diphosphate synthase 1 (*Pc*IDS1) possesses an unusual product regulation mechanism not previously described for scIDSs. It alters the chain length of its products depending on the cofactor: The protein yields C_{10}-GDP in the presence of Co^{2+} or Mn^{2+}, whereas it produces the longer C_{15}-FDP in the presence of Mg^{2+}. GDP is needed for the de novo synthesis of the cyclopentanoid monoterpene iridoids, defensive compounds that are produced during the entire larval stage of *P. cochleariae* (21, 22) (Fig. 1). On the

Author contributions: S.F., A.S., J.G., W. Boland, and A.B. designed research; S.F., R.N., R.R.B., P.R., and G.P. performed research; J.G., W. Boland, and A.B. contributed new reagents/analytic tools; S.F., R.N., A.S., R.R.B., P.R., G.P., W. Brandt, and A.B. analyzed data; and S.F., A.S., J.G., W. Boland, and A.B. wrote the paper.

The authors declare no conflict of interest.

This article is a PNAS Direct Submission.

Data deposition: The *Pc*IDS1 sequence reported in this paper has been deposited in the GenBank database (accession no. KC109782) and the *Pc*IDS1 model has been deposited in the Protein Model DataBase (ID code PM0078683).

[1]To whom correspondence should be addressed. E-mail: aburse@ice.mpg.de.

This article contains supporting information online at www.pnas.org/lookup/suppl/doi:10.1073/pnas.1221489110/-/DCSupplemental.

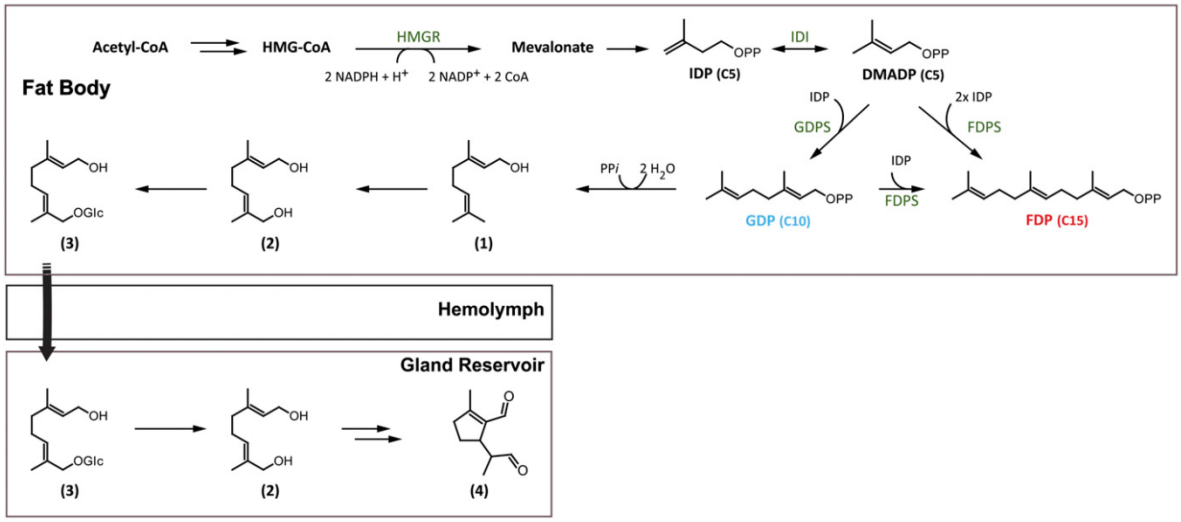

Fig. 1. Biosynthesis of iridoid monoterpene defenses in juvenile *P. cochleariae*: (1) geraniol, (2) 8-hydroxygeraniol, (3) 8-hydroxygeraniol-glucoside, (4) chrysomelidial. HMGR, 3-hydroxy-3-methyl-glutaryl-CoA reductase; IDI, isopentenyl diphosphate isomerase.

other hand, FDP serves as precursor for various primary metabolites and juvenile required hormone. The identification of Co^{2+}, Mn^{2+}, and Mg^{2+} in the juvenile beetles supports the notion that these organisms may control the product specificity of scIDSs by means of changes in local concentrations of these metal ions. Hence, the direction of flux at a branch point in terpene metabolism between defense and primary metabolism is regulated by an unprecedented IDS control mechanism.

Results

Identification and Tissue Distribution of a scIDS in Juvenile *P. cochleariae*. The use of degenerate primers allowed the amplification of a cDNA that encodes a protein of 430 aa (49.3 kDa, pI of 8.63) referred to here as *Pc*IDS1. ClustalW alignments revealed a high amino acid sequence identity of *Pc*IDS1 in relation to other functionally characterized insect scIDSs and showed all the conserved regions known for prenyltransferases (3, 23) (Fig. S1). The sequence also contains an RxxS motif (R_{67}–S_{70}), which could be the cleavage site for a mitochondrial targeting sequence already known from other identified scIDSs (11, 24).

Quantitative real-time assays revealed that *Pc*IDS1 transcripts are generally present in all analyzed larval tissues (Fig. S2*A*). However, the highest transcript abundance was observed in fat body tissue, which had a 5.6-fold higher transcript level compared with gut tissue. The transcript abundance was also reflected in protein level, because *Pc*IDS1 was detectable in all tested tissues, with the strongest signal derived from fat body tissue (Fig. S2*B*). Additionally, overall scIDS activity was determined in all crude extracts of the different larval tissues (Fig. 2*A*). In contrast to the trace amounts of FDP produced by extracts of every tissue tested, GDP-forming activity followed a different pattern. Compared with gut tissue, GDP formation was 141-fold higher in fat body tissue. Our results are consistent with recent findings on the distribution of the pathway to the iridoid defense compounds in *P. cochleariae* larvae. The early steps leading to the formation of the intermediate 8-hydroxygeraniol-glucoside are most likely localized in the fat body tissue. The glucoside is then transferred from there via the hemolymph into the defense glands, where the later steps in formation of chrysomelidial are located (25) (Fig. 1).

***Pc*IDS1 Is Involved in the Production of Defensive Monoterpenoids in Juvenile *P. cochleariae*.** RNAi experiments were performed with *P. cochleariae* to demonstrate the in vivo relevance of *Pc*IDS1. There were no significant differences in the relative growth rate between insects injected with a *PcIDS1*-dsRNA probe or with a control *Gfp* dsRNA probe and noninjected controls (NICs) (Fig. S3). However, transcript quantification 5 d after injection confirmed a significant *PcIDS1* mRNA reduction in fat body tissue (by 95%; $P < 0.001$) in comparison to *PcIDS1* mRNA levels in *Gfp*-treated larvae and NICs (Fig. 2*B*). Accordingly, 5 d after injection, the relative weight of defensive secretions decreased (by 52%; $P < 0.001$) in larvae challenged by *PcIDS1* dsRNA. This reduction continued until by day 13, a defenseless phenotype appeared that lacked secretions. The *Gfp* controls and NICs, on the other hand, produced unaltered amounts of defensive secretions (Fig. 2*C*). Detailed analyses of the relative amount of chrysomelidial per larva revealed a significant decline of this iridoid (by 78%; $P < 0.001$) in *PcIDS1*-treated larvae compared with the *Gfp* group and NICs after 5 d; this decline proceeded until there was a complete loss of secretions (Fig. 2*F*).

To determine if the chrysomelidial reduction is correlated with a decrease of the precursor, 8-hydroxygeraniol-glucoside, we analyzed the hemolymph and fat body tissue of larvae treated with *PcIDS1* dsRNA, *Gfp* dsRNA, and NICs. Seven days after *PcIDS1*-dsRNA injection, the level of precursor in the hemolymph was significantly reduced (by 89%; $P < 0.001$) compared with corresponding *Gfp* controls and NICs. This effect continued further with a reduction of 97% on day 11 (Fig. 2*E*). A similar effect was observed in the fat body tissue, where the amount of 8-hydroxygeraniol-glucoside was diminished (by 64.5 ± 14.08%) after 7 d. In addition to the reduction of chrysomelidial and 8-hydroxygeraniol-glucoside, we observed a significant loss of the overall scIDS activity (by 93%; $P < 0.001$) in the fat body tissue of *PcIDS1*-silenced larvae 7 d after injection compared with *Gfp* controls and NICs (Fig. 2*D*).

Recombinant *Pc*IDS1 Shows Metal Cofactor-Dependent Product Formation. Our results suggest that *Pc*IDS1 is involved in the biosynthesis of the monoterpenoid precursors needed for formation of the defensive compound chrysomelidial. Next, *Pc*IDS1 was expressed in *Escherichia coli* after truncation of the signal sequence at the 5′-end of the coding region, and the enzymatic activity of the purified recombinant protein was studied in vitro.

Like other scIDS proteins, *Pc*IDS1 was inactive without adding divalent metal cations, such as Mg^{2+} or Mn^{2+}. As recent

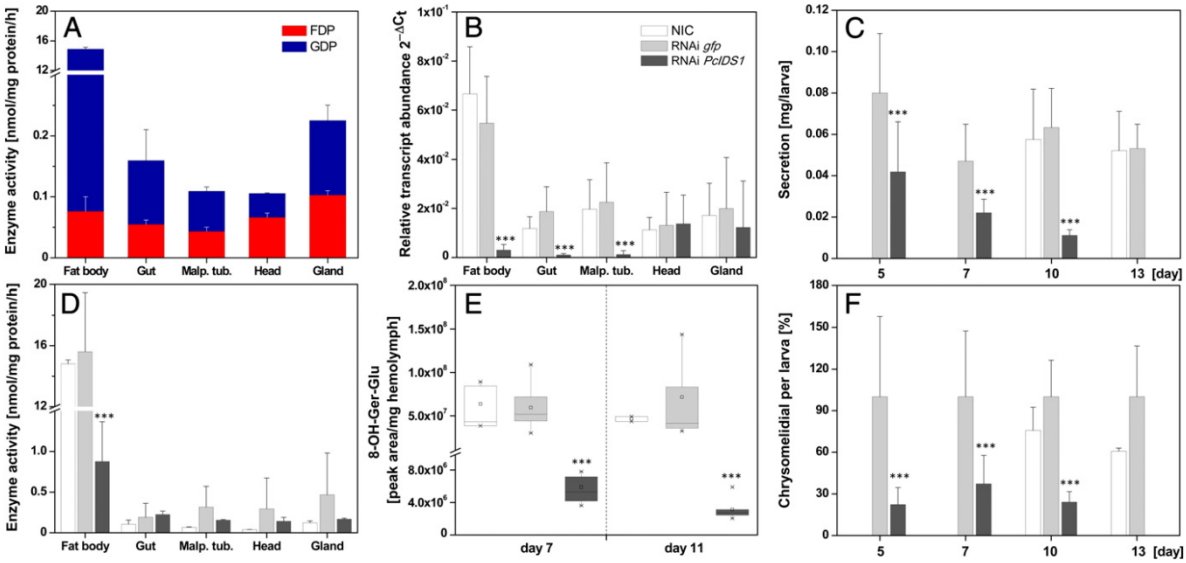

Fig. 2. Silencing *Pc*IDS1 in juvenile *P. cochleariae* by RNAi. (*A*) scIDS activity in tissue extracts of NICs: 10 μg of protein was incubated with 50 μM IDP, 50 μM DMADP, and 10 mM Mg^{2+} for 60 min ($n = 3$). (*B*) Relative transcript abundance ($2^{-\Delta Ct}$) of *Pc*IDS1 in different larval tissues 5 d after dsRNA injection ($n = 3$, ±SD). (*C*) Relative weight of larval secretions observed at different time points after dsRNA injection ($n = 3$, ±SD). (*D*) scIDS activity in tissues extracts 7 d after dsRNA injection. Ten micrograms of protein was incubated with 50 μM IDP, 50 μM DMADP, and 10 mM Mg^{2+} for 60 min ($n = 3$, ±SD). (*E*) Amount of 8-hydroxygeraniol-glucoside (8-OH-Ger-Glu) in hemolymph by HPLC analyses after dsRNA injection ($n = 3$, ±SD). (*F*) GC-MS analyses of chrysomelidial after dsRNA injection ($n = 3$, ±SD). Malp. tub., Malpighian tubules. ***, $p < 0.001$.

studies show, scIDS activity can be modulated by these metal ion cofactors (7, 15, 16, 26, 27); we therefore tested *Pc*IDS1 activity with IDP and two different allylic substrates, DMADP and GDP, in the presence of five different divalent cations. Each ion was tested separately at comparable concentration ranges.

In our assays with DMADP, the maximum overall enzyme activity for each cation was observed at 5 mM for Mg^{2+}, 0.5 mM for Co^{2+} and Mn^{2+}, and 0.1 mM for Ni^{2+} and Zn^{2+} (Fig. 3*A*, Fig. S4*A*, and Table S1). *Pc*IDS1 was far more active with Co^{2+} as an additive than with any other tested metal ion. Intriguingly, not only the overall enzyme activity but the product specificity varied considerably according to the different ions. In the presence of Co^{2+} or Mn^{2+}, with DMADP as a cosubstrate, *Pc*IDS1 produced about 96% GDP and only 4% FDP. In contrast, with Mg^{2+} as an additive, *Pc*IDS1 produced 18% GDP and 82% FDP.

Moreover, the optimal ion concentration changed depending on the allylic substrates. After GDP was substituted for DMADP, leading to the production of FDP, we observed *Pc*IDS1 being most active by addition of 0.5 mM Mg^{2+} compared with any other tested cofactor (Fig. 3*B*, Fig. S4*B*, and Table S1). Overall, Mg^{2+}, Mn^{2+}, and Co^{2+} represent the cofactors most favored in *Pc*IDS1 catalysis. Because Co^{2+} and Mg^{2+} resulted in the highest levels of *Pc*IDS1 activity, we used these cofactors in the following experiments.

In a first approach with DMADP, a constant Co^{2+} concentration of 0.5 mM was complemented with an ascending concentration of Mg^{2+} in a range of 0.001–10 mM (Fig. 4*A*). *Pc*IDS1 formed mainly GDP and only minor amounts of FDP, suggesting that Co^{2+} is the dominant metal ion independent of the tested Mg^{2+} concentration.

In a second approach with DMADP, we measured the enzyme activity with Mg^{2+} constant at 5 mM and an ascending concentration of Co^{2+} in the range of 0.001–10 mM (Fig. 4*B*). At Co^{2+} concentrations lower than 0.05 mM, FDP was the main product, accompanied by a 50% reduction in enzyme activity. However, if Co^{2+} concentrations exceeded 0.1 mM, *Pc*IDS1 activity clearly increased. Simultaneously, a shift from FDP to the reduced chain length of GDP was observed. Even if Mg^{2+} was 100-fold more abundant in the mixture, the enzyme definitely showed a preference for Co^{2+}.

With GDP as a cosubstrate, a constant 0.5 mM Co^{2+}, and an ascending Mg^{2+} concentration, *Pc*IDS1 displayed low FDP-forming activity (Fig. 4*C*). If Mg^{2+} is constant at 5 mM and Co^{2+} concentrations vary, we observed high FDP production only at Co^{2+} concentrations below 0.1 mM. However, as soon as the Co^{2+} concentration ascends, the FDP-forming activity decreases dramatically (Fig. 4*D*). Our findings indicate that the Mg^{2+}-catalyzed activity of *Pc*IDS1 is abolished as soon as Co^{2+} reaches its optimal concentration.

To determine the conformational state of *Pc*IDS1 quaternary structure, size exclusion chromatography was performed. Fig. S5 shows the relative retention volumes of the apoprotein without adding cofactors and *Pc*IDS1 in presence of Co^{2+} (0.5 mM) or Mg^{2+} (5 mM). Surprisingly, we found an obvious difference in the elution volume among the apoprotein (without divalent metal), the *Pc*IDS1-Mg^{2+} complex, and the *Pc*IDS1-Co^{2+} complex. The apoprotein eluted from the column at a retention volume of 76.36 mL (corresponding to 74.6 kDa), whereas *Pc*IDs1-Mg^{2+} and *Pc*IDS1-Co^{2+} eluted at 73.65 mL (corresponding to 93.8 kDa) and 74.46 mL (corresponding to 87.6 kDa), respectively. Given the calculated monomeric mass of 45.8 kDa, this indicates on one hand that the enzyme is always present as a dimer regardless of added cofactor. On the other hand, the difference in the elution volume reflects a change in the hydrodynamic volume of the protein caused by the divalent metal. In the case of Mg^{2+}, the dimeric protein possesses the largest volume, most likely due to a more relaxed conformation. With Co^{2+}, *Pc*IDS1 seems to have a more compact conformation, which may be responsible for the change in product spectrum. As a control, we also analyzed the metal influence on the standard proteins and observed no obvious difference in the elution volume with addition of various amounts of Mg^{2+} or Co^{2+}.

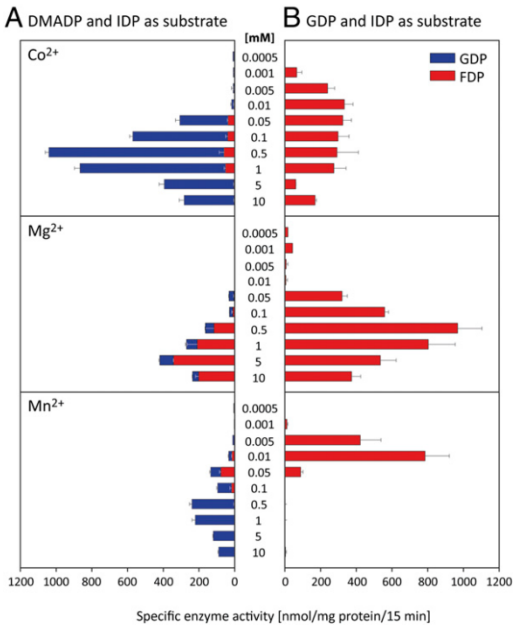

Fig. 3. Effect of metal cofactors on enzyme activity and product formation of *Pc*IDS1. (*A*) Different concentrations of Co^{2+}, Mg^{2+}, and Mn^{2+} were added to *Pc*IDS1 and incubated with 50 μM IDP and 50 μM DMADP ($n = 3$, ±SD). (*B*) Different concentrations of Co^{2+}, Mg^{2+}, and Mn^{2+} were added to *Pc*IDS1 and incubated with 50 μM IDP and 50 μM GDP ($n = 3$, ±SD).

Kinetic Analyses of Purified *Pc*IDS1. All kinetic parameters measured for *Pc*IDS1 are displayed in Table 1. In combination with Co^{2+} and fixed IDP, *Pc*IDS1 has a K_m of 11.6 μM for DMADP (Fig. S6*A*) and a K_m of 24.3 μM for GDP (Fig. S6*E*), suggesting that DMADP is the preferred substrate compared with GDP. Significant differences in the V_{max} were not observed. With Co^{2+} and DMADP fixed at 50 μM, *Pc*IDS1 has a K_m of 0.8 μM for IDP and substrate inhibition at higher concentrations with a K_i of 46.6 μM (Fig. S6*B*). No inhibitory effect of IDP was observed with GDP fixed at 50 μM (Fig. S6*F*).

In combination with Mg^{2+} and fixed IDP, *Pc*IDS1 displayed atypical kinetics for DMADP that resulted in a biphasic curve (Fig. S6*C*). In the first part of the curve from 0.1 to 100 μM DMADP, the reaction seems to follow a Michaelis–Menten kinetic. However, the curve displays a different slope as soon as the DMADP concentration exceeds 50 μM. The K_m for GDP was 1.2 μM with a slight substrate inhibition (Fig. S6*G*). With Mg^{2+} and DMADP fixed at 50 μM, *Pc*IDS1 has a K_m of 11.8 μM for IDP with a slight substrate inhibition (Fig. S6*D*), and with GDP fixed at 50 μM, the K_m of IDP was 7.1 μM (Fig. S6*H*). Analyses of the calculated V_{max} show that Mn^{2+} gave generally lower reaction velocities than did Co^{2+}.

The kinetic parameters substantiate our previous observations that *Pc*IDS1 has a preference for Co^{2+} with DMADP as an allylic cosubstrate giving the C_{10} product GDP. If Mg^{2+} is the metal cofactor, GDP is the favored cosubstrate affording the C_{15} product FDP.

Metal Cofactors Identified in *P. cochleariae* Larvae Have Different Affinities in the Enzyme Complex. Inductively coupled plasma-MS analysis of *P. cochleariae* larvae showed an overall concentration of Co^{2+} in the fat body tissue at ≥0.24 μg/g of dry weight (DW) or 4 nmol/g of DW, and an overall concentration of Mn^{2+} at ≥16.6 μg/g of DW or 0.3 μmol/g of DW, whereas Mg^{2+} was found at a concentration of 2,223 μg/g of DW or 91 μmol/g of DW in the fat body (Table S2).

Quantum mechanical calculations revealed reaction energies of about 40 kcal/mol lower for the formation of complexes containing Co^{2+} or Mn^{2+} compared with those containing Mg^{2+} for association with the diphosphate of DP^{3-} or the aspartate residues of the enzyme (mimicked by propionic acid anions) (Tables S3 and S4). In all cases, the affinity of the metal cations for the diphosphate was more than 200 kcal/mol higher than for the aspartate residues. Based on these gas phase calculations, the deduced minimum equilibrium constant for formation of the diphosphate metal complex is at least 10^{28}-fold higher for Co^{2+} or Mn^{2+} than for Mg^{2+}, which suggests that *Pc*IDS1 may have a considerably higher affinity for Co^{2+} or Mn^{2+} than for Mg^{2+}, although the magnitude of this difference may be reduced somewhat by solvation effects not considered here. Hence, the low concentrations of Co^{2+} or Mn^{2+} in the larval tissue in comparison to Mg^{2+} may be compensated for by their greater complex formation ability with diphosphate. On the other hand, if one compares the affinities of either the metal ion-complexed diphosphate with the aspartate (assuming the metal cations are delivered to the binding site together with the substrate) or, alternatively, the metal-complexed aspartates with the diphosphate (Tables S5 and S6), in both cases, the affinities for Co^{2+} or Mn^{2+} are lower than the affinity for Mg^{2+} in nice agreement with the measured lower $K_{m\ (GDP)}$ (higher affinity) ($Mg^{2+} = 1.18$ μM, $Co^{2+} = 24.3$ μM) and might be an explanation for the experimental differences in product specificity with different divalent metal ions. Note, one order of magnitude in K_m represents 1.4 kcal/mol (ΔG) in interaction energies.

Discussion

Understanding the mechanism of chain-length determination of scIDSs has been a major challenge for researchers of terpene biosynthetic enzymes, and much has been learned about active site features that restrict the length of the enzyme products. The determination of product carbon length by the identity of the metal cofactor apparently provides an alternative mechanism to the regulation of product formation by scIDS. Given that plants possess a number of genes encoding IDSs [e.g., at least 10 in *Arabidopsis thaliana* (8)], whereas insects possess only a few [e.g., 3 in *Bombyx mori* (28)], insects may compensate for this disparity by generating different chain-length products in other ways. In our case, the metal ion-mediated product differences enable the *P. cochleariae* beetles to supply precursors for two terpene pathways, one for monoterpene metabolism (synthesis of chemical defenses) and one for sesquiterpene metabolism (juvenile hormone formation), using only a single enzyme. Instead of "inventing" a new IDS, insects appear to use different cofactors to add an additional product to an enzyme's repertoire, thereby lowering metabolic costs. Such a regulation mechanism may allow faster adaptation to developmental or environmental changes that insects may face, such as metamorphosis or host plant shifts. Due to differences in metal ion identity and concentration, shifts in overall scIDS activity have previously been observed for enzymes from plants [e.g., *Abies grandis* (29)] and for enzymes from insects [e.g., *Myzus persicae* (15), *Choristoneura fumiferana* (30)], but without alterations in product chain length. However, Sen et al. (26) report cofactor-dependent changes of product chain length in crude homogenates of the *corpora allata* of the lepidopteran *Manduca sexta*. The product ratios formed during the coupling of DMADP with IDP by means of scIDS activity showed that FDP formation was stimulated by adding Mg^{2+}, whereas GDP formation increased in the presence of Mn^{2+}. Taken together with our results, these findings should motivate researchers to test alternative cofactors with scIDSs in the future.

*Pc*IDS1 produces mainly GDP (95%) in the presence of Co^{2+} (or Mn^{2+}) with IDP and DMADP as substrates and produces only minor amounts of FDP (4%). In contrast, with Mg^{2+}, the predominant product was FDP (82%); only minor amounts of GDP (18%) were produced. Our kinetic data for *Pc*IDS1 support the observation that the regulation of product distribution by these metal cofactors is biochemically relevant. Comparisons

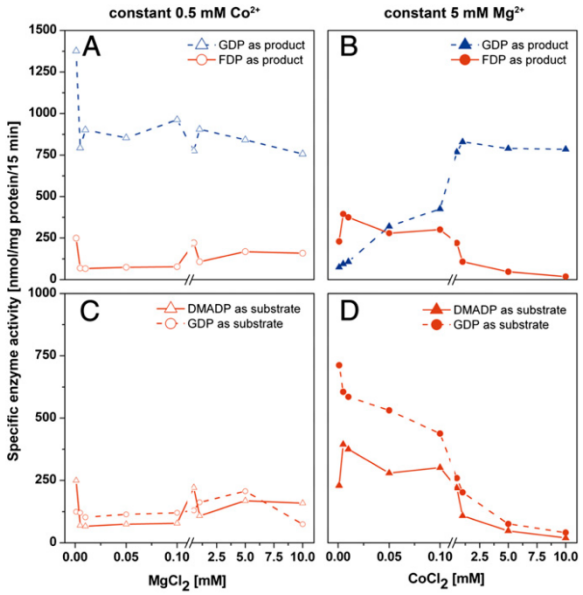

Fig. 4. Effect of mixtures of divalent metal ion cofactors on enzyme activity and product formation of *Pc*IDS1. (*A*) Constant 0.5 mM Co^{2+} with an ascending Mg^{2+} concentration in a range of 0.001 mM up to 10 mM with 50 μM IDP or 50 μM DMADP ($n = 2$). (*B*) Constant 5 mM Mg^{2+} with an ascending Co^{2+} concentration from 0.001 mM up to 10 mM with 50 μM IDP or 50 μM DMADP ($n = 2$). (*C*) FDP formation at constant 0.5 mM Co^{2+} with an ascending Mg^{2+} concentration with 50 μM GDP or 50 μM DMADP ($n = 2$). (*D*) FDP formation at constant 5 mM Mg^{2+} with an ascending Co^{2+} concentration with 50 μM GDP or 50 μM DMADP ($n = 2$).

with kinetic data available from plant GDPSs in the presence of DMADP revealed that the $K_{m(DMADP)}$ of *Pc*IDS1 (11.6 μM) with Co^{2+} corresponds to the K_m of the enzyme from *Anthirrhium majus* (24.1 μM) (31) or *Anthirrhium grandis* (16.7 μM) (29). $K_{m(DMADP)}$ values from insect scIDSs have so far been determined only for the bifunctional GDPSs of *M. persicae* *Mp*IPPS1-S (28.6 μM) (17) and *Mp*IPPS2-S (24.2 μM) (17), as well as *Aphis gossypii* (39.2 μM) (14), and for the FDPS from *Drosophila melanogaster* *Dm*FPPS-1b (33.5 μM) (32). The K_m of *Pc*IDS1 is found within the range of literature values. The combination of DMADP with Mg^{2+} did not allow a K_m calculation due to the biphasic progression of the kinetic curve. Although DMADP reacts initially with IDP to form GDP, in later catalytic cycles, the GDP formed can compete with another molecule of DMADP at the allylic binding site of *Pc*IDS1. If GDP is the preferred allylic substrate in combination with Mg^{2+}, it can lead to the formation of FDP.

The K_m values of *Pc*IDS1 for GDP, which are 24.3 μM and 1.1 μM in the presence of Co^{2+} and Mg^{2+}, respectively, are in the range of K_m values for previously described insect scIDSs, such as those of *A. gossypii* (12.6 μM) (14), *D. melanogaster* FPPS-1b (7 μM) (32), *M. sexta* (0.8 μM) (27), and *M. persicae* (*Mp*IPPS1-S, 25.4 μM; *Mp*IPPS2-S, 15.4 μM) (17). The difference in the *Pc*IDS1 K_m values for different metal cofactors suggests that the enzyme favors GDP as a substrate with Mg^{2+}. The alteration of IDS product specificity by metal ions has so far been described only for long-chain IDSs from microbes. In the presence of Co^{2+} or Mn^{2+}, octaprenyl-, solanesyl-, and decaprenyl-diphosphate synthases gave a variety of polyprenyl products whose chains were longer by up to two isoprene units than those of the products formed in the presence of Mg^{2+} (33–35).

IDS structure elucidation in combination with mutagenesis studies has suggested that product chain length is determined by the size of the hydrophobic pocket in the active center. In particular, the amino acids in the vicinity of the conserved first and second aspartate-rich regions (FARM and SARM motifs, respectively) form a steric hindrance that terminates chain elongation (3, 23, 36, 37). The van der Waals radii of Co^{2+} and Mn^{2+} are 1.73 Å and 1.9 Å, respectively, both of which are larger than that of Mg^{2+} at 0.96 Å (38). These differences may lead to conformational changes of *Pc*IDS1 or to rearrangements of substrate position in the enzymes that influence chain-length elongation. First hints toward conformational changes were obtained by size exclusion chromatography that revealed differences in the quaternary structure due to complex formation with different metal ions. Further homology modeling in combination with site-directed amino acid mutagenesis is needed to explain more fully how changes in cofactors influence the chain-length determination mechanism for *Pc*IDS1.

Mg^{2+} and Mn^{2+} are well-known cofactors for scIDS activity; however, in our biochemical characterization, *Pc*IDS1 showed the highest GDP synthase activity in the presence of Co^{2+}. Despite its rare occurrence in nature, Co^{2+} plays a role as a cofactor in a number of proteins (e.g., methionine aminopeptidase, glucose isomerase) (39). To balance the need for cobalt with its intrinsic toxicity, nature has evolved trafficking systems to maintain metal homeostasis (40). For example, in the transcriptome from *P. cochleariae*, we have identified a transport protein that shows high similarity to the cobalt uptake protein Cot 1 of *Saccharomyces cerevisiae* (41). This finding and the calculated high affinity of Co^{2+} to *Pc*IDS1 underline the possibility that Co^{2+} is an available as well as biologically relevant cofactor for this enzyme despite its low concentration in the larvae.

Using an RNAi approach, we were able to show that the *Pc*IDS1-catalyzed formation of GDP is involved in the production of monoterpenoid defensive compounds in *P. cochleariae* larvae. However, we could not detect a phenotype arising from the loss of formation of the alternate product, FDP. In insects, FDP is the essential precursor for the synthesis of juvenile hormones (42), and it is localized in the *corpora allata* complex found in the head posterior to the brain. Given that RNAi efficiency can differ from tissue to tissue as well as from gene to gene (43), the lack of a phenotype caused by low FDP levels might be attributed to ineffective silencing in the larval head. However, even more important may be the existence of additional prenyltransferases. Aphids, coleopterans, and lepidopterans are known to possess up to three scIDSs, and we are currently searching for additional scIDSs in *P. cochleariae*, which, like many other

Table 1. Kinetic constants for *P. cochleariae* *Pc*IDS1 depend on the identity of both the metal cofactor and allylic substrate

	Co^{2+}				Mg^{2+}			
Fixed substrate	$IDP_{(15\ \mu M)}$	$IDP_{(50\ \mu M)}$	$DMADP_{(50\ \mu M)}$	$GDP_{(50\ \mu M)}$	$IDP_{(50\ \mu M)}$	$IDP_{(50\ \mu M)}$	$DMADP_{(50\ \mu M)}$	$GDP_{(50\ \mu M)}$
Substrate	DMADP	GDP	IDP	IDP	DMADP	GDP	IDP	IDP
$K_{m\ (substrate)}$, μM	11.60	24.31	0.84	1.46	~1103	1.19	11.79	7.08
V_{max}, μmol·min^{-1}·mg^{-1} of protein	0.44	0.41	0.67	0.23	~2.39	0.12	0.17	0.20
$K_{i\ (substrate)}$, μM	n.d.	n.d.	46.62	n.d.	n.d.	1,047	572.7	322.1

n.d., not detectable.

enzymes of this class, may make more than one product. Our work shows that enzymes with an intrinsic promiscuity may also use exogenous factors, such as metal cofactors, to regulate product synthesis. It also serves as a reminder that neither substrate specificity nor product profiles can always be predicted by sequence similarity. Instead, rigorous biochemical testing is needed to establish enzyme function, especially among enzymes of terpene metabolism.

Materials and Methods

A scIDS from *P. cochleariae* was isolated with a degenerated PCR approach and RACE amplification. For further biochemical characterization, heterologous expression in *E. coli* Bl21 star (DE3) and protein purification were performed by affinity chromatography with Ni-nitrilotriacetric acid agarose columns. RNAi techniques were used to determine in vivo relevance, followed by quantitative real-time PCR, the quantification of 8-hydroxygeraniol via liquid chromatography (LC)-tandem MS (MS/MS), the relative quantification of chrysomelidial with GC-MS, and *Pc*IDS1 activity measurements determined by LC-MS/MS. Kinetic analyses and product determination were realized by LC-MS/MS, and calculations were performed with GraphPad Prism (GraphPad Software). Details of beetle rearing, reagents, protein purification/sequencing, antibody production, RNAi techniques, LC-MS/MS, GC-MS, quantitative PCR, sequence analyses, and other methods used in this study are described in *SI Materials and Methods*.

ACKNOWLEDGMENTS. We thank Dr. Dirk Merten for the element analysis and Angelika Berg and Dr. Maritta Kunert for technical assistance. We thank Prof. Jacques M. Pasteels for helpful discussions on aspects of this work and Emily Wheeler for critically reading of the manuscript. This work has been supported by the Deutsche Forschungsgemeinschaft (Grant BU 1862/2-1) and the Max Planck Society.

1. Gershenzon J, Dudareva N (2007) The function of terpene natural products in the natural world. *Nat Chem Biol* 3(7):408–414.
2. Pichersky E, Noel JP, Dudareva N (2006) Biosynthesis of plant volatiles: Nature's diversity and ingenuity. *Science* 311(5762):808–811.
3. Wang KC, Ohnuma S (2000) Isoprenyl diphosphate synthases. *Biochim Biophys Acta* 1529(1-3):33–48.
4. Kharel Y, Koyama T (2003) Molecular analysis of cis-prenyl chain elongating enzymes. *Nat Prod Rep* 20(1):111–118.
5. Liang PH (2009) Reaction kinetics, catalytic mechanisms, conformational changes, and inhibitor design for prenyltransferases. *Biochemistry* 48(28):6562–6570.
6. Gershenzon J, Kreis J (1999) Biochemistry of terpenoids: Monoterpenes, sesquiterpenes, diterpenes, sterols, cardiac glycosides, and steroid saponins. *Biochemistry of Plant Secondary Metabolism*, ed Wink M (Sheffield Academic, Sheffield, UK), pp 222–299.
7. Vandermoten S, Haubruge E, Cusson M (2009) New insights into short-chain prenyltransferases: Structural features, evolutionary history and potential for selective inhibition. *Cell Mol Life Sci* 66(23):3685–3695.
8. Tholl D, Lee S (2011) Terpene specialized metabolism in *Arabidopsis thaliana*. *The Arabidopsis Book*, ed Last R (American Society of Plant Biologists, Rockville, MD), Vol 9, pp e0143.
9. Hsiao YY, et al. (2008) A novel homodimeric geranyl diphosphate synthase from the orchid Phalaenopsis bellina lacking a DD(X)2-4D motif. *Plant J* 55(5):719–733.
10. Schmidt A, et al. (2010) A bifunctional geranyl and geranylgeranyl diphosphate synthase is involved in terpene oleoresin formation in *Picea abies*. *Plant Physiol* 152(2):639–655.
11. Gilg AB, Bearfield JC, Tittiger C, Welch WH, Blomquist GJ (2005) Isolation and functional expression of an animal geranyl diphosphate synthase and its role in bark beetle pheromone biosynthesis. *Proc Natl Acad Sci USA* 102(28):9760–9765.
12. Blomquist GJ, et al. (2010) Pheromone production in bark beetles. *Insect Biochem Mol Biol* 40(10):699–712.
13. Lewis MJ, Prosser IM, Mohib A, Field LM (2008) Cloning and characterisation of a prenyltransferase from the aphid *Myzus persicae* with potential involvement in alarm pheromone biosynthesis. *Insect Mol Biol* 17(4):437–443.
14. Ma G-Y, Sun XF, Zhang YL, Li ZX, Shen ZR (2010) Molecular cloning and characterization of a prenyltransferase from the cotton aphid, *Aphis gossypii*. *Insect Biochem Mol Biol* 40(7):552–561.
15. Vandermoten S, et al. (2008) Characterization of a novel aphid prenyltransferase displaying dual geranyl/farnesyl diphosphate synthase activity. *FEBS Lett* 582(13): 1928–1934.
16. Vandermoten S, et al. (2009) Structural features conferring dual geranyl/farnesyl diphosphate synthase activity to an aphid prenyltransferase. *Insect Biochem Mol Biol* 39(10):707–716.
17. Zhang Y-L, Li Z-X (2012) Functional analysis and molecular docking identify two active short-chain prenyltransferases in the green peach aphid, *Myzus persicae*. *Arch Insect Biochem Physiol* 81(2):63–76.
18. Oldfield E, Lin FY (2012) Terpene biosynthesis: Modularity rules. *Angew Chem Int Ed Engl* 51(5):1124–1137.
19. Brandt W, et al. (2009) Molecular and structural basis of metabolic diversity mediated by prenyldiphosphate converting enzymes. *Phytochemistry* 70(15-16):1758–1775.
20. Aaron JA, Christianson DW (2010) Trinuclear metal clusters in catalysis by terpenoid synthases. *Pure Appl Chem* 82(8):1585–1597.
21. Pasteels JM, Braekman JC, Daloze D, Ottinger R (1982) Chemical defence in chrysomelid larvae and adults. *Tetrahedron* 38(13):1891–1897.
22. Termonia A, Hsiao TH, Pasteels JM, Milinkovitch MC (2001) Feeding specialization and host-derived chemical defense in Chrysomeline leaf beetles did not lead to an evolutionary dead end. *Proc Natl Acad Sci USA* 98(7):3909–3914.
23. Tarshis LC, Proteau PJ, Kellogg BA, Sacchettini JC, Poulter CD (1996) Regulation of product chain length by isoprenyl diphosphate synthases. *Proc Natl Acad Sci USA* 93(26):15018–15023.
24. von Heijne G (1990) The signal peptide. *J Membr Biol* 115(3):195–201.
25. Burse A, et al. (2008) Implication of HMGR in homeostasis of sequestered and *de novo* produced precursors of the iridoid biosynthesis in leaf beetle larvae. *Insect Biochem Mol Biol* 38(1):76–88.
26. Sen SE, Brown DC, Sperry AE, Hitchcock JR (2007) Prenyltransferase of larval and adult M. sexta corpora allata. *Insect Biochem Mol Biol* 37(1):29–40.
27. Sen SE, Sperry AE (2002) Partial purification of a farnesyl diphosphate synthase from whole-body Manduca sexta. *Insect Biochem Mol Biol* 32(8):889–899.
28. Kaneko Y, Kinjoh T, Kiuchi M, Hiruma K (2011) Stage-specific regulation of juvenile hormone biosynthesis by ecdysteroid in *Bombyx mori*. *Mol Cell Endocrinol* 335(2): 204–210.
29. Tholl D, Croteau R, Gershenzon J (2001) Partial purification and characterization of the short-chain prenyltransferases, geranyl diphosphate synthase and farnesyl diphosphate synthase, from Abies grandis (grand fir). *Arch Biochem Biophys* 386(2):233–242.
30. Sen SE, et al. (2007) Purification, properties and heteromeric association of type-1 and type-2 lepidopteran farnesyl diphosphate synthases. *Insect Biochem Mol Biol* 37(8): 819–828.
31. Tholl D, et al. (2004) Formation of monoterpenes in *Antirrhinum majus* and *Clarkia breweri* flowers involves heterodimeric geranyl diphosphate synthases. *Plant Cell* 16(4):977–992.
32. Sen SE, Trobaugh C, Béliveau C, Richard T, Cusson M (2007) Cloning, expression and characterization of a dipteran farnesyl diphosphate synthase. *Insect Biochem Mol Biol* 37(11):1198–1206.
33. Ohnuma S, Koyama T, Ogura K (1992) Chain length distribution of the products formed in solanesyl diphosphate synthase reaction. *J Biochem* 112(6):743–749.
34. Ohnuma S, Koyama T, Ogura K (1993) Alteration of the product specificities of prenyltransferases by metal ions. *Biochem Biophys Res Commun* 192(2):407–412.
35. Fujii H, et al. (1980) Variable product specificity of solanesyl pyrophosphate synthetase. *Biochem Biophys Res Commun* 96(4):1648–1653.
36. Chen AJ, Kroon PA, Poulter CD (1994) Isoprenyl diphosphate synthases: Protein sequence comparisons, a phylogenetic tree, and predictions of secondary structure. *Protein Sci* 3(4):600–607.
37. Szkopińska A, Płochocka D (2005) Farnesyl diphosphate synthase; regulation of product specificity. *Acta Biochim Pol* 52(1):45–55.
38. Heuts JPA, Schipper E, Piet P, German AL (1995) Molecular mechanics calculations on cobalt phthalocyanine dimers. *Theochem-J Mol Struct* 333(1-2):39–47.
39. Kobayashi M, Shimizu S (1999) Cobalt proteins. *Eur J Biochem* 261(1):1–9.
40. Okamoto S, Eltis LD (2011) The biological occurrence and trafficking of cobalt. *Metallomics* 3(10):963–970.
41. Conklin DS, McMaster JA, Culbertson MR, Kung C (1992) COT1, a gene involved in cobalt accumulation in Saccharomyces cerevisiae. *Mol Cell Biol* 12(9):3678–3688.
42. Bellés X, Martín D, Piulachs MD (2005) The mevalonate pathway and the synthesis of juvenile hormone in insects. *Annu Rev Entomol* 50:181–199.
43. Terenius O, et al. (2011) RNA interference in Lepidoptera: An overview of successful and unsuccessful studies and implications for experimental design. *J Insect Physiol* 57(2):231–245.

Supporting Information

Frick et al. 10.1073/pnas.1221489110

SI Materials and Methods

Beetle Rearing and Secretion Collection. *Phaedon cochleariae* (F.) was laboratory-reared as continuous cultures (York chamber, 15 °C and 16-h/8-h light/dark period) on leaves of *Brassica rapa* spp. Larval secretion was collected in glass capillaries (inner diameter = 0.28 mm, outer diameter = 0.78 mm, length = 100 mm; Hirschmann Laborgeraete, Eberstadt, Germany). Sealed capillaries containing samples were stored at −20 °C until needed. Secretions were weighed in the sealed capillaries on an ultramicrobalance (Mettler–Toledo) three times; the weight of empty capillaries was subtracted, and the final weight was averaged.

Isolation and Cloning of a cDNA encoding the *Phaedon cochleariae* isoprenyl diphosphate synthase 1 (*Pc*IDS1). Tissue samples from the head, gut, fat body, Malpighian tubules, and defensive glands were taken from third-instar larvae dissected in Ringer's solution (1) and directly transferred in liquid nitrogen-cooled reaction tubes. Total RNA was extracted with the RNeasy Micro Kit (Qiagen) according to the manufacturer's instructions. Complete removal of DNA was achieved using the RNase-free DNase Set (Qiagen). The quality of the RNA was evaluated by measuring the 260:280-nm absorbance ratio, and the integrity of 18S and 28S ribosomal RNA bands was assessed by electrophoresis on RNA 6000 Nano labchips (Agilent Technologies). RNA concentrations were determined from absorbance values at a wavelength of 260 nm. First-strand cDNA was subsequently transcribed from total RNA using SuperScript III reverse transcriptase (Life Technologies). Up to 1 μg of total RNA was reverse-transcribed according to the manufacturer's instructions using oligo(dT)$_{12–18}$ primer. Degenerated primers were designed against the highly conserved regions of previously identified short-chain isoprenyl diphosphate synthases (scIDSs) from *Myzus persicae*, *Aphis gossypii*, *Agrotis ipsilon*, and *Anthonomus grandis*. PCR amplification using Taq DNA Polymerase (Promega) of a 686-bp core fragment was performed with the primer pair FWD_211_geranyl diphosphate synthase (GDPS) (5′-TTC ATG G(AC)(ACT)(GT)(GT)(GC)TTCCC(AGC)GA-3′) and REV_903_GDPS (5′-GAAGTCAT(CT)(CT)TGA(AC)(CT)TTG-3′). The following cycling profile was carried out in an Eppendorf thermal cycler: 3 min at 94 °C; 35 cycles of 30 s at 94 °C, 30 s at 45 °C, and 1 min at 72 °C; and a final 10-min extension at 72 °C. PCR products were purified using QiaEx II (Qiagen), ligated into pCR2.1-TOPO vector (Life Technologies), and sequenced. To obtain full-length cDNA sequence of *P. cochleariae* isoprenyl diphosphate synthase (IDS), a BD SMART RACE cDNA Amplification Kit (BD Biosciences) was used. For amplification of the 5′-end, site sequence-specific reverse primers were designed as followed: RACE_5_214_Rev (5′-CCCTAGGATGCCGGCCAATCTCACG-3′) and nested primer RACE_5_140_Rev (5′-GTGGACAGGCCCCTGGTCTTCTTGC-3′). The sequence-specific primers for the 3′-end site were RACE_3_447_FWD (5′-GACCAACATGGGCCAATCTTTAGACGC-3′) and nested primer RACE_3_483_FWD (5′-GAAGGATGGGAGGCCCATATTGAGCC-3′). The 5′ and 3′ RACE products were cloned and sequenced. The resulting assembled cDNA sequence contained a 1,290-bp open-reading frame that encodes an IDS similar protein of 430 aa referred to here as *P. cochleariae* isoprenyl diphosphate synthase 1 (*Pc*IDS1). This sequence of *Pc*IDS1was registered at GenBank (accession no. KC109782).

Functional Expression and Purification of Recombinant *Pc*IDS1. The entire encoding sequence of *Pc*IDS1 lacking the predicted signal peptide (based on analysis with SignalP 4.1 (2), available at the prediction servers of the Center for Biological Sequence Analysis, Technical University of Denmark, Lyngby, Denmark) was amplified with the following primers that included the start and stop codons for translation in an *Escherichia coli*-based heterologous expression system: *Pc*IDS1-forward (5′-CACCAGGGCCCTCTCCACGATC-3′) and *Pc*IDS1-reverse (5′-CTATGCATCCCTCTTGTAAATCTTCTT-3′). Template cDNA was synthesized by RT from RNA of whole-body *P. cochleariae* larvae, except for the gut tissue. PCR was performed using an Expand High Fidelity PCR system (Roche Applied Science). PCR was performed for 3 min at 94 °C for denaturation, followed by 10 cycles of 15 s at 94 °C, 30 s at 55 °C, and 90 s at 72 °C; 20 cycles of 15 s at 94 °C, 30 s at 55 °C, and 90 s plus 5 s of elongation for each cycle at 72 °C; and a final extension for 7 min at 72 °C. The resulting cDNA fragment was purified with the Zymoclean Gel DNA Recovery Kit (Zymo) and cloned in the expression vector pET100/D-TOPO (Invitrogen), which has a 6 × His-tag on the N terminus. Plasmids were transferred into the strain *E. coli* TOP10F (Life Technologies) and sequenced. Positive constructs were then transferred into different expression strains, including BL21(DE3) star (Invitrogen), BL21(DE3) pLysS (Life Technologies), and Rosetta (DE3; Novagen), but strain BL21(DE3) star produced the highest amount of soluble and active protein of long and short *Pc*IDS1. Bacterial precultures of 20 mL were grown over 3 d at 18 °C under continuous rotation on LB with 50 μg/mL carbenicillin. Afterward, the cells were pelleted and used to inoculate the 200-mL expression culture. There, we used the Overnight Express Autoinduction System 1 (Novagen) and let them grow over 2 d at 18 °C under continuous rotation to stationary phase according to the manufacturer's recommendations. Bacterial pellets were resuspended in 2 mL of assay buffer containing 25 mM 3-(*N*-morpholino)-2-hydroxypropanesulfonic acid (MOPSO; pH 7.3), 10% (vol/vol) glycerol, and 150 mM NaCl. The suspension was sonicated using a Sonopuls HD2070 (Bandelin) for 4 min, cycle 2, at 60% power. The overexpressed His-tagged proteins were subsequently column-purified by affinity chromatography with Ni-nitrilotriacetic acid agarose columns (Qiagen) using a stepwise imidazole gradient from 10 to 500 mM. The purity of the recombinant proteins was evaluated by SDS/PAGE gel electrophoresis, followed by colloidal Coomassie staining (Roti-Blue Colloidal Coomassie Staining; Carl Roth). The purified *Pc*IDS1 migrated at ∼45.8 kDa (399 aa). Fractions that contained the highest amount of pure recombinant protein were pooled and desalted in assay buffer with a PD-10 Desalting column (Amersham Biosciences) to remove the imidazole.

To see if the affinity tag influenced the enzyme activity, the fusion protein *Pc*IDS1 was subsequently cleaved using the highly specific serine protease EnterokinaseMax (Life Technologies) according to the manufacturer's instructions. After purification and removal of the affinity tag, cleavage was checked by SDS/PAGE and Western blotting using the anti-His antibody. The fusion protein and the cleaved protein were tested for their enzyme activity. Because cleavage of the tag altered neither the activity nor the product profile, the truncated His-tagged fusion protein *Pc*IDS1 was used in all following experiments.

To determine the conformational state of the *Pc*IDS1 quaternary structure, size exclusion chromatography was performed. The protein was added to running buffer [25 mM MOPSO (pH 7.3), 10% (vol/vol) glycerol, and 150 mM NaCl] in the presence of either 5 mM $MgCl_2$ or 0.5 mM $CoCl_2$ and incubated for 10

min at 4 °C. To confirm the overall conformation of the protein with the different metal cofactors, an aliquot of each solution was separated on a SuperdexHiLoad 16/60 200 prep grade (GE Healthcare) column at a flow rate of 1 mL/min. The retention volume of *Pc*IDS1 was detected via its absorption at 280 nm. To calibrated the column, we used cytochrome *c* from horse heart (12.4 kDa), carbonic anhydrase from bovine erythrocytes (29 kDa), BSA (66 kDa), alcohol dehydrogenase from yeast (150 kDa), and β-amylase from sweet potato (200 kDa) in the presence of 10 mM $CoCl_2$ or 10 mM $MgCl_2$. The molecular weight for *Pc*IDS1 was calculated by the formula received from the corresponding standard curve. Without cofactor, $y = -27.133x + 128.38$ ($R^2 = 0.9925$); with Co^{2+}, $y = -27.133x + 128.21$ ($R^2 = 0.9927$); and with Mg^{2+}, $y = -27.122x + 128.26$ ($R^2 = 0.9921$).

Prenyltransferase Assay and Product Distribution Analyses. For kinetic analyses, enzyme assays of *Pc*IDS1 were carried out in a final volume of 200 μL containing 25 mM MOPSO (pH 7.3), 10% (vol/vol) glycerol, 150 mM NaCl, and 5 mM Mg^{2+} or 1 mM Co^{2+}, respectively. As substrates and countersubstrates, isopentenyl diphosphate (IDP), dimethylallyl diphosphate, and geranyl diphosphate (GDP; Sigma–Aldrich) were used. The countersubstrate concentration was kept constant at 50 μM; different experimental conditions are mentioned separately. The analyzed substrate ranged from 0.1 μM up to 100 μM. The reaction was heated to 30 °C and initiated by adding 0.2 μg of protein for Co^{2+} assays or 2 μg of protein for Mg^{2+} assays of the recombinant protein, and it was then incubated further at 30 °C. The water phase was analyzed by direct injection of 1 μL into the HPLC system at different time points from the same reaction mixture to identify the linear reaction velocity for every parameter. Calculation of the kinetic parameters was performed with GraphPad Prism version 5.04 (GraphPad Software) using the built-in enzyme kinetics module.

The pH optimum for the catalytic activity of *Pc*IDS1 was determined to be 7.0–7.5 in the presence of Mg^{2+} or Co^{2+}. However, the enzyme activity was quite stable over a broad range, from pH 4 to pH 8. Even the temperature optimum was not delimited to a narrow range. Acceptable activity with Mg^{2+} or Co^{2+} was measured from 15 °C up to 45 °C, whereas the optimum resided at 28 °C to 32 °C.

Activity testing of purified full-length *Pc*IDS1 in the presence of Mg^{2+} or Co^{2+} showed only about 5% of the activity in both cases in comparison to its truncated form, which lacks the predicted signal sequence.

For enzyme assay from larvae material, the samples were obtained by macerating different tissues with a 2-mL Potter–Elvehjem grinder with a Teflon pestle for 2 min at 4 °C with 300 μL of assay buffer. The suspension was centrifuged at 20,000 × *g*, and the protein concentration of the supernatant was determined. Ten micrograms of protein was used for standard assays and incubated at 30 °C for 60 min. The assays were stopped by adding 500 μL of chloroform and by mixing for 20 s, followed by centrifugation for 5 min at 5,000 × *g*. Subsequently, the water phase was transferred to a glass vial and measured directly by injecting 1 μL into the HPLC system. Protein concentrations were measured according to Bradford and Williams (3) and Bradford (4), using the Coomassie Plus Protein Assay Kit (Thermo Scientific Pierce) with BSA as a standard.

Liquid Chromatography-Tandem MS Method for *Pc*IDS1 Assay Product Determination. Analysis of isoprenoid diphosphates (IDS) was performed according to a modified method (5) on an Agilent 1260 HPLC system (Agilent Technologies) coupled to an API 5000 triple-quadrupole mass spectrometer (AB Sciex Instruments). For separation, a ZORBAX Extended C-18 column (1.8 μm, 50 mm × 4.6 mm; Agilent Technologies) was used. The mobile phase consisted of 5 mM ammonium bicarbonate in water as solvent A and acetonitrile as solvent B, with the flow rate set at 1.2 mL/min and the column temperature kept at 20 °C. Separation was achieved by using a gradient starting at 0% B, increasing to 90% B in 3 min and 100% B in 3.1 min (1-min hold), followed by a change to 0% B in 0.5 min (2.5-min hold) before the next injection. The injection volume for samples and standards [GDP and farnesyl diphosphate (FDP) from Sigma–Aldrich] was 1 μL; autosampler temperature was either 30 °C for assays without or 4 °C for assays with chloroform extraction. The mass spectrometer was used in the negative electrospray ionization (EI) mode. Optimal settings were determined using standards. Levels of ion source gases 1 and 2 were set at 60 and 70 psi, respectively, with a temperature of 700 °C. Curtain gas was set at 30 psi and collision gas was set at 7 psi, with all gases being nitrogen. Ion spray voltage was maintained at −4,200 V. Multiple-reaction monitoring (MRM) was used to monitor analyte parent ion-to-product ion formation: *m/z* 312.9/79 for GDP and *m/z* 380.9/79 for (*E,E*)-FDP. *Cisoid* products like neryl-diphosphate, (*Z,E*)-FDP, or (*Z,Z*)-FDP were not detected. Detection of GDP was omitted when used as substrate. Data analysis was performed using Analyst Software 1.6 Build 3773 (AB Sciex).

***Pc*IDS1 Antibody Production and Immunoblot Analysis.** For synthesis of polyclonal antibodies, a 16-aa peptide (HDLFFKIMKKIY-KRDA) from the N-terminal end of the protein was used. The antibody was affinity-purified with 3 mg epoxy-immobilized antigen that was used for immunization (Davids Biotechnologie).

For immunoblot analysis, crude protein from different larval tissue was extracted in assay buffer as described above. Equal amounts of 5 μg of total protein of each tissue were separated by SDS/PAGE using any-KD acrylamide gels (BIO-RAD). Afterward, the proteins were transferred electrophoretically onto nitrocellulose membranes (BIO-RAD). Membranes were blocked with TBST [20 mM Tris (pH 7.5), 150 mM NaCl, 0.1% (vol/vol) Tween 20] and 10% nonfat milk, followed by incubation with 1:100 of the polyclonal anti-*Pc*IDS1 antibody at 16 °C overnight. After washing with blocking solution and a subsequent incubation with anti-rabbit HRP-conjugated secondary antibody, a final TBST washing was carried out. Signal detection was achieved by enhanced chemiluminescence (Thermo Scientific) and Amersham Hyperfilm ECL (GE Healthcare).

Sequence Comparison and Homology Modeling. Sequence similarity searches were performed using the alignment tool BLAST (6). Nucleotide sequences of different organisms were downloaded from the National Center for Biotechnology Information. To determine the degree of similarity between the members of insect scIDS and full-length *Pc*IDS1, sequence analysis was performed using the ClustalW tool (Lasergene 10 Core Suite; DNASTAR).

The 3D structure of truncated *Pc*IDS1 was modeled using the molecular modeling software YASARA (7). YASARA identified 15 templates based on alignment scores and low E-values suitable for homology modeling. Altogether, 32 models were automatically created and subsequently refined. The model based on the X-ray structure of FDP synthase from *Homo sapiens* deposited in the protein database (1zw5; see www.rcsb.org) (8, 9) appeared to be the most useful one. The structure of the model of *Pc*IDS1 has been deposited at the Protein Model DataBase (http://mi.caspur.it/PMDB/main.php) (10) and has been assigned the ID code PM0078683 for free download. The Mg^{2+} and the ligand binding position of IDP were automatically imported from the template's X-ray structure. The artificial cocrystallized zoledronic acid, [1-hydroxy-2-(1H-imidazol-1-yl)ethane-1,1-diyl]bis(phosphonic acid), was manually replaced by GDP. This model was then refined with the md-refinement tool of YASARA (7). The quality of the final model was checked with PROSA II (11) and PROCHECK (12). The graphical analysis with PROSA II showed one small loop (10 aa) area in positive energy range out-

side the active site. A combined energy z-score of −9.83 clearly indicated a native-like folded structure. Analysis of the calculated model with PROCHECK evaluated the consistency of all stereochemical parameters, such as the Ramachandran plot quality (92.3% of the backbone dihedral angles in most favored areas).

To investigate influences by the replacement of Mg^{2+} with Co^{2+}, the TRIPOS force field was used first (13). Thus, the atom types of Mg^{2+} were modified to Co^{2+}, and short molecular dynamics simulations (10 ps, 300 K) with subsequent energy minimization of GDP in the active site were performed. The Co^{2+} and the interacting side chains of all remaining amino acids except this ligand were kept fixed because the TRIPOS force field is not suitable for protein structure refinement. To estimate the interaction energies of different ions with the diphosphate moiety and aspartate side chains, density functional theory (DFT) B3LYP 6-311G++ calculations were performed using Gaussian 03 (14).

Tissue-Specific Expression of *Pc*IDS1. Quantitative real-time PCR was used for relative quantification (15). cDNA was synthesized from DNA-digested RNA and purified from three larvae per biological replicate using the RNAqueous Micro Kit (Life Technologies). Three biological replicates were analyzed twice. If technical replicates had a difference in the quantification cycle value greater than 1, the assay was repeated. Reference genes [*Pc*RPL8 (EMBL: AFQ22729.1) and *Pc*RPS3 (GenBank: KC109783)] were chosen. Real-time PCR data were acquired on an Mx3000P Real-Time PCR system (Agilent) using Brilliant III SYBR Green qPCR Master Mix (Agilent) according to the manufacturer's instructions. These analyses were performed following the minimum information for publication of quantitative real-time PCR experiments guidelines (16, 17).

RNAi in *P. cochleariae* Larvae. dsRNA was synthesized using the Megascript RNAi kit (Life Technologies) with altering of the elution buffer to 3.5 mM Tris·HCl, 1 mM NaCl, 50 nM Na_2HPO_4, 20 nM KH_2PO_4, 3 mM KCl, and 0.3 mM EDTA (pH 7.0). Off-target prediction was performed for highly specific silencing according to Bodemann et al. (18). The ORFs of full-length *PcIDS1* and *Gfp* were analyzed for off-target prediction by dicing the sequences *in silico* (19) and using the resulting putative 21-nt siRNAs for a BLASTn search linked to our transcriptome database of *P. cochleariae*. No putative off-target effects with other transcripts are predicted with the chosen dsRNA sequences on a critical value of at least 20 continuous nucleotides that have to be identical. The dsRNA synthesis templates with opposite T7-promotor sites were amplified out of sequenced plasmid pIB/V5-His (Life Technologies) containing full-length *PcIDS1* for 850 bp of *PcIDS1* using IDS1_FWD_T7_RNA (5′-TAATACGACTCACTATAGGGAGATCAAGCCAGTCTCCT-3′) as forward primer and IDS1_REV_T7_RNA (5′-TAATACGACTCACTATAGGGAGACTAAGCATCCCTCTTG-3′) as reverse primer and pCR3.1/CT-GFP-TOPO (Life Technologies) for 720 bp of *Gfp* (for primer, see ref. 18), respectively. The concentration of dsRNA was adjusted to 2 μg/μL, and for all injections, 250 nL (500 ng) of dsRNA solution was used.

Late first-instar larvae of *P. cochleariae* were used for injections. These were collected 5 d after hatching and were put in an incubator set to 16 h of light at 14 °C and 8 h of darkness at 12 °C for slow larval development after treatment. A Nano2000 injector (WPI) on a three-axis micromanipulator was used for injecting ice-chilled larvae parasagittal between the pro- and mesothorax.

Relative Quantification of 8-Hydroxygeraniol-Glucoside in *P. cochleariae* Fat Body and Hemolymph. Analysis was done on an Agilent 1260 HPLC system (Agilent Technologies) coupled to an API 5000 triple-quadrupole mass spectrometer (AB Sciex Instruments). For separation, a ZORBAX Eclipse XDB-C-18 column (1.8 μm, 50 mm × 4.6 mm; Agilent Technologies) was used. The mobile phase consisted of 20 mM ammonium formate in water as solvent A and acetonitrile as solvent B, with the flow rate set at 1.0 mL/min and the column temperature kept at 20 °C. Separation was achieved by using a gradient starting at 10% solvent B, increasing to 95% solvent B in 5 min (1-min hold), followed by a change to 10% solvent B in 1 min (1-min hold) before the next injection. Injection volume for samples and standards was 5 μL; the autosampler temperature was 4 °C. The mass spectrometer was used in negative EI mode. Optimal settings were determined using a standard. Ion source gases 1 and 2 were set at 70 psi, with a temperature of 700 °C. Curtain gas was set at 25 psi and collision gas was set at 6 psi, with all gases being nitrogen. Ion spray voltage was maintained at −3000 V. The monitored MRM transition was *m/z* 377.3/331.2. Data analysis was performed using Analyst Software 1.6 Build 3773 (AB Sciex).

Relative Quantification of Chrysomelidial in Defense Secretions of *P. cochleariae*. Secretions were collected and weighed in pulled-out glass capillaries from different instar stages of treated larvae, and they were then diluted 1:200 (wt/vol) in ethyl acetate supplemented with 100 μg/mL methyl benzoate as an internal standard. One microliter was subjected to GC-EI-MS analysis [ThermoQuest Finnigan ITQ GC-MS 2000 (quadrupole) equipped with Phenomenex ZB-5-W/Guardian-column, 25 m (10-m Guardian precolumn) × 0.25 mm, film thickness of 0.25 μm]. Substances were separated splitless using helium as a carrier (1.5 mL/min). Conditions were set as follows: 50 °C (2 min), 20 °C/min to 130 °C, 40 °C/min to 200 °C, 20 °C/min to 220 °C, and 40 °C/min to 300 °C (1 min). Inlet temperature was 220 °C, and transfer line temperature was 280 °C. Chrysomelidial was identified according to Oldham et al. (20). The peak areas were obtained using the Interactive Chemical Information System algorithm that is implemented in the Xcalibur bundle (version 2.0.7; Thermo Scientific). The relative amount of chrysomelidial per larva has been calculated with the following equation, in which *mChry* is the relative amount of chrysomelidial per larva, *AoChry* is the peak area of chrysomelidial, *AoMB* is the peak area of methyl benzoate, and *mSec* is the average mass of secretion per larva:

$$mChry = \left(\frac{AoChry}{AoMB} * dilution\right) * mSec.$$

Fitness Measurements. The development of larval weight was documented using five replicates of three larvae. Larval weight was measured per replicate on an ultramicrobalance in a 24-h ± 3-h period. In accordance with the method used by Kuehnle and Mueller (21), the relative growth rate was calculated using the weight of freshly emerged pupae as the final larval developmental stage.

1. Discher S, et al. (2009) A versatile transport network for sequestering and excreting plant glycosides in leaf beetles provides an evolutionary flexible defense strategy. *ChemBioChem* 10(13):2223–2229.
2. Petersen TN, Brunak S, von Heijne G, Nielsen H (2011) SignalP 4.0: Discriminating signal peptides from transmembrane regions. *Nat Methods* 8(10):785–786.
3. Bradford MM, Williams WL (1976) New, rapid, sensitive method for protein determination. *Fed Proc* 35(3):274.
4. Bradford MM (1976) A rapid and sensitive method for the quantitation of microgram quantities of protein utilizing the principle of protein-dye binding. *Anal Biochem* 72(1-2):248–254.
5. Nagel R, Gershenzon J, Schmidt A (2012) Nonradioactive assay for detecting isoprenyl diphosphate synthase activity in crude plant extracts using liquid chromatography coupled with tandem mass spectrometry. *Anal Biochem* 422(1):33–38.

6. Altschul SF, Lipman DJ (1990) Protein database searches for multiple alignments. *Proc Natl Acad Sci USA* 87(14):5509–5513.
7. Krieger E, et al. (2009) Improving physical realism, stereochemistry, and side-chain accuracy in homology modeling: Four approaches that performed well in CASP8. *Proteins* 77(Suppl 9):114–122.
8. Kavanagh KL, Dunford JE, Bunkoczi G, Russell RG, Oppermann U (2006) The crystal structure of human geranylgeranyl pyrophosphate synthase reveals a novel hexameric arrangement and inhibitory product binding. *J Biol Chem* 281(31):22004–22012.
9. Kavanagh KL, et al. (2006) The molecular mechanism of nitrogen-containing bisphosphonates as antiosteoporosis drugs. *Proc Natl Acad Sci USA* 103(20): 7829–7834.
10. Castrignanò T, De Meo PD, Cozzetto D, Talamo IG, Tramontano A (2006) The PMDB Protein Model Database. *Nucleic Acids Res* 34:D306–D309.
11. Sippl MJ (1990) Calculation of conformational ensembles from potentials of mean force. An approach to the knowledge-based prediction of local structures in globular proteins. *J Mol Biol* 213(4):859–883.
12. Laskowski RA, MacArthur MW, Moss DS, Thornton JM (1993) PROCHECK—A program to check the stereochemical quality of protein structures. *J Appl Cryst* 26(2):283–291.
13. Clark M, Cramer RD, Van Opdenbosch N (1989) Validation of the General Purpose Tripos 5.2 Force Field. *J Comp Chem* 10(8):982–1012.
14. Frisch MJ, et al. (2004) Gaussian 03, Revision C.02. (Gaussian, Wallingford CT).
15. Livak KJ, Schmittgen TD (2001) Analysis of relative gene expression data using real-time quantitative PCR and the $2^{(-\Delta\Delta CT)}$ Method. *Methods* 25(4):402–408.
16. Bustin SA, et al. (2010) MIQE précis: Practical implementation of minimum standard guidelines for fluorescence-based quantitative real-time PCR experiments. *BMC Mol Biol* 11:74–78.
17. Bustin SA, Johnson G, Agrawal SG (2012) [MIQE—Guidelines for developing robust real-time PCR assays]. *Mycoses* 55(Suppl 2):30–34. German.
18. Bodemann RR, et al. (2012) Precise RNAi-mediated silencing of metabolically active proteins in the defence secretions of juvenile leaf beetles. *Proc Biol Sci* 279(1745):4126–4134.
19. Naito Y, et al. (2005) dsCheck: Highly sensitive off-target search software for double-stranded RNA-mediated RNA interference. *Nucleic Acids Res* 33(Web Server issue): W589-91.
20. Oldham NJ, Veith M, Boland W, Dettner K (1996) Iridoid monoterpene biosynthesis in insects—Evidence for a *de novo* pathway occurring in the defensive glands of *Phaedon armoraciae* (Chrysomelidae) leaf beetle larvae. *Naturwissenschaften* 83(10): 470–473.
21. Kuehnle A, Mueller C (2011) Responses of an oligophagous beetle species to rearing for several generations on alternative host-plant species. *Ecol Entomol* 36(2):125–134.

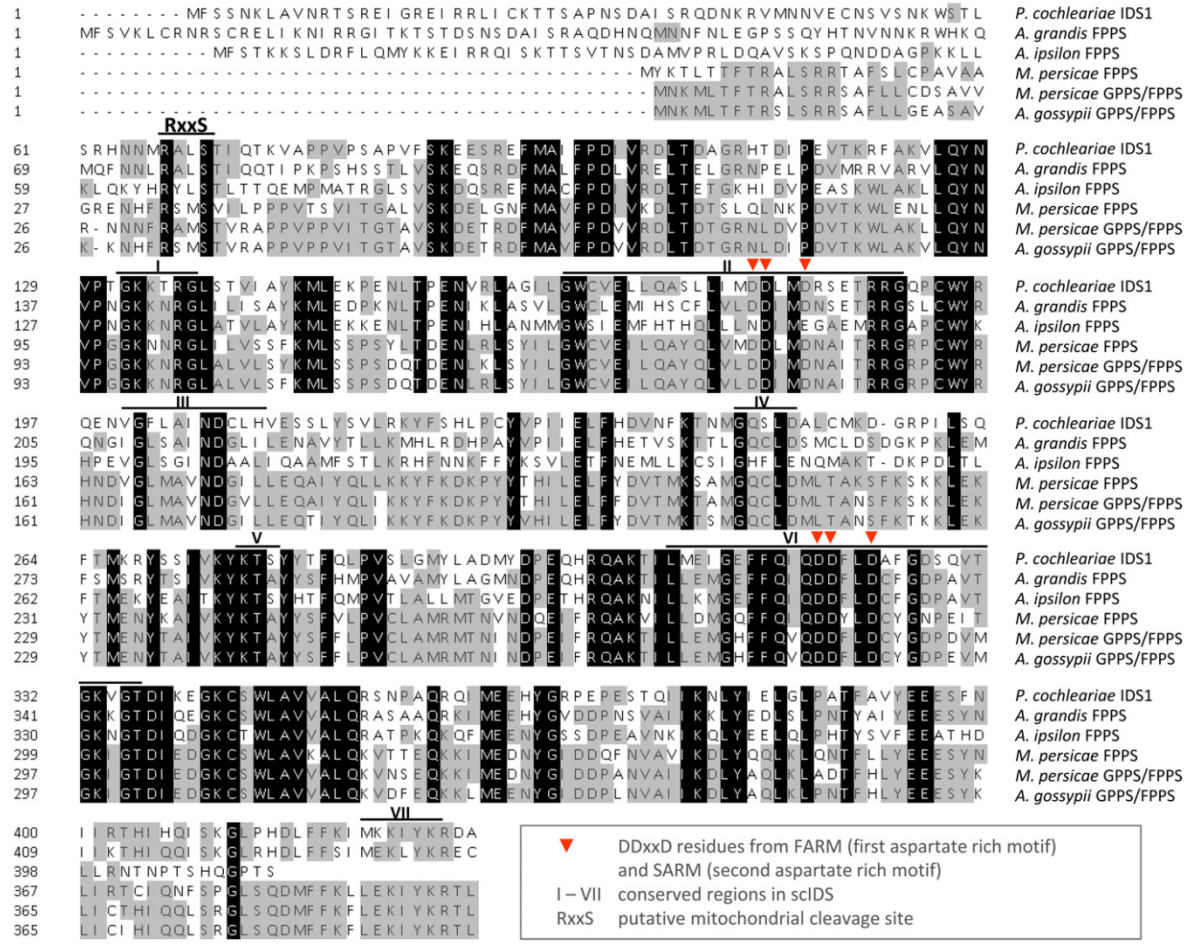

Fig. S1. Amino acid alignment (ClustalW) of full-length *Pc*IDS1 from *P. cochleariae* with other insect scIDSs. Sequence identity to other farnesyl diphosphate synthases (FDPSs): *Anthonomus grandis* (54.1%) (GenBank: AAX78434), *Myzus persicae* (45.4%) (GenBank: ABY19313), and *Agrotis ipsilon* (45.2%) (GenBank CAA08918). Sequence identity to bifunctional FDPSs/GDPSs: *Aphis gossypii* (48.6%) (EMBL: ACT79808) and *M. persicae* (48.4%) (EMBL: ABY19312). (Residues in black are identical in all sequences; gray residues are >50% identical in aligned sequences.)

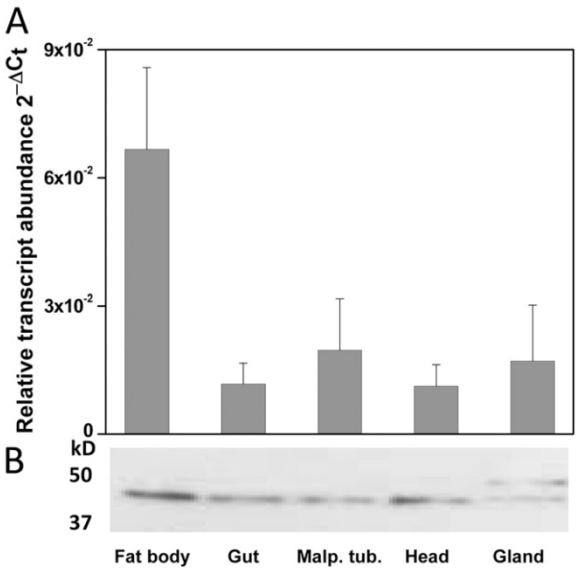

Fig. S2. (*A*) Relative transcript abundance ($2^{\Delta Ct}$) of *PcIDS1* in different larval tissues. (*B*) Western blot analyses of 5 μg of protein per lane probed with sequence-specific antibodies against *Pc*IDS1, followed by ECL detection. Malp. tub, Malpighian tubules.

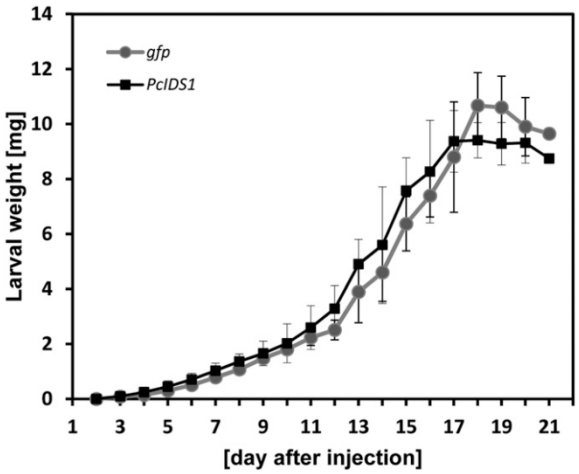

Fig. S3. Relative growth rate of RNAi-induced larvae from *P. cochleariae*. The development of larval weight was documented and measured in a 24-h ± 3-h period. No significant differences in the relative growth rate were observed between *Gfp*- and *PcIDS1*-injected larvae. The final larval developmental stage was the weight of freshly emerged pupae (n = 15, ±SD).

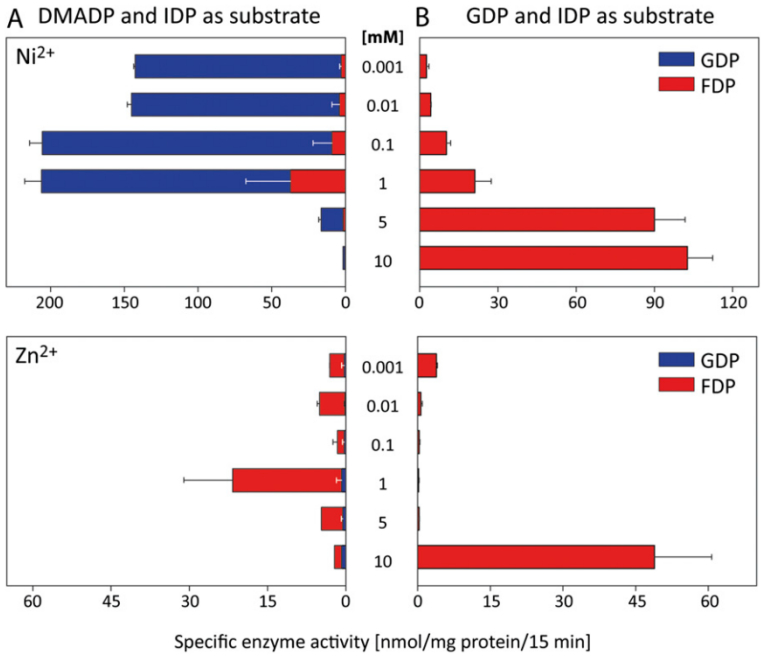

Fig. S4. Effect of metal cofactors regarding product formation and enzyme activity of *Pc*IDS1. (*A*) Different concentrations of Ni^{2+} and Zn^{2+} were added to *Pc*IDS1 and incubated with 50 μM IDP and 50 μM dimethylallyl diphosphate (DMADP; $n = 3$, ±SD). (*B*) Different concentrations of Ni^{2+} and Zn^{2+} were added to *Pc*IDS1 and incubated with 50 μM IDP and 50 μM GDP ($n = 3$, ±SD).

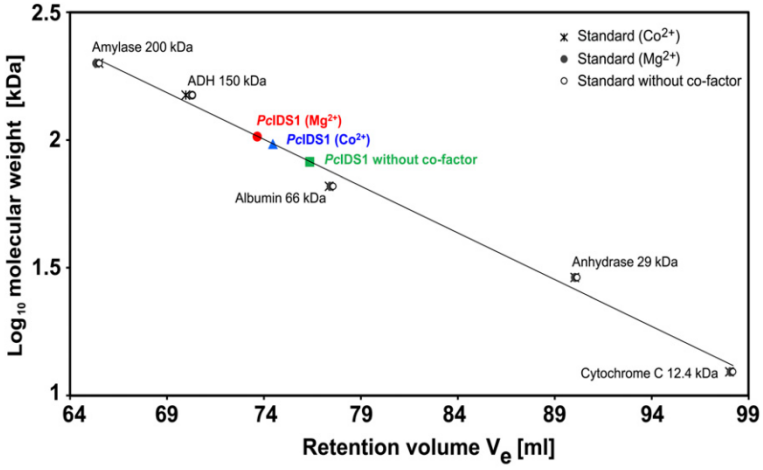

	Elution volume			MW log10			calc. MW (kDa)		
	No co-factor	Co^{2+}	Mg^{2+}	No co-factor	Co^{2+}	Mg^{2+}	No co-factor	Co^{2+}	Mg^{2+}
*Pc*IDS1	76.3	74.4	73.6	1.91	1.98	2.01	74.6	87.6	93.8
Amylase	65.5	65.4	65.3	2.31	2.31	2.31	207.5	204.9	208.5
ADH	70.3	69.9	70.2	2.14	2.14	2.13	138.1	140.1	137.2
Albumin	77.5	77.3	77.4	1.87	1.87	1.87	74.5	74.8	74.7
Anhydrase	90.1	90.0	90.0	1.40	1.40	1.40	25.6	25.5	25.6
Cytochrome C	98.1	98.0	98.0	1.11	1.11	1.11	12.9	12.9	12.9

Fig. S5. Analytical size exclusion chromatography of *Pc*IDS1. The plot shows the relative retention volumes of the protein molecular weight standards and the calculated standard curve by linear regression dependent on the divalent ions. The relative retention volumes of the apoprotein *Pc*IDS1 are shown by the green rectangle. The shifts of the retention volume dependent on the divalent metal cofactor are represented by the red dot in the presence of Mg^{2+} and the blue triangle in the presence of Co^{2+}.

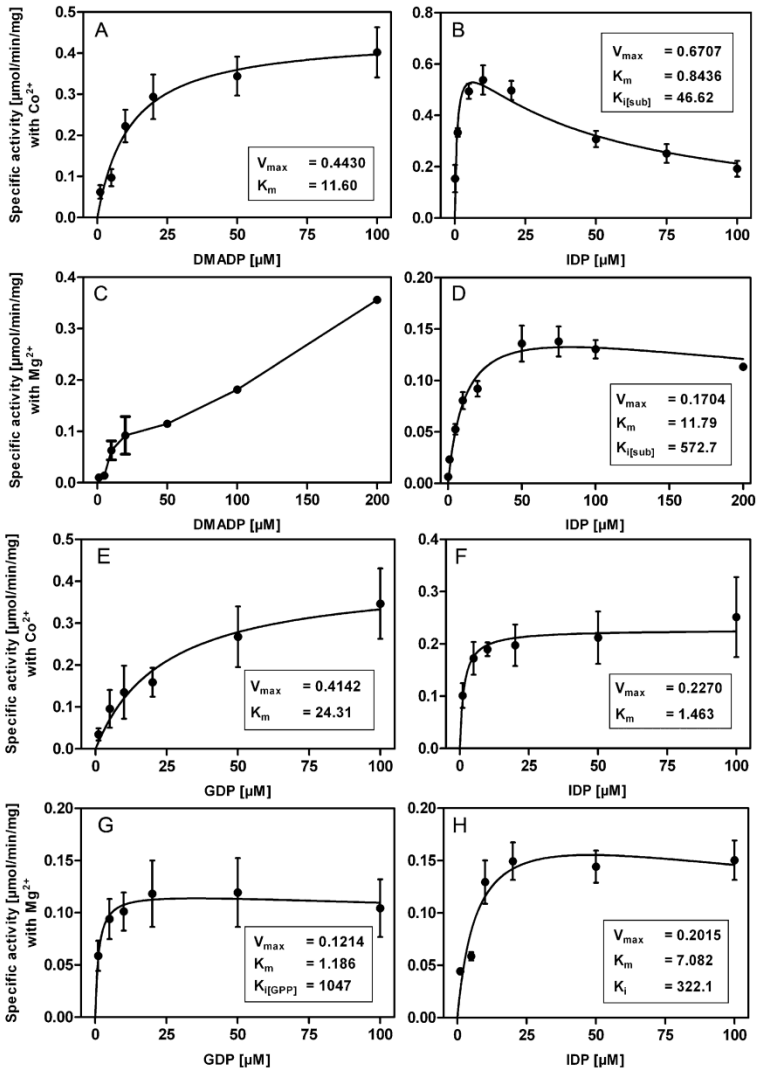

Fig. S6. Kinetic analyses of *Pc*IDS1 with nonlinear regression and built-in function calculated with GraphPad Prism version 5.04. (*A*) Calculation according to the Michaelis–Menten kinetic of $K_{m(DMADP)}$ with Co^{2+} and 15 µM IDP. (*B*) Calculation with substrate inhibition of $K_{m(IDP)}$ with Co^{2+} and 50 µM dimethylallyl diphosphate (DMADP). (*C*) Enzyme activity data with variable DMADP in the presence of Mg^{2+} and 50 µM IDP. (*D*) Calculation with substrate inhibition of $K_{m(IDP)}$with Mg^{2+} and 50 µM DMADP. (*E*) Calculation according to the Michaelis–Menten kinetic of $K_{m(GDP)}$ with Co^{2+} and 50 µM IDP as countersubstrate. (*F*) Calculation according to the Michaelis–Menten kinetic of $K_{m(IDP)}$ with Co^{2+} and 50 µM GDP as countersubstrate. (*G*) Calculation with substrate inhibition of $K_{m(GDP)}$ with Mg^{2+} and 50 µM IDP as countersubstrate. (*H*) Calculation with substrate inhibition of $K_{m(IDP)}$ with Mg^{2+} and 50 µM GDP as countersubstrate.

Table S1. Enzyme activity of *Pc*IDS1 with different metal cofactors

Substrate	Ion	Optimal cofactor concentration, mM	Total activity, nmol/mg of protein per 15 min (±SD)	GDP activity, % of total activity
DMADP	Co^{2+}	0.5	1,022.33 (±72.2)	95.9
	Mg^{2+}	5	418.85 (±6.2)	18.3
	Mn^{2+}	0.5	239.66 (±16.2)	98.8
	Ni^{2+}	0.1	206.8 (±41.3)	81.9
	Zn^{2+}	0.1	21.69 (±24.1)	96.3
GDP	Co^{2+}	0.01	333.56 (±48.13)	
	Mg^{2+}	0.5	967.25 (±136.4)	
	Mn^{2+}	0.01	785.07 (±136.5)	
	Ni^{2+}	0.001	102.68 (±9.6)	
	Zn^{2+}	0.001	48.90 (±11.8)	

DMADP, dimethylallyl diphosphate.

Table S2. ICP-OES and ICP-MS analyses of fat body and gut tissue of *P. cochleariae* larvae

		Fat body 1		Fat body 2		Gut	
Element	Method	DW, μg/g (±SD)	DW, μmol/g	DW, μg/g (±SD)	DW, μmol/g	DW, μg/g (±SD)	DW, μmol/g
Ca	ICP-OES	753.2 (±0.3)	18.7	788 (±16)	19.6	893 (±12)	22.2
Co	ICP-MS	0.243 (±0.005)	0.0041	0.198 (±0.005)	0.0033	0.297 (±0.001)	0.005
Cu	ICP-MS	14.09 (±0.07)	0.221	14.9 (±0.2)	0.234	12.88 (±0.03)	0.203
Fe	ICP-MS	41.7 (±0.1)	0.746	41.8 (±0.5)	0.748	92.6 (±0.04)	1.658
K	ICP-OES	12,075 (±274)	308.8	12,112 (±71)	309.8	18,299 (±4)	468
Mg	ICP-OES	2,223 (±41)	91.4	2,255.5 (±0.5)	92.8	2,205.2 (±0.4)	90.7
Mn	ICP-MS	16.51 (±0.04)	0.301	16.706 (±0.002)	0.304	47.3 (±0.4)	0.861
Na	ICP-OES	462 (±11)	20.1	463 (±5)	20.1	499.2 (±0.4)	21.7
Ni	ICP-MS	0.36 (±0.01)	0.0061	0.3598 (±0.0007)	0.0061	0.88 (±0.08)	0.0149
Zn	ICP-MS	62.3 (±0.3)	0.952	62.66 (±0.02)	0.958	141.1 (±0.03)	2.158

DW, dry weight; ICP-MS, inductively coupled plasma mass spectrometry; ICP-OES, inductively coupled plasma optical emission spectrometry.

Table S3. Energies of the compounds and resulting reaction energies for the formation of diphosphate metal complexes in kilocalories per mole calculated with density functional theory (DFT) B3LYP 6-311G++ (d.p)

	Products energy	Educts energy			
X	X-DP^{3-}	X	DP^{3-}	Reaction energy	Δ to Mg^{2+}
Mg^{2+}	−885,175.2	−125,023.7	−759,218.5	−933.0	0
Co^{2+}	−16,277,257.6	−867,059.6	−759,218.5	−979.6	−46.6
Mn^{2+}	−1,481,820.2	−721,619.3	−759,218.5	−982.4	−49.4

X, metal cation.

Table S4. Energies of the compounds and resulting reaction energies for the formation of propionic acid metal complexes in kilocalories per mole calculated with DFT B3LYP 6-311G++ (d.p)

	Products energy	Educts energy			
X	$X(CH_3CH_2COO^-)_2$	X	$(CH_3CH_2COO^-)_2$	Reaction energy	Δ to Mg^{2+}
Mg^{2+}	−461,861.2	−125,023.7	−336,166.4	−671.1	0
Co^{2+}	−1,203,933.8	−867,059.6	−336,166.4	−712.6	−41.5
Mn^{2+}	−1,058,498.3	−721,619.3	−336,166.4	−707.8	−36.7

X, metal cation.

Table S5. Energies of the compounds and resulting reaction energies for the formation of metal complexes with both propionic acid and diphosphate using the metal cation diphosphate complex as educt in kilocalories per mole calculated with DFT B3LYP 6-311G++ (d.p)

	Products energy	Educts energy			
X	$CH_3CH_2COO^- \times (P_2O_7H_3)^-$	$X\ (P_2O_7H_3)^-$	$CH_3CH_2COO^-$	Reaction energy	Δ to Mg^{2+}
Mg^{2+}	−1,054,033.6	−885,711.5	−168,083.2	−238.9	0
Co^{2+}	−1,796,098.5	−1,627,782.5	−168,083.2	−232.8	6.1
Mn^{2+}	−1,650,660.9	−1,482,341.6	−168,083.2	−236.1	2.8

X, metal cation.

Table S6. Energies of the compounds and resulting reaction energies for the formation of metal complexes with both propionic acid and diphosphate using the metal cation propionic acid complex as educt in kilocalories per mole calculated with DFT B3LYP 6-311G++ (d.p)

	Products energy	Educts energy			
X	$CH_3CH_2COO^- \times (P_2O_7H_3)^-$	$(P_2O_7H_3)^-$	$CH_3CH_2COO^-\ X$	Reaction energy	Δ to Mg^{2+}
Mg^{2+}	−1,054,033.6	−760,331.1	−293,532.0	−170.5	0
Co^{2+}	−1,796,098.5	−760,331.1	−1,035,599.4	−168.0	2.5
Mn^{2+}	−1,650,660.9	−760,331.1	−890,171.2	−158.6	11.9

X, metal cation.

4. General Discussion

The published findings of this thesis focus on the role of IDS in terpene biosynthesis in plants and insects. Despite the importance of IDS, regulation of terpene biosynthesis can also occur at earlier steps in the MEP and MVA pathways. The aim of this general discussion is to embed the function of IDS into this larger framework and compare the findings from insects and plants where possible, as well as to discuss the development and limitations of new analytical techniques.

4.1 Regulation of DMADP and IDP biosynthesis

DMADP and IDP are used by IDS to produce longer prenyl diphosphates, and both substrates can be produced by either the MEP or MVA pathway. Usually only one of the two pathways is present in a given organism, as in insects were only the MVA pathway can be found. The exception to this generalization are plants where both pathways occur, but are differentially localized (Hemmerlin et al., 2012). Therefore it is convenient to discuss the regulation of IDP and DMADP production separately for plants and insects.

4.1.1 Regulatory mechanisms of MEP and MVA pathways in plants

The MVA pathway in plants is localized to the cytosol and mainly supplies IDP and DMADP for the formation of sesquiterpenes and triterpenes (e.g. sterols). Regulation of the MVA pathway is mostly attributed to 3-hydroxy-3-methyl-glutaryl-CoA reductase (HMGR), the only membrane bound enzyme in this pathway (Bach et al., 1986; Bach et al., 1991; Campos and Boronat, 1995). HMGR activity depends on protein abundance and is regulated either transcriptionally or by degradation of the enzyme (Re et al., 1995), but also can be affected by posttranslational modifications (Hemmerlin et al., 2012). Plants usually have two to five copies of HMGR, and it is speculated that various isoforms are used for diverse purposes and are differentially regulated (Loguercio and Wilkins, 1998; Hemmerlin et al., 2012). It was shown that HMGR responds to various abiotic and biotic stresses (Wegener et al., 1997; Alex et al., 2000; Hartmann et al., 2000; Wentzinger et al., 2002; Kai et al., 2006; Rinaldi et al., 2007; Nieto et al., 2009) and can control the flux towards sterols (Bach, 1986; Hagen and Grunewald, 2000; Harker et al., 2003; Harker et al., 2003; Suzuki et al., 2004) and to a certain degree to secondary metabolites (Stermer and Bostock, 1987; Choi et al., 1994; Lange et al., 1998). HMGR has both

soluble and membrane-bound domains with the membrane-bound part being critical for post-translational regulation. Overexpression of the soluble part of HMGR alone led to increased accumulation of end products, like sterols and sterol esters (Ayora-Talavera et al., 2002; Harker et al., 2003; Holmberg et al., 2003; Muñoz-Bertomeu et al., 2007; Sales et al., 2007; Aquil et al., 2009). Overexpression of the whole enzyme did not lead to more sterols, but sterol esters, which are even more important as end products in case of HMGR overexpression, were not quantified in those publications (Re et al., 1995; Köhle et al., 2002).

The plastidal MEP pathway mostly supplies IDP and DMADP for the formation of monoterpenes, diterpenes and tetraterpenes. Here the controlling mechanisms are not as clear as for the MVA pathway. This is due to the more recent discovery of the MEP pathway, but also because of analytical problems in quantifying enzyme activity *in planta* and the lethality of knock-out mutants of all MEP pathway enzyme e.g. in *A. thaliana* (Hemmerlin et al., 2012). Despite these difficulties, the strongest evidence points towards DXS (Lois et al., 2000; Estévez et al., 2001; Rodríguez-Concepción et al., 2001; Dudareva et al., 2005; Guevara-García et al., 2005; Khemvong and Suvachittanont, 2005; Kishimoto and Ohmiya, 2006; Morris et al., 2006; Muñoz-Bertomeu et al., 2006; Duchêne et al., 2009; Harada et al., 2009; Kim et al., 2009; Wiberley et al., 2009) and in fewer cases DXR (Julliard and Douce, 1991; Mahmoud and Croteau, 2001; Carretero-Paulet et al., 2002; Bede et al., 2006; Carretero-Paulet et al., 2006; Kolotilin et al., 2007) for having the most control over the MEP pathway. HDR in some cases can fine tune the MEP pathway flux, as shown in tomato, pine and orange (Botella-Pavía et al., 2004; Alquezar et al., 2008; Flores-Pérez et al., 2008; Kim et al., 2009). Similar to HMGR for the MVA pathway, DXS and HDR are present in gene families, thought to be regulated differently under various situations (Hemmerlin et al., 2012).

Although both MEP and MVA pathways show a different localization and can be regulated independently from each other, there is some evidence of a metabolic crosstalk between plastids and cytosol. For example, it was shown that transport of intermediates can take place from plastid towards the cytosol (Soler et al., 1993; Bick and Lange, 2003; Flügge and Gao, 2005; Gutensohn et al., 2013), but also the other way around (Soler et al., 1993; Nagata et al., 2002; Hemmerlin et al., 2003; Schuhr et al., 2003; Gutiérrez-Nava et al., 2004; Skorupinska-Tudek et al., 2008). The most likely molecules to be transported are IDP and GDP towards the cytosol and FDP towards the plastid, but neither a mechanism of transport nor the exact identity of the transported molecule(s) are known (Hemmerlin et al., 2012). Therefore it still is not clear if the pools of IDP and DMADP or other prenyl diphosphates are actually connected.

4.1.2 Regulatory mechanisms of the MVA pathway in insects

In contrast to plants, only the MVA pathway can be found in animals, and here HMGR was identified as the most important regulatory enzyme. HMGR is controlled on the transcriptional and post transcriptional level similar to HMGR in plants. Sterols were identified as the key negative regulator for HMGR in most animals (Burg and Espenshade, 2011). In contrast to plants and most animals, insects do not use the MVA pathway for *de novo* production of sterols, but rely on sterols supplied with their food (Clayton, 1964; Jing et al., 2013). In insects HMGR is therefore not regulated by sterols, as demonstrated with a *Drosophila melanogaster* cell line supplied with exogenous sterols (Brown et al., 1983; Havel et al., 1986; Seegmiller et al., 2002). Instead the expression of HMGR and to a lesser degree of 3-hydroxy-3-methyl-glutaryl-CoA synthase (HMGS) can be regulated by application of juvenile hormone III in bark beetles (Tittiger et al., 1999; Tittiger et al., 2000; Hall et al., 2002; Hall et al., 2002; Tittiger et al., 2003; Keeling et al., 2006; Bearfield et al., 2009). Knock out of HMGR leads to lethal heart defects in *D. melanogaster*, caused by an altered protein prenylation and RNAi knock down inhibits oviposition in *Helicoverpa armigera* (Yi et al., 2006; Wang et al., 2013).

In insects that produce terpenes belonging to the secondary metabolism, higher expression levels of HMGR and sometimes HMGS can be found in the terpene producing tissues, like the midgut of bark beetles (Bearfield et al., 2009), glands of termite soldiers of the species *Nasatitermes takasagoensis* (Hojo et al., 2012) or the fatty body tissue of *P. cochleariae* (Burse et al., 2007; Burse et al., 2008). For the HMGR of *P. cochleariae*, it was shown that enzyme activity can be inhibited by 8-hydroxygeraniol in crude protein extracts from fat body tissue or in heterologously overexpressed protein. Inhibition by geraniol, the precursor of 8-hydroxygeraniol, was less pronounced (Burse et al., 2008). In the same publication it was also shown that the inhibition by 8-hydroxygeraniol is strongest in leaf beetles producing iridoid defense compounds *de novo*, but also *D. melanogaster* HMGR can be inhibited to a certain degree by this compound. Questions about the specificity of this inhibition remain and whether the HMGR of insects producing defensive terpenes is differentially regulated in comparison to insects only needing the MVA pathway for their primary metabolism. It might also be interesting to compare the regulatory influence of HMGR and IDS of *P. cochleariae* in future research.

4.2 Prenyl diphosphate detection

The next step in terpene biosynthesis after the MEP and MVA pathways are IDS, which use IDP and DMADP to produce longer chain prenyl diphosphates. To study the role of IDS for terpene biosynthesis, it is crucial to have the analytical means to detect the reaction products of those enzymes, especially in enzyme assays with heterologously expressed IDS to identify their product spectrum. In addition, quantification of IDS activity in total protein extracts from plants and of the *in vivo* concentrations of reaction products under various conditions will help to broaden our knowledge about a potential regulatory role of IDS in terpene biosynthesis.

4.2.1 IDS enzyme activity in vitro

Recently a publication revealed that of the over 5,800 annotated IDS only 46 were biochemically characterized in detail (Wallrapp et al., 2013). In this particular publication 79 additional IDS were biochemically characterized. However even with this significant increase of IDS with known product specificity, assigning the length of prenyl diphosphate products by means of sequence comparison is still not accurate. Thus there is a need for a fast and reliable method identifying the product distribution of individual IDS.

Up to now the established essays for detection of prenyl diphosphates made use of radioactively-labeled [^{14}C]-IPP as substrate followed by acid or alkaline hydrolysis. The prenyl alcohols generated were then measured using radio-gas chromatography (radio-GC), radio-high-performance liquid chromatography (radio-HPLC), thin layer chromatography (TLC) or liquid scintillation counting (LSC)(Zhang and Poulter, 1993; Cunillera et al., 1996; Martin et al., 2002; Masferrer et al., 2002; Gilg et al., 2005; Manzano et al., 2006; Schmidt and Gershenzon, 2007, 2008; Chang et al., 2010; Kim et al., 2010; Schmidt et al., 2010). Those methods involve radioactive isotopes and hydrolysis, and are therefore rather laborious, time-consuming and frequently imprecise. In addition, cleavage of the diphosphate under highly acidic conditions usually generates more than one reaction product, making interpretation and quantification rather complicated (Schilmiller et al., 2009). If instead of using acid conditions, phosphatases are used to cleave the diphosphate enzymatically, the pH needs to be shifted first from the optimum for IDS towards that of the phosphatase used. Moreover prenyl diphosphates can be suboptimal substrates for commercially available phosphatases (Kurokawa et al., 1971).

The method described in Manuscript 1 avoids both issues by using an HPLC-MS/MS based method that improves the signal to noise ratio by two orders of magnitude in comparison to a radio-HPLC based assay. The method can be used for short-chain products up to GGDP and can distinguish between different stereoisomers. This is becoming more and more of an issue due to the discovery of a family of short-chain *cis*-IDS in several tomato species (Sallaud et al., 2009; Schilmiller et al., 2009; Akhtar et al., 2013). For prenyl diphosphates larger than GGDP, radioactive assays followed by thin layer chromatography are still the method of choice, for reasons discussed later under 3.2.3 (Wallrapp et al., 2013). Furthermore, besides the identification of the product profile, the same method can also be used to quantify enzyme activity of either heterologously expressed proteins or total protein extracts of animals or plants. The ability to quantify enzyme activity is a necessary basis for studying the importance of individual IDS *in vivo* by manipulating their expression. Another advantage of the non-radioactive method becomes apparent when metal cofactors besides Mg^{2+} are used in IDS assays. Most other IDS assay methods involve the cleavage of the diphosphate before analysis, but metals such as Co^{2+} have been shown to inhibit the activity of an *E. coli* alkaline phosphatase (Wang et al., 2005). This would block quantitative cleavage of phosphate groups and thereby prevent quantitative detection of the products formed, leading ultimately to incorrect activity data. The IDS characterized in Manuscript 3 is able to accept either Mg^{2+} or Co^{2+} as a metal cofactor and displays a different prenyl diphosphate product length depending on the metal used.

4.2.2 Prenyl diphosphate quantification *in vivo*

The method developed in Manuscript 1 was also the basis for successfully quantifying prenyl diphosphates *in vivo*, used in Manuscript 2. To the best of my knowledge, this is the first time that GDP, FDP and GGDP were quantified *in planta* together. The most recent method describing quantification of GGDP alone dates back to 1983. Here 1.5 kg of etiolated oat seedlings were used as starting material and 6 purification steps were needed (Benz et al., 1983). The method described in Manuscript 2, needs about 2000 times less plant material (0.75 g) and only 1 purification step. This increases the reliability of the quantification of prenyl diphosphates *in vivo* and makes it more suitable for larger sample sizes. In the aforementioned publication, the amounts of GGDP detected in oat seedlings were 10 times higher than amounts found in *P. abies* needles. This might be rationalized by the etiolated state of these seedlings, so

that high amounts of GGDP might be needed for the synthesis of chlorophyll to initiate photosynthesis. Quantification of GDP was performed in several publications using acid hydrolysis, where geraniol is formed from GDP and rearranges to linalool that is subsequently quantified by proton transfer reaction mass spectrometry (PTR-MS). Using acid hydrolysis, significantly larger amounts of GDP (200 fold) were reported for spruce (20 pmol mg^{-1} FW) compared to 0.1 nmol g^{-1} FW measured in Manuscript 2 (Nogués et al., 2006; Ghirardo et al., 2010). This difference might be caused by the presence of already formed linalool or the conversion of other terpenes to linalool under the highly acidic conditions, as already discussed by the authors themselves (Ghirardo et al., 2010). In contrast, the quantification of prenyl diphosphates without acid hydrolysis, as done in Manuscript 2, is not affected by those contaminations and allows for the use of an internal standard.

4.2.3 Limitations

Despite the already mentioned advantages of this LC-MS/MS based method for prenyl diphosphate detection, e.g. speed and reliability, it still has some limitations. At present it can be only used for the detection of GDP, FDP and GGDP. While IDP and DMADP can also be detected, they cannot be separated and elute very early in the chromatogram with the flow-through, preventing any attempt at quantification. Prenyl diphosphates larger than GGDP are difficult to detect for two reasons. They are not commercially available and chemical synthesis becomes more and more laborious with increasing size due to the increase in the number of possible stereoisomers. In addition, ionization of larger diphosphates is suppressed in the ion source of the mass spectrometer. This effect is already seen for GGDP compared to FDP and GDP. (Manuscript 1). Tuning the LC-MS/MS for the detection of solanesyl diphosphate (C_{45}) failed, because no ions were formed even after increasing the sample concentration by 100 fold (unpublished data), but geranylfarnesyl diphosphate (C_{25}) was successfully detected from enzymatic assays (unpublished data). Which prenyl diphosphates between C_{30}-C_{45} can be detected has to be elucidated in future experiments.

Quantification of GDP, FDP and GGDP *in vivo* is possible, but needs relatively large quantities of plant material (ca. 1 g). Therefore with the current detection limit it is not possible to compare differences in the *in vivo* concentration of those prenyl diphosphates between different cell types of a given tissue, as can be done for transcript abundance, enzyme activity and terpene quantification (Abbott et al., 2010).

Although in Manuscript 2 internal standards were used for the quantification of GDP, FDP and GGDP. These standards only share a similar structure with the analytes and are chromatographically separated, it would be more desirable to use isotopically labeled compounds instead (Stokvis et al., 2005). Recently a procedure for chemical synthesis of hexadeuterated FDP and GGDP was published, which would be useful in supplying standards for more reliable prenyl diphosphate quantification *in vivo* (Subramanian et al., 2013).

4.3 Prenyl diphosphate chain length determination of IDS

The analytical ability to quantify prenyl diphosphates of different chain length *in vitro* as well as *in vivo* will help to deepen our knowledge about terpene biosynthesis in general, and is also a useful tool to understand the molecular mechanism of chain length determination in short-chain IDS. A topic researchers attempted to understand for decades. Here mostly side directed mutagenesis approaches were used, changing single or multiple amino acid residues close to the FARM region in short-chain IDS. Most notably here are amino acids in positions 4, 5, 8 and 11 before the FARM, they form a pocket accommodating the growing prenyl carbon chain. Increasing the size of those amino acids, causes steric hindrance and limits the length of the formed prenyl diphosphate, this is also known as the molecular ruler theory (Wang and Ohnuma, 2000; Liang et al., 2002; Vandermoten et al., 2009; Vandermoten et al., 2009; Oldfield and Lin, 2012). Newer findings also indicate the importance of the dimer interface between the two identical subunits, to be relevant for the product specificity (Ogawa et al., 2011; Chang et al., 2013). For long-chain IDS it is known that the purified enzyme is in need of detergents or phospholipids for an effective turnover. These lipids and detergents help in removal of the produced prenyl diphosphates from the active site. In addition to the increase in enzyme activity, usage of different detergents produce varying prenyl diphosphate chain length (Pan et al., 2013). For short-chain IDS to my best knowledge this was not observed.

Despite the knowledge about changes of chain length produced by an individual IDS, some IDS naturally release prenyl diphosphates of different size. Which is more frequently found for long-chain IDS under *in vitro* conditions (Hsieh et al., 2011; Pan et al., 2013; Wallrapp et al., 2013), however also short-chain IDS are not restricted to release products of one length. This was recently demonstrated for IDS from aphids and bark beetles producing GDP and FDP and for IDS1 from *Picea abies* producing GDP and GGDP without release of intermediately formed FDP (Vandermoten et al., 2008; Vandermoten et al., 2009; Schmidt et al., 2010; Keeling et al.,

2013). The product specificity of the aphid and bark beetle IDS can be modulated by the ratio of IDP towards DMADP (Vandermoten et al., 2008; Vandermoten et al., 2009; Keeling et al., 2013), being also demonstrated for other IDS, including long-chain IDS (Wallrapp et al., 2013).

Besides those known factors influencing the chain length, in Manuscript 3 the metal cofactor was identified to be of great importance. Influences of the metal cofactor on the product profile of an IDS was shown before for an long-chain IDS were exchanging Mg^{2+} to Co^{2+} increased the product size by one C_5 unit (Ohnuma et al., 1993). For short-chain IDS Mg^{2+} was shown to be the preferred cofactor and other metals usually decrease the enzyme activity, but changes in product composition by different metal cofactors were not investigated before (Tholl et al., 2001; Sen et al., 2007; Sen et al., 2007; Sen et al., 2007; Vandermoten et al., 2009; Barbar et al., 2013). The IDS characterized in Manuscript 3 in contrast is able to accept either Mg^{2+} or Co^{2+} as a metal cofactor, without any reduction in enzyme activity. Instead changing the metal cofactor from Mg^{2+} to Co^{2+} will decreases the product size by one C_5 unit, from FDP to GDP. If both metal cofactors are available, Co^{2+} is the preferred one. Both metals have differing atomic radii, which might induce changes in the protein structure resulting in variations of the active site pocket size. Exchange of metal cofactors is a newly described way for determining the product specificity of IDS. However the exact mechanism and the relevance for other insects and also for plant IDS still has to be demonstrated.

4.4 Importance of IDS for the regulation of terpene biosynthesis

Despite the newly developed analytical techniques for prenyl diphosphate detection, which have resulted in more knowledge about IDS product specificity *in vitro* and prenyl diphosphate concentrations *in vivo*, the regulatory role of IDS for terpene biosynthesis can only be assessed by manipulation of IDS enzyme abundance and activity either by overexpression or knock out/down experiments. In this part of the discussion the results gained by overexpression of *Pa*IDS1 in *P. glauca* (Manuscript 2) and RNAi mediated knock down of *Pc*IDS1 in *P. cochleariae* (Manuscript 3) will be compared with similar approaches from the literature.

4.4.1 RNAi and knock out of IDS

Very little information is present in the literature about knock down or knock out of plant or insect IDS. In plants, the double knock out of FDPS1 and FDPS2 in *Arabidopsis thaliana*, induced a lethal developmental arrest at very early embryo stages (Closa et al., 2010). In contrast to this, knock down by viral induced gene silencing (VIGS) of an FDPS in *Nicotiana attenuata* reduced the transcript abundance, FDPS enzyme activity and the sterol content, but the plants were still viable (Jassbi et al., 2008). The advantage of a knock down over a knock out approach becomes evident from previous manuscripts, especially when the enzyme being studied is involved in primary metabolism like FDPS. In plants, as in most other organisms, FDP and therefore FDPS are needed for *de novo* sterol synthesis. Sterols are essential in regulation of membrane fluidity and permeability and can also act as hormones in case of brassinosteroids (Schaller, 2003), thus a complete knock-out would be inviable. The remaining activity of the FDPS in knock down experiments might be sufficient to supply primary metabolism and still give an observable phenotype without lethal effects. Knock down of a GGDPS in *N. attenuata*, which presumably is only involved in secondary metabolism, reduced the amount of diterpene glycosides. This impaired defense against the tobacco hornworm, *Manduca sexta*, but had no adverse side effects on general plant viability in the absence of herbivory (Jassbi et al., 2008).

RNAi mediated knock down of the *Phaedon cochleariae* IDS1, produced a phenotype not making any terpene defense compounds several days after injection, due to reduction of IDS1 transcript levels and thereby IDS enzyme activity, but did not alter larval development (Manuscript 3). This particular IDS has a dual product specificity as it can produce GDP and FDP. In contrast to plants, insects and among them *P. cochleariae* have lost the ability to produce sterols *de novo* and strictly depend on sterols from their food source. Therefore IDS1 is not involved in sterol biosynthesis (Clayton, 1964; Jing et al., 2013). Nevertheless insects still need FDP to produce juvenile hormones (JH) for an adequate larval development (Belles et al., 2005). Since juvenile development is not affected in IDS1 RNAi-treated larvae, it has to be assumed that the remaining IDS activity is either sufficient to supply FDP for JH biosynthesis or RNAi is not working with the same efficacy in different tissues, a fact already discussed in the literature (Belles, 2010). Similar to these results, RNAi-mediated knock down of a GDPS/FDPS from the mountain pine beetle, *Dendroctonus ponderosae*, does not have large effects on the viability of these beetles (Keeling et al., 2013). Although instead of larvae, fully developed adult beetle were used, which were also artificially treated with juvenile hormone, the same publication

showed that RNAi-mediated knock down of a GGDPS in *D. ponderosae* inhibits the biosynthesis of the anti-aggregation pheromone frontalin (Keeling et al., 2013).

4.4.2 Overexpression of IDS

Overexpression of IDS was only successfully utilized in plants, not in animals, with the results depending on the individual IDS and the plant species used. FDPS1 overexpression either of a short or long form causes severe alterations in cytokinin homeostasis and induces senescence in *A. thaliana* (Masferrer et al., 2002; Manzano et al., 2006). In contrast, overexpression of FDPS from different origins in *Artemisia annua* increases the artemisinin amount without severe effects on plant vitality, as observed in *A. thaliana*, although some phenotypic variations in leaf morphology were noticed (Han et al., 2006; Banyai et al., 2010; Kai et al., 2011). Here it has to be noted that the biosynthesis of artemisinin may be somewhat unique, since IDP and DMADP are not exclusively supplied by the MVA pathway as expected for a sesquiterpene. Instead, one IDP unit originates from the MEP pathway (Towler and Weathers, 2007; Schramek et al., 2010). Unlike the previously mentioned IDS which are all localized in the cytosol, overexpression of IDS localized to the plastid, like the native GGDPS of *Salvia miltiorrhiza* in hairy root cultures increased the tanshinone amount (Kai et al., 2011) and overexpression of a GDPS in mint increased the total monoterpene content (Lange et al., 2011). Overexpression of the bifunctional GDP/GGDP producing IDS1 in *P. glauca* is increasing the total terpene amount (Manuscript 2), but not in the expected way. In contrast to an increase in the major terpenes of mint and *S. miltiorrhiza* after IDS overexpression, in *P. glauca* a minor class of terpenes increased by more than 10,000 fold. Combining the previously mentioned findings, it appears that overexpression of IDS in plants is influenced by the subcellular compartment in which the enzyme is expressed and might depend on the proportion of IDP and DMADP supplied by the MVA and MEP pathways. This proposition was already tested by overexpressing a TPS or a TPS together with an IDS either in the cytosol or plastid of *Nicotiana tabacum* (Wu et al., 2006). The authors chose a monoterpene or sesquiterpene producing TPS together with an IDS producing GDP or FDP. Overexpression of an IDS producing FDP in combination with a sesquiterpene producing TPS increased the amount of sesquiterpenes compared to overexpression of the TPS alone. The increase was higher if both enzymes were localized in the plastid, rather than in the cytosol, indicating regulatory differences between the two compartments. Unfortunately, in their other experiments the authors used an IDS thought to

produce GDP as its main product that actually makes medium/long-chain prenyl diphosphates instead (Hsieh et al., 2011). Therefore the results showing nearly no increase in terpene production after combined overexpression are simply further evidence confirming that this IDS makes longer products.

After overexpression of IDS1 in *P. glauca*, the *in planta* concentrations of prenyl diphosphates increased. To the best of my knowledge, there are no other studies investigating the *in vivo* concentrations of prenyl diphosphates after overexpression of IDS or other manipulations of terpene biosynthesis. Therefore those changes cannot be compared with other values from the literature. However the results demonstrate a direct link between the transcript abundance and total IDS enzyme activity and the quantities of GDP, FDP and GGDP found *in planta*. Furthermore, they also clearly show that the functionality of IDS overexpression depends on differences not only between the different cellular compartments (Wu et al., 2006), but also on the combination of promoter and investigated tissue.

4.4.3 Comparison of prenyl diphosphate pool sizes in plants

The previous chapters showed that manipulations of the expression of an IDS, either by knock out/down or overexpression can alter the terpene amount of an organism. But, the mechanism for this is not clear yet. Quantification of GDP, FDP and GGDP allows us to compare their concentrations with those of their direct precursors, namely IDP and DMADP. Depending on the resulting ratios, assumptions can be made on whether IDS are a limiting step in terpene biosynthesis or not. Prenyl diphosphate amounts in *P. glauca* vary between 0.1-0.5 nmol g^{-1} FW in needle tissue, whereas DMADP can be found in amounts more than 100 fold higher in *Populus* x *canescens* (21-36 nmol g^{-1} DW) and in even higher amounts in several pine species (50-650 nmol g^{-1} FW) and *P. abies* (100 nmol g^{-1} FW) in leaf or needle tissue (Rosenstiel et al., 2002; Behnke et al., 2007; Ghirardo et al., 2010). Even though only DMADP was quantified in spruce or poplar, an equilibrium between DMADP and IDP is established by isopentenyl diphosphate isomerase (Berthelot et al., 2012). Recently the DMADP:IDP ratio in kudzu (*Pueraria montana*) was determined to be around 2 in light adapted plants (Zhou et al., 2013). Although different methods and different species were used for quantifying prenyl diphosphates, the available data indicate that the IDS substrates, DMADP and IDP, are present in higher amounts than the IDS products, GDP, FDP and GGDP. Therefore IDS enzyme activity might be an overall limiting step in terpene biosynthesis.

A possible complication in relating prenyl diphosphate pool sizes to flux rates is that some plants produce the C_5 product, isoprene, from DMADP (Monson et al., 2013). Isoprene is produced either by an isoprene synthase, a specialized TPS only accepting DMADP as a substrate, or by a TPS that can accept DMADP in addition to GDP (Sharkey et al., 2013). Although isoprene may be produced in large amounts, its physiological role is still under debate, even though it has been shown to increase thermotolerance in poplar (Behnke et al., 2007; Monson et al., 2013). Plants emitting isoprene might have to adapt their terpene metabolism to produce greater amounts of DMADP by adjusting the flux of the MEP pathway and/or the ratio between IDP and DMADP established by isopentenyl diphosphate isomerase. On the other hand, isoprene synthase also could be a drain on DMADP increasing the proportion of IDP instead thereby optimizing the conditions for particular IDS to produce a certain prenyl diphosphate length. To date, nearly nothing is known about the interplay of IDS, IDI and isoprene synthase and the enzymes of the MEP and MVA pathways. However, such information is crucial to understand the regulation of terpene biosynthesis.

4.5 Storage and mode of action of terpenes

Knowledge about terpene biosynthesis and its regulation will give us the means to alter the qualitative and quantitative amount of terpenes of an organism. However since terpenes are used by plants to defend themselves against pathogens and herbivores and are used by insects as a defense against predators, both plants and insects need to store those terpenes to be readily available in case of an attack. Moreover the stored terpenes should have toxic or deterrent properties towards the attacking organism.

Yet only few terpenes are known to have distinct molecular targets, like cardenolides that target the Na^+/K^+-ATPases (Agrawal et al., 2012). Many terpenes are thought to act in a more general way by disturbing membrane integrity (Cox et al., 2000; Carson et al., 2002; Hammer et al., 2004; Di Pasqua et al., 2006; Turina et al., 2006; Di Pasqua et al., 2007; Witzke et al., 2010). This mode of toxicity, although not being specific has the advantage that resistance is less likely to be acquired by the attacking organism. However this mode of toxicity may not only apply to the attackers, but may also affect the producing organism itself. Therefore most organisms producing and storing terpenes have developed specialized structures for their storage. In plants this includes the resin channels or resin blisters in bark or needles of conifers (Franceschi et al., 2005), the trichomes of the Lamiaceae, e.g. mint and basil (Pichersky et al., 2006; Lange

et al., 2011), or Solanaceae, e.g. tomato and tobacco (Sallaud et al., 2009; Heiling et al., 2010; Tissier et al., 2013) and for insects this includes the defensive glands of leaf beetles and rove beetles among others (Termonia et al., 2001; Schierling and Dettner, 2013). If terpenes are not confined to storage structures, plants and insects may circumvent toxicity by altering their polarity. This can be done by adding sugars to make the terpene more polar and prevent integration into the membrane (Termonia et al., 2001; Aharoni et al., 2003; Burse et al., 2007; Jassbi et al., 2008; Heiling et al., 2010; Dinh et al., 2013). Alternatively, terpenes can be esterified to various fatty acids (Liljenberg and Karunen, 1978; Ekman, 1980; Karunen et al., 1980; Lütke-Brinkhaus et al., 1985; McKibben et al., 1985; Jondiko and Pattenden, 1989; Reiter and Lorbeer, 2001; Dunphy, 2006; Biedermann et al., 2008), which makes them too big to integrate into membranes and too lipophilic to be compatible with the amphiphilic nature of membranes. Terpene esters are likely to accumulate in storage structures for general lipids, like oil bodies (Gaude et al., 2007). Terpene esterification has been described in *A. thaliana* for phytol in senescent leaves or after feeding phytol artificially (Ischebeck et al., 2006), and the same class of molecules has also been found in other plants (Csupor, 1970; Liljenberg, 1977; Anderson et al., 1984; Pereira et al., 2002; Gaude et al., 2007). In senescent leaves, as plastids including the chlorophyll molecule are degraded, the high abundance of chlorophyll should lead to large amounts of free phytol after chlorophyll cleavage. To prevent these from becoming toxic, they are stored in an esterified form. Overexpression of IDS1 in white spruce appears to create a similar scenario. Here geranylgeraniol accumulates over time due to hydrolysis of high levels of GGDP and is therefore esterified to several fatty acids. The toxicity of geranylgeraniol is demonstrated by the lower survival rate of *Lymantria monacha* larvae feeding on IDS1 overexpressing white spruce that have large quantities of those esters present (Manuscript 2). Here the esters may be cleaved by the high quantities of esterases present in the gut of *Lymantria* species (Kapin and Ahmad, 1980) and affect the larval growth.

4.6 Future perspectives

This dissertation has increased our understanding of the *in vivo* significance of IDS in plants and insects, added an alternative mechanism for product chain length determination in IDS and advanced the methodology of prenyl diphosphate detection, as well as opening up directions for future research. Since it is now possible to quantify prenyl diphosphate metabolites *in planta*, this methodology can be applied to questions about pathway regulation. For example, it

would be advantageous to compare prenyl diphosphate concentrations in spruce with those from other plants to determine whether a correlation exists between the amount of terpene end products produced by a plant and the prenyl diphosphate concentrations present. It would also be of great interest to investigate how prenyl diphosphate concentrations might change upon herbivory, or simulation thereof by methyl jasmonate application.

To further improve our knowledge about the regulation of terpene biosynthesis and especially the role of IDS therein, the approach of overexpressing biosynthetic genes used in Manuscript 2 should be supplemented by an RNAi approach. Since the results of Manuscript 2 showed that IDS are not the only key enzymes of terpene biosynthesis in plants, the combined overexpression of IDS, IDI and/or TPS could gain further insights into the regulation. Quite recently a similar approach was used in *Nicotiana benthamiana* were transient overexpression of a diterpene TPS together with DXS and GGDPS increased the diterpene content 3.5 fold in comparison to overexpression of TPS alone, TPS+DXS or TPS+GGDPS (Brückner and Tissier, 2013). It would be of great interest if a stable overexpression in a different species, e.g. spruce, would have the same results.

The transport and storage of terpenes should also be investigated since the enhancement of terpene production might also lead to unexpected side effects, like the formation of geranylgeranyl fatty acid esters. A successful overproduction of desired terpenes might only be possible if there is a specialized structure to store them and secretory and/or transport mechanisms to move the compounds to the storage site. Transport here most likely occurs with the help of ABC-transporters, yet only two of these transporters were described recently, one in the plant *Nicotiana tabaccum* and one in the plant pathogen *Grosmannia clavigera* (Crouzet et al., 2013; Wang et al., 2013).

This thesis revealed that the identity of the divalent metal ion cofactor can alter the chain length of IDS product for an enzyme from the leaf beetle *Phaedon cochleariae*. Now, it should be tested if this phenomenon is specific for the *Phaedon cochleariae* enzyme or can also be observed with IDS from other insects or even plants. It might also be worth investigating how this mechanism for chain length determination interacts with the molecular ruler theory, using a site directed mutagenesis approach to identify critical amino acid residues near the active site or the dimer interface of the *Phaedon cochleariae* IDS1.

5. Summary

Terpenes are essential primary and secondary metabolites in every living organism. As secondary metabolites they are important defensive compounds of plants and insects. The biosynthesis of terpenes starts with the formation of two C_5 intermediates, isopentenyl diphosphate (IDP) and dimethylallyl diphosphate (DMADP), formed by the mevalonate (MVA) pathway or methylerythritol phosphate (MEP) pathway. In the next step of biosynthesis, isoprenyl diphosphate synthases (IDS) condense DMADP with a varying number of IDP molecules to produce longer prenyl diphosphates, like geranyl- (GDP, C_{10}), farnesyl- (FDP, C_{15}) and geranylgeranyl diphosphate (GGDP, C_{20}). GDP, FDP and GGDP are substrates for terpene synthases that produce the various terpene skeletons which can be further modified by other enzymes and give rise to the enormous structural diversity of more than 60,000 known terpene structures. IDS have a critical role in terpene biosynthesis since they are located at a central point where the pathway branches towards products of different sizes. But, there are still many open questions about what factors control the product specificity of these enzymes and the details of their regulatory role in terpene biosynthesis.

The published findings of the present dissertation begin with the description of a new LC-MS/MS based method for identification of the product specificity of individual IDS and the quantification of total IDS activity in protein extracts from plants. The method can detect the different isomeric forms of the short-chain prenyl diphosphates GDP, FDP and GGDP. This was the methodical basis for investigations on the regulatory function of *Picea abies* IDS1 after overexpression in *Picea glauca*. Here it was shown that overexpression under the control of an ubiquitin promoter is only functional in needles, but not in bark of *Picea glauca*. In needles overexpression increases the total IDS-activity 7-fold and the *in vivo* concentrations of GDP and GGDP 4- and 8-fold. Despite those increases in terpene precursors, monoterpenes and diterpenes of the defensive oleoresin, as well as the other major terpenoid products, carotenoids and sterols, were unaltered. Instead large amounts of geranylgeranyl fatty acid esters were formed that were shown to have defensive properties against the needle feeding insect *Lymantria monacha*. Comparison of the *in vivo* amount of GDP, FDP and GGDP with that of DMADP showed, that IDS form a metabolic bottleneck in plant terpene biosynthesis.

Besides of plants also insect employ terpenes to defend themselves against predators. Therefore also insects need IDS to produce those terpenes. One example here is the

horseradish leaf beetle *Phaedon cochleariae,* which has pairs of dorsal glands, that excrete the terpene chrysomelidial in case of an attack. Here an IDS, named IDS1, was identified that can produce either GDP or FDP, depending on the metal ion cofactor used. The results of the kinetic measurements and the structural modelling show that variations of the cofactor are an alternative way for IDS enzymes to alter the chain length of the prenyl diphosphate produced. With an RNAi approach it was revealed that IDS1 is indeed a key enzyme in chrysomelidial biosynthesis. RNAi mediated transcript suppression, reduced the total IDS enzyme activity, the amount of intermediates in the larvae and the volume of the defensive secretions.

6. Zusammenfassung

Terpene sind essentielle primäre und sekundäre Metaboliten und kommen daher in jedem lebenden Organismus vor. Als sekundäre Metaboliten haben sie große Bedeutung als defensive Verbindungen von Pflanzen und Insekten. Die Terpenbiosynthese beginnt mit der Produktion von Isopentenyldiphosphat (IDP) und Dimethylallyldiphosphat (DMADP), welche entweder auf dem Mevalonat- (MVA) oder dem Methylerythriolphosphat-Weg (MEP) erfolgt. Im nächsten Schritt der Terpenbiosynthese nutzen Isopentenyldiphosphat Synthasen (IDS) DMADP und 1-3 IDP Einheiten um längere Prenyldiphosphate, wie Geranyl-(GDP, C_{10}), Farnesyl- (FDP, C_{20}) und Geranylgeranyldiphosphat (GGDP, C_{20}), zu produzieren. GDP, FDP und GGDP ihrerseits sind die Substrate von Terpensynthasen, die für eine Vielzahl von Terpenstrukturen verantwortlich sind. Diese Terpenstrukturen können in nachfolgenden enzymatischen Reaktionen weiter zu über 60.000 bekannten Strukturen modifiziert werden. IDS wirken daher an einem zentralen Punkt der Terpenbiosynthese, an welchem sich diese in Produkte verschiedener Kettenlängen verzweigt. Darüber hinaus regulieren IDS den Fluss der Terpenbiosynthese. Zu Produktspezifität und der regulatorischen Rolle von IDS in der Terpenbiosynthese gibt es jedoch immer noch ungeklärte Fragen.

Die veröffentlichten Ergebnisse dieser Dissertation beschreiben im ersten Teil eine neu entwickelte LC-MS/MS basierte Methode, mit welcher sich die Reaktionsprodukte der IDS, sowie die IDS-Gesamtaktivität in Pflanzenextrakten bestimmen lässt. Es kann dabei zwischen den verschiedenen Isomeren von GDP, FDP und GGDP unterschieden werden. Diese Methode bildet im zweiten Teil der vorliegenden Arbeit eine Grundlage für Untersuchungen zur regulatorischen Funktion der *Picea abies* IDS1 mittels Überexpressionsstudien in *Picea glauca*. Hier konnte gezeigt werden, dass eine funktionale Überexpression des IDS1-Gens unter der Aktivität eines Ubiquitinpromotors nur in Nadeln, jedoch nicht in der Borke möglich ist. Die Überexpression führte in den Nadeln zu einer 7-fach höheren IDS-Gesamtaktivität und zu 4- und 8-fach höheren GDP und GGDP Konzentrationen *in vivo*. Trotz der erhöhten Konzentrationen der Terpenvorstufen GDP und GGDP wurden keine vermehrten Mengen von Monoterpenen und Diterpenen im Fichtenharz gefunden. Die Mengen an Sterolen und Karotenoiden waren ebenfalls unverändert. Stattdessen wurden hohe Mengen an Geranylgeranylfettsäureestern produziert, für welche eine Funktion in der Abwehr von nadelfressenden *Lymantria monacha* Larven gezeigt werden konnte. Der Vergleich der *in vivo* Konzentrationen von GDP, FDP und

GGDP mit der von DMADP deutet darauf hin, dass IDS ein limitierender Schritt in der Terpenbiosynthese sind.

Im dritten Kapitel wurde die Bedeutung von IDS für die Terpenbiosynthese von Insekten untersucht. Der Meerrettichblattkäfer *Phaedon cochleariae* nutzt das Terpen Chrysomelidial um sich gegen Prädatoren zu verteidigen. IDS1 wurde aus *Phaedon cochleariae* isoliert und charakterisiert. Diese IDS zeigt eine Abhängigkeit in ihrer Produktspezifität von Metallionen, die als Cofaktor in der enzymatischen Katalyse wirken. Bei Variation der Metallionen wird entweder hauptsächlich GDP oder FDP produziert. Die Resultate der kinetischen Messungen und der Strukturmodellierung zeigen, dass Metallionen-Cofaktoren ein alternativer Mechanismus für die Regulation der Produktspezifität sind. Mithilfe von RNAi-Versuchen konnte gezeigt werden, dass die IDS1 ein Schlüsselenzym der Chrysomelidialbiosynthese ist. Die RNAi vermittelte Transkriptverminderung von IDS1 führte dabei zu einer niedrigeren IDS-Gesamtaktivität, sowie zu weniger Chrysomelidial und Intermediaten von dessen Biosynthese in *P. cochleariae* Larven.

7. References

Aaron JA, Christianson DW (2010) Trinuclear metal clusters in catalysis by terpenoid synthases. Pure and Applied Chemistry **82:** 1585-1597

Abbott E, Hall D, Hamberger B, Bohlmann J (2010) Laser microdissection of conifer stem tissues: Isolation and analysis of high quality RNA, terpene synthase enzyme activity and terpenoid metabolites from resin ducts and cambial zone tissue of white spruce (*Picea glauca*). BMC Plant Biology **10:** 106-121

Agrawal AA, Petschenka G, Bingham RA, Weber MG, Rasmann S (2012) Toxic cardenolides: chemical ecology and coevolution of specialized plant-herbivore interactions. New Phytologist **194:** 28-45

Aharoni A, Giri AP, Deuerlein S, Griepink F, de Kogel WJ, Verstappen FWA, Verhoeven HA, Jongsma MA, Schwab W, Bouwmeester HJ (2003) Terpenoid metabolism in wild-type and transgenic Arabidopsis plants. Plant Cell **15:** 2866-2884

Akhtar TA, Matsuba Y, Schauvinhold I, Yu G, Lees HA, Klein SE, Pichersky E (2013) The tomato *cis*–prenyltransferase gene family. Plant Journal **73:** 640-652

Alex D, Bach TJ, Chye ML (2000) Expression of *Brassica juncea* 3-hydroxy-3-methylglutaryl CoA synthase is developmentally regulated and stress-responsive. Plant Journal **22:** 415-426

Alquezar B, Rodrigo MJ, Zacarías L (2008) Regulation of carotenoid biosynthesis during fruit maturation in the red-fleshed orange mutant Cara Cara. Phytochemistry **69:** 1997-2007

Anderson WH, Gellerman JL, Schlenk H (1984) Effect of drought on phytyl wax esters in *Phaseolus* leaves. Phytochemistry **23:** 2695-2696

Aquil S, Husaini AM, Abdin MZ, Rather GM (2009) Overexpression of the HMG-CoA reductase gene leads to enhanced artemisinin biosynthesis in transgenic *Artemisia annua* plants. Planta Medica **75:** 1453-1458

Arigoni D, Sagner S, Latzel C, Eisenreich W, Bacher A, Zenk MH (1997) Terpenoid biosynthesis from 1-deoxy-d-xylulose in higher plants by intramolecular skeletal rearrangement. Proceedings of the National Academy of Sciences of the United States of America **94:** 10600-10605

Ayora-Talavera T, Chappell J, Lozoya-Gloria E, Loyola-Vargas VM (2002) Overexpression in Catharanthus roseus hairy roots of a truncated hamster 3-hydroxy-3-methylglutaryl-CoA reductase gene. Applied Biochemistry and Biotechnology - Part A Enzyme Engineering and Biotechnology **97:** 135-145

Bach TJ (1986) Hydroxymethylglutaryl-CoA reductase, a key enzyme in phytosterol synthesis? Lipids **21:** 82-88

Bach TJ, Rogers DH, Rudney H (1986) Detergent-solubilization, purification, and characterization of membrane-bound 3-hydroxy-3-methylglutaryl-coenzyme A reductase from radish seedlings. European journal of biochemistry / FEBS **154:** 103-111

Bach TJ, Wettstein A, Boronat A, Ferrer A, Enjuto M, Gruissem W, Narita JO (1991) Properties and molecular cloning of plant HMG-CoA reductase. Physiology and Biochemistry of Sterols**:** 29-49

Banyai W, Kirdmanee C, Mii M, Supaibulwatana K (2010) Overexpression of farnesyl pyrophosphate synthase (FPS) gene affected artemisinin content and growth of *Artemisia annua* L. Plant Cell, Tissue and Organ Culture **103:** 255-265

Barbar A, Couture M, Sen SE, Béliveau C, Nisole A, Bipfubusa M, Cusson M (2013) Cloning, expression and characterization of an insect geranylgeranyl diphosphate synthase from *Choristoneura fumiferana*. Insect Biochemistry and Molecular Biology **43:** 947-958

Bearfield JC, Henry AG, Tittiger C, Blomquist GJ, Ginzel MD (2009) Two regulatory mechanisms of monoterpenoid pheromone production in *Ips spp.* of bark beetles. Journal of Chemical Ecology **35:** 689-697

Beck G, Coman D, Herren E, Ruiz-Sola MÁ, Rodríguez-Concepción M, Gruissem W, Vranová E (2013) Characterization of the GGPP synthase gene family in *Arabidopsis thaliana*. Plant Molecular Biology **82:** 393-416

Bede JC, Musser RO, Felton GW, Korth KL (2006) Caterpillar herbivory and salivary enzymes decrease transcript levels of *Medicago truncatula* genes encoding early enzymes in terpenoid biosynthesis. Plant Molecular Biology **60:** 519-531

Behnke K, Ehlting B, Teuber M, Bauerfeind M, Louis S, Hänsch R, Polle A, Bohlmann J, Schnitzler J-P (2007) Transgenic, non-isoprene emitting poplars don't like it hot. Plant Journal **51:** 485-499

Belles X (2010) Beyond Drosophila: RNAi In Vivo and Functional Genomics in Insects. *In* Annual Review of Entomology, Vol 55, pp 111-128

Belles X, Martin D, Piulachs MD (2005) The mevalonate pathway and the synthesis of juvenile hormone in insects. *In* Annual Review of Entomology, Vol 50, pp 181-199

Benz J, Fischer I, Rüdiger W (1983) Determination of phytyl diphosphate and geranylgeranyl diphosphate in etiolated oat seedlings. Phytochemistry **22:** 2801-2804

Berthelot K, Estevez Y, Deffieux A, Peruch F (2012) Isopentenyl diphosphate isomerase: A checkpoint to isoprenoid biosynthesis. Biochimie **94:** 1621-1634

Bhatnagar D, Soran H, Durrington PN (2008) Hypercholesterolaemia and its management. BMJ **337**

Bick JA, Lange BM (2003) Metabolic cross talk between cytosolic and plastidial pathways of isoprenoid biosynthesis: Unidirectional transport of intermediates across the chloroplast envelope membrane. Archives of Biochemistry and Biophysics **415:** 146-154

Biedermann M, Haase-Aschoff P, Grob K (2008) Wax ester fraction of edible oils: Analysis by on-line LC-GC-MS and GC x GC-FID. European Journal of Lipid Science and Technology **110:** 1084-1094

Blomquist GJ, Figueroa-Teran R, Aw M, Song M, Gorzalski A, Abbott NL, Chang E, Tittiger C (2010) Pheromone production in bark beetles. Insect Biochemistry and Molecular Biology **40:** 699-712

Blum MS, Brand JM, Wallace JB, Fales HM (1972) Chemical characterization of defensive secretion of a chrysomelid larva. Life Sciences Pt-2 Biochemistry General and Molecular Biology **11:** 525-531

Blum MS, Wallace JB, Duffield RM, Brand JM, Fales HM, Sokoloski EA (1978) Chrysomelidial in defensive secretions of leaf bettle *Gastrophysa cyanea* Melsheimer. Journal of Chemical Ecology **4:** 47-53

Bohlmann J, Keeling CI (2008) Terpenoid biomaterials. Plant Journal **54:** 656-669

Botella-Pavía P, Besumbes Ó, Phillips MA, Carretero-Paulet L, Boronat A, Rodríguez-Concepción M (2004) Regulation of carotenoid biosynthesis in plants: Evidence for a key role of hydroxymethylbutenyl diphosphate reductase in controlling the supply of plastidial isoprenoid precursors. Plant Journal **40:** 188-199

Brown K, Havel CM, Watson JA (1983) Isoprene synthesis in isolated embryonic Drosphila cells. 2. Regulation of 3-hydroxy-3-methylglutaryl coenzyme-A reductase activity. Journal of Biological Chemistry **258:** 8512-8518

Brückmann M, Termonia A, Pasteels JM, Hartmann T (2002) Characterization of an extracellular salicyl alcohol oxidase from larval defensive secretions of *Chrysomela populi* and *Phratora vitellinae* (Chrysomelina). Insect Biochemistry & Molecular Biology **32:** 1517-1523

Brückner K, Tissier A (2013) High-level diterpene production by transient expression in Nicotiana benthamiana. Plant Methods **9:** 46

Bueno E, Mesa S, Bedmar EJ, Richardson DJ, Delgado MJ (2012) Bacterial adaptation of respiration from oxic to microoxic and anoxic conditions: redox control. Antioxidants & Redox Signaling **16:** 819-852

Burg JS, Espenshade PJ (2011) Regulation of HMG-CoA reductase in mammals and yeast. Progress in Lipid Research **50:** 403-410

Burse A, Frick S, Discher S, Tolzin-Banasch K, Kirsch R, Strauss A, Kunert M, Boland W (2009) Always being well prepared for defense: The production of deterrents by juvenile Chrysomelina beetles (Chrysomelidae). Phytochemistry **70:** 1899-1909

Burse A, Frick S, Schmidt A, Buechler R, Kunert M, Gershenzon J, Brandt W, Boland W (2008) Implication of HMGR in homeostasis of sequestered and de novo produced precursors of the iridoid biosynthesis in leaf beetle larvae. Insect Biochemistry and Molecular Biology **38:** 76-88

Burse A, Schmidt A, Frick S, Kuhn J, Gershenzon J, Boland W (2007) Iridoid biosynthesis in Chrysomelina larvae: Fat body produces early terpenoid precursors. Insect Biochemistry & Molecular Biology **37:** 255-265

Campos N, Boronat A (1995) Targeting and topology in the membrane of plant 3-hydroxy-3-methylglutaryl Coenzyme A reductase. Plant Cell **7:** 2163-2174

Carretero-Paulet L, Ahumada I, Cunillera N, Rodríguez-Concepción M, Ferrer A, Boronat A, Campos N (2002) Expression and molecular analysis of the Arabidopsis DXR gene encoding 1-deoxy-D-xylulose 5-phosphate reductoisomerase, the first committed enzyme of the 2-C-methyl-D-erythritol 4-phosphate pathway. Plant Physiology **129:** 1581-1591

Carretero-Paulet L, Cairó A, Botella-Pavía P, Besumbes O, Campos N, Boronat A, Rodríguez-Concepción M (2006) Enhanced flux through the methylerythritol 4-phosphate pathway

in Arabidopsis plants overexpressing deoxyxylulose 5-phosphate reductoisomerase. Plant Molecular Biology **62:** 683-695

Carson CF, Mee BJ, Riley TV (2002) Mechanism of action of *Melaleuca alternifolia* (tea tree) oil on *Staphylococcus aureus* determined by time-kill, lysis, leakage, and salt tolerance assays and electron microscopy. Antimicrobial Agents and Chemotherapy **46:** 1914-1920

Cazzonelli CI, Pogson BJ (2010) Source to sink: regulation of carotenoid biosynthesis in plants. Trends in Plant Science **15:** 266-274

Chang C-K, Teng K-H, Lin S-W, Chang T-H, Liang P-H (2013) Control activity of yeast geranylgeranyl diphosphate synthase from dimer interface through H-Bonds and hydrophobic interaction. Biochemistry **52:** 2783-2792

Chang T-H, Hsieh F-L, Ko T-P, Teng K-H, Liang P-H, Wang AH-J (2010) Structure of a heterotetrameric geranyl pyrophosphate synthase from mint (*Mentha piperita*) reveals intersubunit regulation. Plant Cell **22:** 454-467

Chen F, Tholl D, Bohlmann J, Pichersky E (2011) The family of terpene synthases in plants: A mid-size family of genes for specialized metabolism that is highly diversified throughout the kingdom. Plant Journal **66:** 212-229

Chen F, Tholl D, D'Auria JC, Farooq A, Pichersky E, Gershenzon J (2003) Biosynthesis and emission of terpenoid volatiles from Arabidopsis flowers. The Plant Cell Online **15:** 481-494

Choi D, Bostock RM, Avdiushko S, Hildebrand DF (1994) Lipid-derived signals that discriminate wound- and pathogen-responsive isoprenoid pathways in plants: Methyl jasmonate and the fungal elicitor arachidonic acid induce different 3-hydroxy-3-methylglutaryl-coenzyme A reductase genes and antimicrobial isoprenoids in *Solanum tuberosum* L. Proceedings of the National Academy of Sciences of the United States of America **91:** 2329-2333

Christianson DW (2008) Unearthing the roots of the terpenome. Current Opinion in Chemical Biology **12:** 141-150

Clayton RB (1964) The utilization of sterols by insects. Journal of Lipid Research **5:** 3-19

Closa M, Vranova E, Bortolotti C, Bigler L, Arró M, Ferrer A, Gruissem W (2010) The *Arabidopsis thaliana* FPP synthase isozymes have overlapping and specific functions in isoprenoid biosynthesis, and complete loss of FPP synthase activity causes early developmental arrest. Plant Journal **63:** 512-525

Clouse SD, Sasse JM (1998) BRASSINOSTEROIDS: Essential Regulators of Plant Growth and Development. Annual Review of Plant Physiology and Plant Molecular Biology **49:** 427-451

Cox SD, Mann CM, Markham JL, Bell HC, Gustafson JE, Warmington JR, Wyllie SG (2000) The mode of antimicrobial action of the essential oil of *Melaleuca alternifolia* (tea tree oil). Journal of Applied Microbiology **88:** 170-175

Crouzet J, Roland J, Peeters E, Trombik T, Ducos E, Nader J, Boutry M (2013) NtPDR1, a plasma membrane ABC transporter from Nicotiana tabacum, is involved in diterpene transport. Plant Molecular Biology **82:** 181-192

Csupor L (1970) [Phytol in yellow leaves.] (in german) Planta Medica **19:** 37-43

Cunillera N, Arró M, Delourme D, Karst F, Boronat A, Ferrer A (1996) *Arabidopsis thaliana* contains two differentially expressed farnesyl diphosphate synthase genes. Journal of Biological Chemistry **271:** 7774-7780

Daloze D, Pasteels JM (1994) Isolation of 8-hydroxygeraniol-8-O-beta-D-glucoside, a probable intermediate in biosynthesis of iridoid monoterpenes, from defensive secretions of *Plagiodera versicolora* and *Gastrophysa viridula* (Coleoptera, Chrysomelidae). Journal of Chemical Ecology **20:** 2089-2097

Degenhardt J, Köllner TG, Gershenzon J (2009) Monoterpene and sesquiterpene synthases and the origin of terpene skeletal diversity in plants. Phytochemistry **70:** 1621-1637

Dhar MK, Koul A, Kaul S (2013) Farnesyl pyrophosphate synthase: a key enzyme in isoprenoid biosynthetic pathway and potential molecular target for drug development. New Biotechnology **30:** 114-123

Di Pasqua R, Betts G, Hoskins N, Edwards M, Ercolini D, Mauriello G (2007) Membrane toxicity of antimicrobial compounds from essential oils. Journal of Agricultural and Food Chemistry **55:** 4863-4870

Di Pasqua R, Hoskins N, Betts G, Mauriello G (2006) Changes in membrane fatty acids composition of microbial cells induced by addiction of thymol, carvacrol, limonene, cinnamaldehyde, and eugenol in the growing media. Journal of Agricultural and Food Chemistry **54:** 2745-2749

Dinh SN, Galis I, Baldwin IT (2013) UVB radiation and 17-hydroxygeranyllinalool diterpene glycosides provide durable resistance against mirid (*Tupiocoris notatus*) attack in field-grown *Nicotiana attenuata* plants. Plant, Cell & Environment **36:** 590-606

Dobler S, Petschenka G, Pankoke H (2011) Coping with toxic plant compounds - The insect's perspective on iridoid glycosides and cardenolides. Phytochemistry **72:** 1593-1604

Duchêne E, Butterlin G, Claudel P, Dumas V, Jaegli N, Merdinoglu D (2009) A grapevine (*Vitis vinifera* L.) deoxy-d-xylulose synthase gene colocates with a major quantitative trait loci for terpenol content. Theoretical and Applied Genetics **118:** 541-552

Dudakovic A, Tong HX, Hohl RJ (2011) Geranylgeranyl diphosphate depletion inhibits breast cancer cell migration. Investigational New Drugs **29:** 912-920

Dudareva N, Andersson S, Orlova I, Gatto N, Reichelt M, Rhodes D, Boland W, Gershenzon J (2005) The nonmevalonate pathway supports both monoterpene and sesquiterpene formation in snapdragon flowers. Proceedings of the National Academy of Sciences of the United States of America **102:** 933-938

Dunphy PJ (2006) Location and biosynthesis of monoterpenyl fatty acyl esters in rose petals. Phytochemistry **67:** 1110-1119

Ekman R (1980) Geranylgeranyl esters in norway spruce wood. Phytochemistry **19:** 321-322

Espenshade PJ, Hughes AL (2007) Regulation of sterol synthesis in eukaryotes. *In* Annual Review of Genetics, Vol 41. Annual Reviews, Palo Alto, pp 401-427

Estévez JM, Cantero A, Reindl A, Reichler S, León P (2001) 1-deoxy-D-xylulose-5-phosphate synthase, a limiting enzyme for plastidic isoprenoid biosynthesis in plants. Journal of Biological Chemistry **276:** 22901-22909

Fernández-Grandon GM, Woodcock CM, Poppy GM (2013) Do asexual morphs of the peach-potato aphid, *Myzus persicae*, utilise the aphid sex pheromone? Behavioural and electrophysiological responses of M. persicae virginoparae to (4a*S*,7*S*,7a*R*)-nepetalactone and its effect on aphid performance. Bulletin of entomological research **103:** 466-472

Fischer M, Meyer S, Oswald M, Claudel P, Karst F (2013) Metabolic engineering of monoterpenoid production in yeast. *In* TJ Bach, M Rohmer, eds, Isoprenoid Synthesis in Plants and Microorganisms. Springer New York, pp 65-71

Flores-Pérez U, Pérez-Gil J, Rodríguez-Villalón A, Gil MJ, Vera P, Rodríguez-Concepción M (2008) Contribution of hydroxymethylbutenyl diphosphate synthase to carotenoid biosynthesis in bacteria and plants. Biochemical and Biophysical Research Communications **371:** 510-514

Flügge UI, Gao W (2005) Transport of isoprenoid intermediates across chloroplast envelope membranes. Plant Biology **7:** 91-97

Franceschi VR, Krokene P, Christiansen E, Krekling T (2005) Anatomical and chemical defenses of conifer bark against bark beetles and other pests. New Phytologist **167:** 353-376

Gaude N, Bréhélin C, Tischendorf G, Kessler F, Dörmann P (2007) Nitrogen deficiency in Arabidopsis affects galactolipid composition and gene expression and results in accumulation of fatty acid phytyl esters. The Plant Journal **49:** 729-739

Gershenzon J, Kreis J (1999) Biochemistry of terpenoids: monoterpenes, sesquiterpenes, diterpenes, sterols, cardiac glycosides, and steroid saponins. *In* M Wink, ed, Biochemistry of Plant Secondary Metabolism. Sheffield Academic Press, Sheffield, UK, pp 222–299

Ghirardo A, Koch K, Taipale R, Zimmer INA, Schnitzler J-P, Rinne J (2010) Determination of de novo and pool emissions of terpenes from four common boreal/alpine trees by 13CO2 labelling and PTR-MS analysis. Plant, Cell & Environment **33:** 781-792

Gilg AB, Bearfield JC, Tittiger C, Welch WH, Blomquist GJ (2005) Isolation and functional expression of an animal geranyl diphosphate synthase and its role in bark beetle pheromone biosynthesis. Proceedings of the National Academy of Sciences of the United States of America **102:** 9760-9765

Gilg AB, Tittiger C, Blomquist GJ (2009) Unique animal prenyltransferase with monoterpene synthase activity. Naturwissenschaften **96:** 731-735

Guevara-García A, San Román C, Arroyo A, Cortés ME, De La Gutiérrez-Nava ML, León P (2005) Characterization of the Arabidopsis clb6 mutant illustrates the importance of posttranscriptional regulation of the methyl-d-erythritol 4-phosphate pathway. Plant Cell **17:** 628-643

Gutensohn M, Orlova I, Nguyen TTH, Davidovich-Rikanati R, Ferruzzi MG, Sitrit Y, Lewinsohn E, Pichersky E, Dudareva N (2013) Cytosolic monoterpene biosynthesis is supported by plastid-generated geranyl diphosphate substrate in transgenic tomato fruits. Plant Journal **75:** 351-363

Gutiérrez-Nava MDLL, Gillmor CS, Jiménez LF, Guevara-García A, Léon P (2004) Chloroplast Biogenesis genes act cell and noncell autonomously in early chloroplast development. Plant Physiology **135:** 471-482

Hagen C, Grunewald K (2000) Fosmidomycin as an inhibitor of the non-mevalonate terpenoid pathway depresses synthesis of secondary carotenoids in flagellates of the green alga *Haematococcus pluvialis*. Journal of Applied Botany **74:** 137-140

Hall GM, Tittiger C, Andrews GL, Mastick GS, Kuenzli M, Luo X, Seybold SJ, Blomquist GJ (2002) Midgut tissue of male pine engraver, *Ips pini*, synthesizes monoterpenoid pheromone component ipsdienol de novo. Naturwissenschaften **89:** 79-83

Hall GM, Tittiger C, Blomquist GJ, Andrews GL, Mastick GS, Barkawi LS, Bengoa C, Seybold SJ (2002) Male Jeffrey pine beetle, *Dendroctonus jeffreyi*, synthesizes the pheromone component frontalin in anterior midgut tissue. Insect Biochemistry & Molecular Biology **32:** 1525-1532

Hammer KA, Carson CF, Riley TV (2004) Antifungal effects of *Melaleuca alternifolia* (tea tree) oil and its components on *Candida albicans*, *Candida glabrata* and *Saccharomyces cerevisiae*. Journal of Antimicrobial Chemotherapy **53:** 1081-1085

Han JL, Liu BY, Ye HC, Wang H, Li ZQ, Li GF (2006) Effects of overexpression of the endogenous farnesyl diphosphate synthase on the artemisinin content in *Artemisia annua* L. Journal of Integrative Plant Biology **48:** 482-487

Harada H, Fujisawa M, Teramoto M, Sakurai N, Suzuki H, Shibata D, Misawa N (2009) Simple functional analysis of key genes involved in astaxanthin biosynthesis using Arabidopsis cultured cells. Plant Biotechnology **26:** 81-92

Harker M, Hellyer A, Clayton JC, Duvoix A, Lanot A, Safford R (2003) Co-ordinate regulation of sterol biosynthesis enzyme activity during accumulation of sterols in developing rape and tobacco seed. Planta **216:** 707-715

Harker M, Holmberg N, Clayton JC, Gibbard CL, Wallace AD, Rawlins S, Hellyer SA, Lanot A, Safford R (2003) Enhancement of seed phytosterol levels by expression of an N-terminal truncated *Hevea brasiliensis* (rubber tree) 3-hydroxy-3-methylglutaryl-CoA reductase. Plant Biotechnol. J. **1:** 113-121

Hartmann MA, Wentzinger L, Hemmerlin A, Bach TJ (2000) Metabolism of farnesyl diphosphate in tobacco BY-2 cells treated with squalestatin. Biochemical Society Transactions **28:** 794-796

Havel C, Rector ER, Watson JA (1986) sopentenoid synthesis in isolated embryonic Drosophila cells - possible regulation of 3-hydroxy-3-methylglutaryl coenzyme A reductase - activity by shunted mevalonate carbon. Journal of Biological Chemistry **261:** 150-156

Hedden P, Thomas SG (2012) Gibberellin biosynthesis and its regulation. Biochemical Journal **444:** 11-25

Heiling S, Schuman MC, Schoettner M, Mukerjee P, Berger B, Schneider B, Jassbi AR, Baldwin IT (2010) Jasmonate and ppHsystemin regulate key malonylation steps in the biosynthesis of 17-hydroxygeranyllinalool diterpene glycosides, an abundant and effective direct defense against herbivores in *Nicotiana attenuata*. The Plant Cell Online **22:** 273-292

Hemmerlin A, Harwood JL, Bach TJ (2012) A raison d'être for two distinct pathways in the early steps of plant isoprenoid biosynthesis? Progress in Lipid Research **51:** 95-148

Hemmerlin A, Hoeffler JF, Meyer O, Tritsch D, Kagan IA, Grosdemange-Billiard C, Rohmer M, Bach TJ (2003) Cross-talk between the cytosolic mevalonate and the plastidial methylerythritol phosphate pathways in tobacco bright yellow-2 cells. Journal of Biological Chemistry **278:** 26666-26676

Hilker M, Schulz S (1994) composition of larval secretion of *Chrysomela lapponica* (Coleoptera, Chrysomelidae) and its dependence on host-plant. Journal of Chemical Ecology **20:** 1075-1093

Hojo M, Maekawa K, Saitoh S, Shigenobu S, Miura T, Hayashi Y, Tokuda G, Maekawa H (2012) Exploration and characterization of genes involved in the synthesis of diterpene defence secretion in nasute termite soldiers. Insect Molecular Biology **21:** 545-557

Holmberg N, Harker M, Wallace AD, Clayton JC, Gibbard CL, Safford R (2003) Co-expression of N-terminal truncated 3-hydroxy-3-methylglutaryl CoA reductase and C24-sterol methyltransferase type 1 in transgenic tobacco enhances carbon flux towards end-product sterols. Plant Journal **36:** 12-20

Hsieh F-L, Chang T-H, Ko T-P, Wang AH-J (2011) Structure and mechanism of an Arabidopsis medium/long-chain-length prenyl pyrophosphate synthase. Plant Physiology **155:** 1079-1090

Huang M, Sanchez-Moreiras AM, Abel C, Sohrabi R, Lee S, Gershenzon J, Tholl D (2012) The major volatile organic compound emitted from *Arabidopsis thaliana* flowers, the sesquiterpene (E)-β-caryophyllene, is a defense against a bacterial pathogen. New Phytologist **193:** 997-1008

Ischebeck T, Zbierzak AM, Kanwischer M, Dörmann P (2006) A salvage pathway for phytol metabolism in Arabidopsis. Journal of Biological Chemistry **281:** 2470-2477

Jassbi AR, Gase K, Hettenhausen C, Schmidt A, Baldwin IT (2008) Silencing geranylgeranyl diphosphate synthase in *Nicotiana attenuata* dramatically impairs resistance to tobacco hornworm. Plant Physiology **146:** 974-986

Jing X, Grebenok RJ, Behmer ST (2013) Sterol/steroid metabolism and absorption in a generalist and specialist caterpillar: Effects of dietary sterol/steroid structure, mixture and ratio. Insect Biochemistry and Molecular Biology **43:** 580-587

Jondiko IJO, Pattenden G (1989) Terpenoids and an apocarotenoid from seeds of *Bixa orellana*. Phytochemistry **28:** 3159-3162

Julliard JH, Douce R (1991) Biosynthesis of the thiazole moiety of thiamin (vitamin B1) in higher plant chloroplasts. Proceedings of the National Academy of Sciences of the United States of America **88:** 2042-2045

Kai G, Miao Z, Zhang L, Zhao D, Liao Z, Sun X, Zhao L, Tang K (2006) Molecular cloning and expression analyses of a new gene encoding 3-hydroxy-3-methylglutaryl-CoA synthase from *Taxus* x *media*. Biologia Plantarum **50:** 359-366

Kai GY, Xu H, Zhou CC, Liao P, Xiao JB, Luo XQ, You LJ, Zhang L (2011) Metabolic engineering tanshinone biosynthetic pathway in *Salvia miltiorrhiza* hairy root cultures. Metabolic Engineering **13:** 319-327

Kaneko Y, Kinjoh T, Kiuchi M, Hiruma K (2011) Stage-specific regulation of juvenile hormone biosynthesis by ecdysteroid in *Bombyx mori*. Molecular and Cellular Endocrinology **335:** 204-210

Kang J-H, Gonzales-Vigil E, Matsuba Y, Pichersky E, Barry C (2014) Determination of residues responsible for substrate and product specificity of *Solanum habrochaites* short-chain *cis*-prenyltransferases. Plant Physiology **164**: 80-91

Kannenberg EL, Poralla K (1999) Hopanoid biosynthesis and function in bacteria. Naturwissenschaften **86:** 168-176

Kapin MA, Ahmad S (1980) Esterases in larval tissues of gypsy moth, *Lymantria dispar* (L.): Optimum assay conditions, quantification and characterization. Insect Biochemistry **10:** 331-337

Karunen P, Mikola H, Ekman R (1980) Occurrence of steryl and wax esterrs in *Dicranum elongatum*. Physiologia Plantarum **48:** 554-559

Keeling CI, Bearfield JC, Young S, Blomquist GJ, Tittiger C (2006) Effects of juvenile hormone on gene expression in the pheromone-producing midgut of the pine engraver beetle, *Ips pini*. Insect Molecular Biology **15:** 207-216

Keeling CI, Bohlmann J (2006) Diterpene resin acids in conifers. Phytochemistry **67:** 2415-2423

Keeling CI, Chiu CC, Aw T, Li M, Henderson H, Tittiger C, Weng H-B, Blomquist GJ, Bohlmann J (2013) Frontalin pheromone biosynthesis in the mountain pine beetle, *Dendroctonus ponderosae*, and the role of isoprenyl diphosphate synthases. Proceedings of the National Academy of Sciences of the United States of America **110:** 18838-18843

Keena MA (2003) Survival and development of *Lymantria monacha* (Lepidoptera: Lymantriidae) on North American and introduced Eurasian tree species. Journal of economic Entomology **96:** 43-52

Keena MA, Vandel A, Pultar O (2010) Phenology of *Lymantria monacha* (Lepidoptera: Lymantriidae) laboratory reared on spruce foliage or a newly developed artificial diet. Annals of the Entomological Society of America **103:** 949-955

Khemvong S, Suvachittanont W (2005) Molecular cloning and expression of a cDNA encoding 1-deoxy-D-xylulose-5- phosphate synthase from oil palm *Elaeis guineensis* Jacq. Plant Science **169:** 571-578

Kim O, Bang K, Jung S, Kim Y, Hyun D, Kim S, Cha S (2010) Molecular characterization of ginseng farnesyl diphosphate synthase gene and its up-regulation by methyl jasmonate. Biologia Plantarum **54:** 47-53

Kim YB, Kim SM, Kang MK, Kuzuyama T, Lee JK, Park SC, Shin SC, Kim SU (2009) Regulation of resin acid synthesis in *Pinus densiflora* by differential transcription of genes encoding multiple 1-deoxy-d-xylulose 5-phosphate synthase and 1-hydroxy-2-methyl-2-(E)-butenyl 4-diphosphate reductase genes. Tree Physiology **29:** 737-749

Kishimoto S, Ohmiya A (2006) Regulation of carotenoid biosynthesis in petals and leaves of chrysanthemum (*Chrysanthemum morifolium*). Physiologia Plantarum **128:** 436-447

Klimetzek D, Vite JP (1989) Tierische Schädlinge. *In* H Schmidt-Vogt, ed, Die Fichte, Vol 2. Verlag Paul Parey, Hamburg and Berlin, pp 40-131

Köhle A, Sommer S, Yazaki K, Ferrer A, Boronat A, Li SM, Heide L (2002) High level expression of chorismate pyruvate-lyase (UbiC) and HMG-CoA reductase in hairy root cultures of *Lithospermum erythrorhizon*. Plant and Cell Physiology **43:** 894-902

Köksal M, Hu H, Coates RM, Peters RJ, Christianson DW (2011) Structure and mechanism of the diterpene cyclase ent-copalyl diphosphate synthase. Nature Chemical Biology **7:** 431-433

Kolotilin I, Koltai H, Tadmor Y, Bar-Or C, Reuveni M, Meir A, Nahon S, Shlomo H, Chen L, Levin I (2007) Transcriptional profiling of high pigment-2^{dg} tomato mutant links early fruit plastid biogenesis with its overproduction of phytonutrients. Plant Physiology **145:** 389-401

Kuhn J, Pettersson EM, Feld BK, Nie L, Tolzin-Banasch K, M'Rabet SM, Pasteels J, Boland W (2007) Sequestration of plant-derived phenolglucosides by larvae of the leaf beetle *Chrysomela lapponica*: Thioglucosides as mechanistic probes. Journal of Chemical Ecology **33:** 5-24

Kurokawa T, Ogura K, Seto S (1971) Formation of polyprenyl phosphates by a cell-free enzyme of. Biochemical and Biophysical Research Communications **45:** 251-257

Lange BM, Turner GW (2013) Terpenoid biosynthesis in trichomes-current status and future opportunities. Plant Biotechnology Journal **11:** 2-22

Lange BM, Mahmoud SS, Wildung MR, Turner GW, Davis EM, Lange I, Baker RC, Boydston RA, Croteau RB (2011) Improving peppermint essential oil yield and composition by metabolic engineering. Proceedings of the National Academy of Sciences of the United States of America **108:** 16944-16949

Lange BM, Severin K, Bechthold A, Heide L (1998) Regulatory role of microsomal 3-hydroxy-3-methylglutaryl-coenzyme A reductase for shikonin biosynthesis in *Lithospermum erythrorhizon* cell suspension cultures. Planta **204:** 234-241

Liang P-H, Ko T-P, Wang AH-J (2002) Structure, mechanism and function of prenyltransferases. European Journal of Biochemistry **269:** 3339-3354

Lieutier F, Day K, Battisti A, Grégoire J, Evans H (2004) Bark and wood boring insects in living trees in Europe, A Synthesis. Springer

Liljenberg C (1977) Occurrence of phytolpyrophosphate and acyl esters of phytol in irradiated dark-grown barley seedlings and their possible role in biosynthesis of chlorophyll. Physiologia Plantarum **39:** 101-105

Liljenberg C, Karunen P (1978) Changes in content of phytyl and geranylgeranyl esters of germinating *Polytrichum commune* spores. Physiologia Plantarum **44:** 369-372

Loguercio LL, Wilkins TA (1998) Structural analysis of a HMG-CoA-reductase pseudogene: Insights into evolutionary processes affecting the hmgr gene family in allotetraploid cotton (*Gossypium hirsutum* L.). Current Genetics **34:** 241-249

Lois LM, Rodríguez-Concepción M, Gallego F, Campos N, Boronat A (2000) Carotenoid biosynthesis during tomato fruit development: Regulatory role of 1-deoxy-D-xylulose 5-phosphate synthase. Plant Journal **22:** 503-513

Lombard J, Moreira D (2011) Origins and early evolution of the mevalonate pathway of isoprenoid biosynthesis in the three domains of life. Molecular Biology and Evolution **28:** 87-99

Lorenz M, Boland W, Dettner K (1993) Biosynthesis of iridodials in the defense glands of beetle larvae (Chrysomelinae). Angewandte Chemie-International Edition in English **32:** 912-914

Lütke-Brinkhaus F, Weiss G, Kleinig H (1985) Prenyl lipid formation in spinach-chloroplasts and in a cell-free system of *Synechococcus* (Cyanobacteria)- Polyprenols, chlorophylls, and fatty-acid prenyl esters. Planta **163:** 68-74

Mahmoud SS, Croteau RB (2001) Metabolic engineering of essential oil yield and composition in mint by altering expression of deoxyxylulose phosphate reductoisomerase and menthofuran synthase. Proceedings of the National Academy of Sciences of the United States of America **98:** 8915-8920

Manzano D, Busquets A, Closa M, Hoyerová K, Schaller H, Kaminek M, Arró M, Ferrer A (2006) Overexpression of farnesyl diphosphate synthase in Arabidopsis mitochondria triggers light-dependent lesion formation and alters cytokinin homeostasis. Plant Molecular Biology **61:** 195-213

Martin D, Tholl D, Gershenzon J, Bohlmann J (2002) Methyl jasmonate induces traumatic resin ducts, terpenoid resin biosynthesis, and terpenoid accumulation in developing xylem of Norway spruce stems. Plant Physiology **129:** 1003-1018

Martin DM, Faldt J, Bohlmann J (2004) Functional characterization of nine Norway spruce TPS genes and evolution of gymnosperm terpene synthases of the TPS-d subfamily. Plant Physiology **135:** 1908-1927

Martin DM, Gershenzon J, Bohlmann J (2003) Induction of volatile terpene biosynthesis and diurnal emission by methyl jasmonate in foliage of Norway spruce. Plant Physiology **132:** 1586-1599

Martin VJJ, Pitera DJ, Withers ST, Newman JD, Keasling JD (2003) Engineering a mevalonate pathway in *Escherichia coli* for production of terpenoids. Nature Biotechnology **21:** 796-802

Masferrer A, Arró M, Manzano D, Schaller H, Fernández-Busquets X, Moncaleán P, Fernández B, Cunillera N, Boronat A, Ferrer A (2002) Overexpression of *Arabidopsis thaliana* farnesyl diphosphate synthase (FPS1S) in transgenic Arabidopsis induces a cell death/senescence-like response and reduced cytokinin levels. Plant Journal **30:** 123-132

Matsumi R, Atomi H, Driessen AJM, van der Oost J (2011) Isoprenoid biosynthesis in Archaea – Biochemical and evolutionary implications. Research in Microbiology **162:** 39-52

Maury J, Asadollahi MA, Formenti LR, Schalk M, Nielsen J (2013) Metabolic engineering of isoprenoid production: reconstruction of multistep heterologous pathways in tractable hosts. *In* TJ Bach, M Rohmer, eds, Isoprenoid Synthesis in Plants and Microorganisms. Springer New York, pp 73-89

McKibben GH, Thompson MJ, Parrott WL, Thompson AC, Lusby WR (1985) Identification of feeding stimulants for boll-weevils from cotton buds and anthers. Journal of Chemical Ecology **11:** 1229-1238

Meinwald J, Jones TH, Eisner T, Hicks K (1977) Defense-mechanisms of arthropods .56. new methylcyclopentanoid terpenes from larval defensive secretion of a chrysomelid beetle (*Plagiodera versicolora*). Proceedings of the National Academy of Sciences of the United States of America **74:** 2189-2193

Mitchell JW, Mandava N, Worley JF, Plimmer JR, Smith MV (1970) Brassins - a new family of plant hormones from rape pollen. Nature **225:** 1065-1066

Monson RK, Jones RT, Rosenstiel TN, Schnitzler JP (2013) Why only some plants emit isoprene. Plant Cell & Environment **36:** 503-516

Morris WL, Ducreux LJM, Hedden P, Millam S, Taylor MA (2006) Overexpression of a bacterial 1-deoxy-D-xylulose 5-phosphate synthase gene in potato tubers perturbs the isoprenoid metabolic network: Implications for the control of the tuber life cycle. Journal of Experimental Botany **57:** 3007-3018

Morrone D, Lowry L, Determan M, Hershey D, Xu M, Peters R (2010) Increasing diterpene yield with a modular metabolic engineering system in *E. coli*: comparison of MEV and MEP isoprenoid precursor pathway engineering. Applied Microbiology and Biotechnology **85:** 1893-1906

Muñoz-Bertomeu J, Arrillaga I, Ros R, Segura J (2006) Up-Regulation of 1-deoxy-d-xylulose-5-phosphate synthase enhances production of essential oils in transgenic spike lavender. Plant Physiology **142:** 890-900

Muñoz-Bertomeu J, Sales E, Ros R, Arrillaga I, Segura J (2007) Up-regulation of an N-terminal truncated 3-hydroxy-3-methylglutaryl CoA reductase enhances production of essential oils and sterols in transgenic *Lavandula latifolia*. Plant Biotechnology Journal **5:** 746-758

Nagata N, Suzuki M, Yoshida S, Muranaka T (2002) Mevalonic acid partially restores chloroplast and etioplast development in Arabidopsis lacking the non-mevalonate pathway. Planta **216:** 345-350

Nieto B, Forés O, Arró M, Ferrer A (2009) Arabidopsis 3-hydroxy-3-methylglutaryl-CoA reductase is regulated at the post-translational level in response to alterations of the sphingolipid and the sterol biosynthetic pathways. Phytochemistry **70:** 58-64

Nogués I, Brilli F, Loreto F (2006) Dimethylallyl diphosphate and geranyl diphosphate pools of plant species characterized by different isoprenoid emissions. Plant Physiology **141:** 721-730

Nowicka B, Gruszka J, Kruk J (2013) Function of plastochromanol and other biological prenyllipids in the inhibition of lipid peroxidation—A comparative study in model systems. Biochimica et Biophysica Acta - Biomembranes **1828:** 233-240

Nystedt B, Street NR, Wetterbom A, Zuccolo A, Lin YC, Scofield DG, Vezzi F, Delhomme N, Giacomello S, Alexeyenko A, Vicedomini R, Sahlin K, Sherwood E, Elfstrand M, Gramzow L, Holmberg K, Hallman J, Keech O, Klasson L, Koriabine M, Kucukoglu M, Kaller M, Luthman J, Lysholm F, Niittyla T, Olson A, Rilakovic N, Ritland C, Rossello JA, Sena J, Svensson T, Talavera-Lopez C, Theissen G, Tuominen H, Vanneste K, Wu ZQ, Zhang B, Zerbe P, Arvestad L, Bhalerao R, Bohlmann J, Bousquet J, Garcia Gil R, Hvidsten TR, de Jong P, MacKay J, Morgante M, Ritland K, Sundberg B, Thompson SL, Van de Peer Y, Andersson B, Nilsson O, Ingvarsson PK, Lundeberg J, Jansson S (2013)

The Norway spruce genome sequence and conifer genome evolution. Nature **497:** 579-584

Ogawa T, Yoshimura T, Hemmi H (2011) Connected cavity structure enables prenyl elongation across the dimer interface in mutated geranylfarnesyl diphosphate synthase from *Methanosarcina mazei*. Biochemical and Biophysical Research Communications **409:** 333-337

Ohnuma S, Koyama T, Ogura K (1993) Alteration of the product specificities of prenyltransferases by metal-ions. Biochemical and Biophysical Research Communications **192:** 407-412

Oldfield E, Lin F-Y (2012) Terpene Biosynthesis: Modularity Rules. Angewandte Chemie-International Edition **51:** 1124-1137

Paddon CJ, McPhee D, Westfall PJ, Benjamin KR, Pitera DJ, Regentin R, Fisher K, Fickes S, Leavell MD, Newman JD (2013) Microbially derived semisynthetic artemisinin. *In* TJ Bach, M Rohmer, eds, Isoprenoid Synthesis in Plants and Microorganisms. Springer New York, pp 91-106

Pan J-J, Ramamoorthy G, Poulter CD (2013) Dependence of the product chain-length on detergents for long-chain E-polyprenyl diphosphate synthases. Biochemistry **52:** 5002-5008

Pasteels JM, Braekman JC, Daloze D, Ottinger R (1982) Chemical defence in chrysomelid larvae and adults. Tetrahedron **38:** 1891-1897

Pasteels JM, Duffey S, Rowellrahier M (1990) Toxins in chrysomelid beetles - possible evolutionary sequence from denovo synthesis to derivation from food-plant chemicals. Journal of Chemical Ecology **16:** 211-222

Pereira AS, Siqueira DS, Elias VO, Simoneit BRT, Cabral JA, Aquino Neto FR (2002) Three series of high molecular weight alkanoates found in Amazonian plants. Phytochemistry **61:** 711-719

Pettersson M, Unelius CR, Valterova I, Borg-Karlson AK (2008) Semiochemicals related to the aphid *Cinara pilicornis* and its host, *Picea abies*: A method to assign nepetalactone diastereomers. Journal of Chromatography A **1180:** 165-170

Phillips MA, Croteau RB (1999) Resin-based defenses in conifers. Trends in Plant Science **4:** 184-190

Pichersky E, Gershenzon J (2002) The formation and function of plant volatiles: Perfumes for pollinator attraction and defense. Current Opinion in Plant Biology **5:** 237-243

Pichersky E, Noel JP, Dudareva N (2006) Biosynthesis of plant volatiles: Nature's diversity and ingenuity. Science **311:** 808-811

Piller LE, Abraham M, Dörmann P, Kessler F, Besagni C (2012) Plastid lipid droplets at the crossroads of prenylquinone metabolism. Journal of Experimental Botany **63:** 1609-1618

Ponzio C, Gols R, Pieterse CMJ, Dicke M (2013) Ecological and phytohormonal aspects of plant volatile emission in response to single and dual infestations with herbivores and phytopathogens. Functional Ecology **27:** 587-598

Re EB, Jones D, Learned RM (1995) Co-expression of native and introduced genes reveals cryptic regulation of HMG CoA reductase expression in Arabidopsis. Plant Journal **7:** 771-784

Reiter B, Lorbeer E (2001) Analysis of the wax ester fraction of olive oil and sunflower oil by gas chromatography and gas chromatography-mass spectrometry. Journal of the American Oil Chemists Society **78:** 881-888

Rinaldi C, Kohler A, Frey P, Duchaussoy F, Ningre N, Couloux A, Wincker P, Le Thiec D, Fluch S, Martin F, Duplessis S (2007) Transcript profiling of poplar leaves upon infection with compatible and incompatible strains of the foliar rust *Melampsora larici-populina*. Plant Physiology **144:** 347-366

Rodríguez-Concepción M (2006) Early steps in isoprenoid biosynthesis: Multilevel regulation of the supply of common precursors in plant cells. Phytochemistry Reviews **5:** 1-15

Rodríguez-Concepción M, Ahumada I, Diez-Juez E, Sauret-Güeto S, María Lois L, Gallego F, Carretero-Paulet L, Campos N, Boronat A (2001) 1-Deoxy-D-xylulose 5-phosphate reductoisomerase and plastid isoprenoid biosynthesis during tomato fruit ripening. Plant Journal **27:** 213-222

Rosenstiel TN, Fisher AJ, Fall R, Monson RK (2002) Differential accumulation of dimethylallyl diphosphate in leaves and needles of isoprene- and methylbutenol-emitting and nonemitting species. Plant Physiology **129:** 1276-1284

Sales E, Muñoz-Bertomeu J, Arrillaga I, Segura J (2007) Enhancement of cardenolide and phytosterol levels by expression of an N-terminally truncated 3-hydroxy-3-methylglutaryl CoA reductase in transgenic *Digitalis minor*. Planta Medica **73:** 605-610

Sallaud C, Rontein D, Onillon S, Jabès F, Duffé P, Giacalone C, Thoraval S, Escoffier C, Herbette G, Leonhardt N, Causse M, Tissier A (2009) A novel pathway for sesquiterpene biosynthesis from Z,Z-farnesyl pyrophosphate in the wild tomato *Solanum habrochaites*. The Plant Cell Online **21:** 301-317

Schaller H (2003) The role of sterols in plant growth and development. Progress in Lipid Research **42:** 163-175

Schierling A, Dettner K (2013) The pygidial defense gland system of the Steninae (Coleoptera, Staphylinidae): Morphology, ultrastructure and evolution. Arthropod Structure & Development **42:** 197-208

Schilmiller AL, Schauvinhold I, Larson M, Xu R, Charbonneau AL, Schmidt A, Wilkerson C, Last RL, Pichersky E (2009) Monoterpenes in the glandular trichomes of tomato are synthesized from a neryl diphosphate precursor rather than geranyl diphosphate. Proceedings of the National Academy of Sciences of the United States of America **106:** 10865-10870

Schmidt A, Gershenzon J (2007) Cloning and characterization of isoprenyl diphosphate synthases with farnesyl diphosphate and geranylgeranyl diphosphate synthase activity from Norway spruce (*Picea abies*) and their relation to induced oleoresin formation. Phytochemistry **68:** 2649-2659

Schmidt A, Gershenzon J (2008) Cloning and characterization of two different types of geranyl diphosphate synthases from Norway spruce (*Picea abies*). Phytochemistry **69:** 49-57

Schmidt A, Nagel R, Krekling T, Christiansen E, Gershenzon J, Krokene P (2011) Induction of isoprenyl diphosphate synthases, plant hormones and defense signalling genes correlates with traumatic resin duct formation in Norway spruce (*Picea abies*). Plant Molecular Biology **77:** 577-590

Schmidt A, Wächtler B, Temp U, Krekling T, Séguin A, Gershenzon J (2010) A bifunctional geranyl and geranylgeranyl diphosphate synthase is involved in terpene oleoresin formation in *Picea abies*. Plant Physiology **152:** 639-655

Schramek N, Wang H, Römisch-Margl W, Keil B, Radykewicz T, Winzenhörlein B, Beerhues L, Bacher A, Rohdich F, Gershenzon J, Liu B, Eisenreich W (2010) Artemisinin biosynthesis in growing plants of *Artemisia annua*. A 13CO2 study. Phytochemistry **71:** 179-187

Schuhr CA, Radykewicz T, Sagner S, Latzel C, Zenk MH, Arigoni D, Bacher A, Rohdich F, Eisenreich W (2003) Quantitative assessment of crosstalk between the two isoprenoid biosynthesis pathways in plants by NMR spectroscopy. Phytochemistry Reviews **2:** 3-16

Schulz S, Gross J, Hilker M (1997) Origin of the defensive secretion of the leaf beetle *Chrysomela lapponica*. Tetrahedron **53:** 9203-9212

Seegmiller AC, Dobrosotskaya I, Goldstein JL, Ho YK, Brown MS, Rawson RB (2002) The SREBP pathway in Drosophila: Regulation by palmitate, not sterols. Developmental Cell **2:** 229-238

Sen SE, Brown DC, Sperry AE, Hitchcock JR (2007) Prenyltransferase of larval and adult *M. sexta* corpora allata. Insect Biochemistry and Molecular Biology **37:** 29-40

Sen SE, Cusson M, Trobaugh C, Beliveau C, Richard T, Graham W, Mimms A, Roberts G (2007) Purification, properties and heteromeric association of type-1 and type-2 lepidopteran farnesyl diphosphate synthases. Insect Biochemistry and Molecular Biology **37:** 819-828

Sen SE, Trobaugh C, Beliveau C, Richard T, Cusson M (2007) Cloning, expression and characterization of a dipteran farnesyl diphosphate synthase. Insect Biochemistry and Molecular Biology **37:** 1198-1206

Sharkey TD, Gray DW, Pell HK, Breneman SR, Topper L (2013) Isoprene synthase genes form a monophyletic clade of acyclic terpene synthases in the TPS-B terpene synthase family. Evolution **67:** 1026-1040

Shibata M, Mikota T, Yoshimura A, Iwata N, Tsuyama M, Kobayashi Y (2004) Chlorophyll formation and photosynthetic activity in rice mutants with alterations in hydrogenation of the chlorophyll alcohol side chain. Plant Science **166:** 593-600

Skorupinska-Tudek K, Poznanski J, Wojcik J, Bienkowski T, Szostkiewicz I, Zelman-Femiak M, Bajda A, Chojnacki T, Olszowska O, Grunler J, Meyer O, Rohmer M, Danikiewicz W, Swiezewska E (2008) Contribution of the mevalonate and methylerythritol phosphate pathways to the biosynthesis of dolichols in plants. Journal of Biological Chemistry **283:** 21024-21035

Soe ARB, Bartram S, Gatto N, Boland W (2004) Are iridoids in leaf beetle larvae synthesized de novo or derived from plant precursors? A methodological approach. Isotopes in Environmental and Health Studies **40:** 175-180

Soetens P, Pasteels JM, Daloze D (1993) A simple method for in-vivo testing of glandular enzymatic-activity on potential precursors of larval defensive compounds in *Phratora* species (Coleoptera, Chrysomelinae). Experientia **49:** 1024-1026

Soler E, Clastre M, Bantignies B, Marigo G, Ambid C (1993) Uptake of isopentenyl diphosphate by plastids isolated from *Vitis vinifera* L. cell suspensions. Planta **191:** 324-329

Song M, Kim AC, Gorzalski AJ, MacLean M, Young S, Ginzel MD, Blomquist GJ, Tittiger C (2013) Functional characterization of myrcene hydroxylases from two geographically distinct *Ips pini* populations. Insect Biochemistry and Molecular Biology **43:** 336-343

Staniek A, Bouwmeester H, Fraser PD, Kayser O, Martens S, Tissier A, van der Krol S, Wessjohann L, Warzecha H (2013) Natural products - modifying metabolite pathways in plants. Biotechnology journal **8:** 1159-1171

Stermer BA, Bostock RM (1987) Involvement of 3-hydroxy-3-methylglutaryl coenzyme A reductase in the regulation of sesquiterpenoid phytoalexin synthesis in potato. Plant Physiology **84:** 404-408

Stokvis E, Rosing H, Beijnen JH (2005) Stable isotopically labeled internal standards in quantitative bioanalysis using liquid chromatography/mass spectrometry: necessity or not? Rapid Communications in Mass Spectrometry **19:** 401-407

Subramanian T, Subramanian KL, Sunkara M, Onono FO, Morris AJ, Spielmann HP (2013) Syntheses of deuterium labeled prenyldiphosphate and prenylcysteine analogues for in vivo mass spectrometric quantification. Journal of Labelled Compounds & Radiopharmaceuticals **56:** 370-375

Suzuki M, Kamide Y, Nagata N, Seki H, Ohyama K, Kato H, Masuda K, Sato S, Kato T, Tabata S, Yoshida S, Muranaka T (2004) Loss of function of 3-hydroxy-3-methylglutaryl coenzyme A reductase 1 (HMG1) in Arabidopsis leads to dwarfing, early senescence and male sterility, and reduced sterol levels. Plant Journal **37:** 750-761

Symmes EJ, Dewhirst SY, Birkett MA, Campbell CAM, Chamberlain K, Pickett JA, Zalom FG (2012) The sex pheromones of mealy plum (*Hyalopterus pruni*) and leaf-curl plum (*Brachycaudus helichrysi*) aphids: Identification and field trapping of male and gynoparous aphids in prune orchards. Journal of Chemical Ecology **38:** 576-583

Termonia A, Hsiao TH, Pasteels JM, Milinkovitch MC (2001) Feeding specialization and host-derived chemical defense in Chrysomeline leaf beetles did not lead to an evolutionary dead end. Proceedings of the National Academy of Sciences of the United States of America **98:** 3909-3914

Termonia A, Pasteels JM (1999) Larval chemical defence and evolution of host shifts in Chrysomela leaf beetles. Chemoecology **9:** 13-23

Tholl D (2006) Terpene synthases and the regulation, diversity and biological roles of terpene metabolism. Current Opinion in Plant Biology **9:** 297-304

Tholl D, Croteau R, Gershenzon J (2001) Partial purification and characterization of the short-chain prenyltransferases, geranyl diphosphate synthase and farnesyl diphosphate synthase, from *Abies grandis* (grand fir). Archives of Biochemistry and Biophysics **386:** 233-242

Tholl D, Lee S (2011) Terpene specialized metabolism in *Arabidopsis thaliana*. The Arabidopsis Book / American Society of Plant Biologists **9:** e0143

Tissier A (2012a) Glandular trichomes: what comes after expressed sequence tags? Plant Journal **70:** 51-68

Tissier A (2012b) Trichome Specific Expression: Promoters and Their Applications. *In* YO Çiftçi, ed, Transgenic Plants - Advances and Limitations. InTech Open Access Company, Rijeka, Croatia, pp 353–378

Tissier A, Sallaud C, Rontein D (2013) Tobacco trichomes as a platform for terpenoid biosynthesis engineering. *In* TJ Bach, M Rohmer, eds, Isoprenoid Synthesis in Plants and Microorganisms. Springer New York, pp 271-283

Tittiger C, Barkawi LS, Bengoa CS, Blomquist GJ, Seybold SJ (2003) Structure and juvenile hormone-mediated regulation of the HMG-CoA reductase gene from the Jeffrey pine beetle, *Dendroctonus jeffreyi*. Molecular and Cellular Endocrinology **199:** 11-21

Tittiger C, Blomquist GJ, Ivarsson P, Borgeson CE, Seybold SJ (1999) Juvenile hormone regulation of HMG-R gene expression in the bark beetle *Ips paraconfusus* (Coleoptera : Scolytidae): implications for male aggregation pheromone biosynthesis. Cellular and Molecular Life Sciences **55:** 121-127

Tittiger C, O'Keeffe C, Bengoa CS, Barkawi LS, Seybold SJ, Blomquist GJ (2000) Isolation and endocrine regulation of an HMG-CoA synthase cDNA from the male Jeffrey pine beetle, *Dendroctonus jeffreyi* (Coleoptera : Scolytidae). Insect Biochemistry and Molecular Biology **30:** 1203-1211

Towler M, Weathers P (2007) Evidence of artemisinin production from IPP stemming from both the mevalonate and the nonmevalonate pathways. Plant Cell Reports **26:** 2129-2136

Turina AdV, Nolan MV, Zygadlo JA, Perillo MA (2006) Natural terpenes: Self-assembly and membrane partitioning. Biophysical Chemistry **122:** 101-113

Vandermoten S, Charloteaux B, Santini S, Sen SE, Beliveau C, Vandenbol M, Francis F, Brasseur R, Cusson M, Haubruge E (2008) Characterization of a novel aphid prenyltransferase displaying dual geranyl/farnesyl diphosphate synthase activity. FEBS Letters **582:** 1928-1934

Vandermoten S, Haubruge E, Cusson M (2009) New insights into short-chain prenyltransferases: structural features, evolutionary history and potential for selective inhibition. Cellular and Molecular Life Sciences **66:** 3685-3695

Vandermoten S, Mescher MC, Francis F, Haubruge E, Verheggen FJ (2012) Aphid alarm pheromone: An overview of current knowledge on biosynthesis and functions. Insect Biochemistry and Molecular Biology **42:** 155-163

Vandermoten S, Santini S, Haubruge E, Heuze F, Francis F, Brasseur R, Cusson M, Charloteaux B (2009) Structural features conferring dual geranyl/farnesyl diphosphate synthase activity to an aphid prenyltransferase. Insect Biochemistry and Molecular Biology **39:** 707-716

Veith M, Dettner K, Boland W (1996) Stereochemistry of an alcohol oxidase from the defensive secretion of larvae of the leaf beetle *Phaedon armoraciae* (Coleoptera: Chrysomelidae). Tetrahedron **52:** 6601-6612

Veith M, Lorenz M, Boland W, Simon H, Dettner K (1994) Biosynthesis of iridoid monoterpenes in insects - Defensive secretions from larvae of leaf beetles (Coleoptera, Chrysomelidae). Tetrahedron **50:** 6859-6874

Veith M, Oldham NJ, Dettner K, Pasteels JM, Boland W (1997) Biosynthesis of defensive allomones in leaf beetle larvae: Stereochemistry of salicylalcohol oxidation in *Phratora vitellinae* and comparison of enzyme substrate and stereospecificity with alcohol oxidases from several iridoid producing leaf beetles. Journal of Chemical Ecology **23:** 429-443

Wallrapp FH, Pan J-J, Ramamoorthy G, Almonacid DE, Hillerich BS, Seidel R, Patskovsky Y, Babbitt PC, Almo SC, Jacobson MP, Poulter CD (2013) Prediction of function for the polyprenyl transferase subgroup in the isoprenoid synthase superfamily. Proceedings of the National Academy of Sciences of the United States of America **110:** E1196-1202

Wang J, Stieglitz KA, Kantrowitz ER (2005) Metal Specificity Is Correlated with Two Crucial Active Site Residues in *Escherichia coli* Alkaline Phosphatase. Biochemistry **44:** 8378-8386

Wang KC, Ohnuma S (2000) Isoprenyl diphosphate synthases. Biochimica et Biophysica Acta-Molecular and Cell Biology of Lipids **1529:** 33-48

Wang Y, Lim L, DiGuistini S, Robertson G, Bohlmann J, Breuil C (2013) A specialized ABC efflux transporter GcABC-G1 confers monoterpene resistance to Grosmannia clavigera, a bark beetle-associated fungal pathogen of pine trees. New Phytologist **197:** 886-898

Wang ZJ, Dong YC, Desneux N, Niu CY (2013) RNAi Silencing of the *Ha*HMG-CoA Reductase Gene Inhibits Oviposition in the *Helicoverpa armigera* Cotton Bollworm. Plos One **8**

Wasko BM, Dudakovic A, Hohl RJ (2011) Bisphosphonates induce autophagy by depleting geranylgeranyl diphosphate. Journal of Pharmacology and Experimental Therapeutics **337:** 540-546

Wegener A, Gimbel W, Werner T, Hani J, Ernst D, Sandermann Jr H (1997) Molecular cloning of ozone-inducible protein from *Pinus sylvestris* L. with high sequence similarity to vertebrate 3-hydroxy-3-methylglutaryl-CoA-synthase. Biochimica et Biophysica Acta - Gene Structure and Expression **1350:** 247-252

Wellenstein G (ed.) 1942. Die Nonne in Ostpreußen (1933-1937). Freilandstudien der Waldstation für Schädlingsbekämpfung in Jagdhaus Rominten. Monographien zur angewandten Entomologie, Nummer 15, Parey, Berlin 1942

Wentzinger LF, Bach TJ, Hartmann MA (2002) Inhibition of squalene synthase and squalene epoxidase in tobacco cells triggers an up-regulation of 3-hydroxy-3-methylglutaryl coenzyme a reductase. Plant Physiology **130:** 334-346

Wiberley AE, Donohue AR, Westphal MM, Sharkey TD (2009) Regulation of isoprene emission from poplar leaves throughout a day. Plant, Cell & Environment **32:** 939-947

Witzke S, Duelund L, Kongsted J, Petersen M, Mouritsen OG, Khandelia H (2010) Inclusion of terpenoid plant extracts in lipid bilayers investigated by molecular dynamics simulations. Journal of Physical Chemistry B **114:** 15825-15831

Wu SQ, Schalk M, Clark A, Miles RB, Coates R, Chappell J (2006) Redirection of cytosolic or plastidic isoprenoid precursors elevates terpene production in plants. Nature Biotechnology **24:** 1441-1447

Yalovsky S (2011) Protein prenylation CaaX processing in plants. *In* F Tamanoi, CA Hrycyna, MO Bergo, eds, Enzymes, Vol 29: Protein Prenylation, Pt A, Vol 29. Elsevier Science Bv, Sara Burgerhartstraat 25, Po Box 211, 1000 Ae Amsterdam, Netherlands, pp 163-182

Yi P, Han Z, Li XM, Olson EN (2006) The mevalonate pathway controls heart formation in Drosophila by isoprenylation of G gamma 1. Science **313:** 1301-1303

Zhang DL, Poulter CD (1993) Analysis and purification of phosphorylated isoprenoids by reversed-phase HPLC. Analytical Biochemistry **213:** 356-361

Zhao T, Krokene P, Hu J, Christiansen E, Björklund N, Långström B, Solheim H, Borg-Karlson A-K (2011) Induced terpene accumulation in Norway spruce inhibits bark beetle colonization in a dose-dependent manner. PLoS One **6:** e26649

Zhou C, Li Z, Wiberley-Bradford AE, Weise SE, Sharkey TD (2013) Isopentenyl diphosphate and dimethylallyl diphosphate/isopentenyl diphosphate ratio measured with recombinant isopentenyl diphosphate isomerase and isoprene synthase. Analytical Biochemistry **440:** 130-136

Zulak KG, Bohlmann J (2010) Terpenoid biosynthesis and specialized vascular cells of conifer defense. Journal of Integrative Plant Biology **52:** 86-97

Zverina EA, Lamphear CL, Wright EN, Fierke CA (2012) Recent advances in protein prenyltransferases: substrate identification, regulation, and disease interventions. Current Opinion in Chemical Biology **16:** 544-552

8. Eigenständigkeitserklärung

Hiermit erkläre ich, entsprechend § 5 Absatz 4 der Promotionsordnung der Biologisch-Pharmazeutischen Fakultät der Friedrich Schiller Universität Jena, das mir die geltende Promotionsordnung bekannt ist. Die vorliegende Dissertation habe ich eigenständig und nur unter Verwendung angegebener Quellen und Hilfsmittel angefertigt, wobei von Dritten übernommene Textabschnitte entsprechend gekennzeichnet wurden. Alle Personen, die einen entscheidenden Beitrag zu den Manuskripten geleistet haben, sind in Kapitel 2 aufgeführt beziehungsweise in der Danksagung erwähnt. Die Hilfe eines Promotionsberaters wurde nicht in Anspruch genommen noch haben Dritte geldwerte Leistungen für Arbeiten im Zusammenhang mit der vorliegenden Dissertation erhalten. Gemäß den Durchführungsbestimmungen der Promotionsordnung für eine publikationsbasierte Dissertation wurde die Beschreibung des von mir geleisteten Eigenanteils von dem Betreuer der Dissertation, Prof. Dr. Jonathan Gershenzon, mit Unterschrift bestätigt und der Fakultät vorgelegt. Zu keinem früheren Zeitpunkt wurde diese Dissertation, eine in wesentlichen Teilen ähnliche Arbeit oder eine andere Abhandlung bei einer Hochschule als Dissertation eingereicht.

Raimund Nagel

Jena, den

9. Acknowledgements

Foremost I want to thank Axel Schmidt for introducing me to the topic of my dissertation, his excellent supervision and the constant support, even if things were not working out in the first place.

Professor Jonathan Gershenzon I want to thank for giving me the opportunity to work in his lab and to give me the freedom to pursue my own ideas.

I am deeply grateful to the Zwillenberg-Tietz-Stiftung for funding the final year of my dissertation and to the Max-Planck-Gesellschaft for general funding.

I also want to thank all members of the Gershenzon Department, in particular Jan, Aileen, Andrea, Meret and the other PhD students for all the discussions, help and the moral support during the dissertation, Marion for her technical assistance especially by creating “my” transgenic trees. Michael for answering all my questions about analytical equipment and procedures, and the constant help he offers to everybody and Angela for managing the Department so enthusiastically.

The Beetle group of the Boland Department I thank for the great cooperation and especially Sindy for sharing her project with me.

Since you do not only live for science, I want to thank Ulli, Jens, Cora, Nicci + Torsten and Michael for the shared happiness and their moral support during the rough times of this dissertation.

I also want to thank the members of my WG (Ulli W., Matti, Nora und Christina) for many wonderful evenings and weekends.

My parents, my sister and the extended family I thank for their constant support and encouragement along the way. “Other things might change, but we start and end with family” [A. Brandt]

10. Curriculum Vitae

Personal

Name:	Raimund Nagel
Date of birth:	27th September 1983
Place of birth:	Halberstadt
Gender:	male
Marital status:	single
Nationality:	German

Education

2010-current	PhD student at the Max Planck Institute for Chemical Ecology, Jena Department of Biochemistry Supervisor: Prof. Dr. Jonathan Gershenzon
2009	Diploma at the Max Planck Institute for Chemical Ecology, Jena Department of Biochemistry Supervisor: Prof. Dr. Jonathan Gershenzon
2004-2009	Studies in Biochemistry at the Friedrich-Schiller-University, Jena
2003-2004	Civil Service, Cecilienstift Halberstadt
2003	Abitur at Landesschule Pforta, Bad Kösen OT Schulpforte

10.1 Publications

Nagel, R., Berasategui, A., Paetz, C., Gershenzon, J., Schmidt, A. (2014) Overexpression of an isoprenyl diphosphate synthase in spruce leads to unexpected terpene diversion products that function in plant defense. Plant Physiology, doi:10.1104/pp.113.228940 (in press).

Kulkarni, R., Pandit, S. S., Chidley, H., Nagel, R., Schmidt, A., Gershenzon, J., Pujari, K., Giri, A., Gupta, V. (2013). Characterization of three novel isoprenyl diphosphate synthases from the terpenoid rich mango fruit. Plant Physiology and Biochemistry, 71, 121-131.

Frick, S., Nagel, R., Schmidt, A., Bodemann, R., Rahfeld, P., Pauls, G., Brandt, W., Gershenzon, J., Boland, W., Burse, A. (2013). Metal ions control product specificity of isoprenyl diphosphate synthases in the insect terpenoid pathway. Proceedings of the National Academy of Sciences of the United States of America, 110 (11), 4194-4199.

Nagel, R., Gershenzon, J., Schmidt, A. (2012). Nonradioactive assay for detecting isoprenyl diphosphate synthase activity in crude plant extracts using liquid chromatography coupled with tandem mass spectrometry. Analytical Biochemistry, 422, 33-38.

Schmidt, A., Nagel, R., Krekling, T., Christiansen, E., Gershenzon, J., Krokene, P. (2011). Induction of isoprenyl diphosphate synthases, plant hormones and defense signalling genes correlates with traumatic resin duct formation in Norway spruce (*Picea abies*). Plant Molecular Biology, 77 (6), 577-590.

10.2 Oral presentations

Nagel R. Diversion products of terpenoid-based oleoresin biosynthesis function in defense. TERPNET 2013 - 11th International Meeting on Biosynthesis, Function and Biotechnology of Isoprenoids in Terrestrial and Marine Organisms in Terrestrial and Marine Organisms, TERPNET 2013; COST Action FA1006 "Plant Engine"; COST Action FA1106 "QualityFruit"; EU-SMARTCELL, Kolympari, Crete, GR, Jun 2013

Nagel R. Unexpected sied-branch products of terpenoid-based oleoresin biosynthesis function in plant defense. 8th Plant Science Student Conference, Leibnitz-Institut für Pflanzengenetik und Kulturpflanzenforschung (IPK), Gatersleben, DE, Jun 2012

Nagel R. Molecular and analytical characterization of terpene biosynthesis in transgenic spruce lines over-expressing isoprenyl diphosphate synthases. 11th IMPRS Symposium, MPI for Chemical Ecology, Dornburg, DE, Feb 2012

Nagel R. Molecular and analytical characterization of terpene biosynthesis in transgenic spruce lines over-expressing isoprenyl diphosphate synthases. 7th Plant Science Student Conference, Leibniz-Institut für Pflanzenbiochemie (IPB), Halle (Saale), DE, Jun 2011

10.3 Poster presentations

Nagel R., Berasategui A., Gershenzon J., Schmidt A. Diversion products of terpenoid-based oleoresin biosynthesis function in defense. 9th Plant Science Student Conference, Leibniz-Institut für Pflanzenbiochemie (IPB), Halle (Saale), DE, Mai 2013

Nagel R., Gershenzon J., Schmidt A. Unexpected side-products of terpenoid-based oleoresin biosynthesis function in plant defense. 3rd Banff Conference on Plant Metabolism, Alberta, CA, Jul 2012

Nagel R., Gershenzon J., Schmidt A. Measurement of isoprenyl diphosphate synthase activity in plant crude extracts by HPLC-MS/MS. ICE Symposium, MPI for Chemical Ecology, Jena, DE, Sep 2011

Nagel R., Gershenzon J., Schmidt A. Measurement of isoprenyl diphosphate synthase activity in plant crude extracts by HPLC-MS/MS. TERPNET 2011 - 10th International Meeting: Biosynthesis and Function of Isoprenoids in Plants, Microorganisms and Parasites, Linnæus University, Kalmar, SE, May 2011

Nagel R., Johnson M.D., Nagy N.E., Gershenzon J., Schmidt A. Molecular and analytical characterization of terpene biosynthesis in transgenic spruce. TERPNET 2011 - 10th International Meeting: Biosynthesis and Function of Isoprenoids in Plants, Microorganisms and Parasites, Linnæus University, Kalmar, SE, May 2011

Nagel R., Lohse-Trautsch J., Nagy N.E., Gershenzon J., Schmidt A. Molecular and analytical characterization of terpene biosynthesis in transgenic spruce. 24th Conference of Molecular Biology of Plants, Dabringhausen, DE, Feb 2011

Nagel R. Molecular and analytical characterization of terpene biosynthesis in transgenic spruce. 10th IMPRS Symposium, MPI for Chemical Ecology, Dornburg, DE, Feb 2011

Nagel R., Nagy N.E., Gershenzon J., Schmidt A. Regulation of terpenoid biosynthesis in transgenic white spruce (*Picea glauca*). 6th Plant Science Student Conference, Gatersleben, DE, Jun 2010